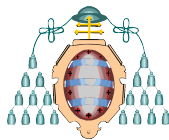


Deformation mechanisms, Rheology and Tectonics

31 August - 2 September, 2011

Facultad de Geología
Universidad de Oviedo
Oviedo, Spain



UNIVERSIDAD
DE OVIEDO



Fundación Universidad de Oviedo

ABSTRACT VOLUME

Contents

Oral programme
Poster programme
Abstracts (in alphabetical order)
List of conference participants
Acknowledgements
Blank pages

The volume was compiled and edited by the Organising Committee

Organizing Committee

Sergio Llana-Fúnez, *Universidad de Oviedo*

Marco A. López-Sánchez, *Universidad de Oviedo*

Francisco J. Fernández-Rodríguez, *Universidad de Oviedo*

Miguel Gutiérrez-Medina, *Universidad de Cantabria*

Alberto Marcos Vallaure, *Universidad de Oviedo*

Juan Luis Alonso, *Universidad de Oviedo*

Fernando Bastida, *Universidad de Oviedo*

Jesús Aller, *Universidad de Oviedo*

Ángela Suárez Rodríguez, *IGME*

+

Fundación Universidad de Oviedo

Scientific Committee

Georg Dresen, *GFZ-Potsdam*

Ernie Rutter, *University of Manchester*

Simon Brocklehurst, *University of Manchester*

Dave Prior, *University of Otago*

Andrés Pérez-Estaún, *Institute of Earth Sciences, CSIC, Barcelona*

Fernando Bastida, *Universidad de Oviedo*

Jesús Aller, *Universidad de Oviedo*

Sergio Llana-Fúnez, *Universidad de Oviedo*

Front cover: *I. Parga Pondal, R. Vegas, A. Marcos. (1982)*

Mapa Xeolóxico do Macizo Hespérico Escala 1:500.000.

Publicacións da Área de Xeoloxía e Minería do Seminario de Estudos Galegos.

Memoir 19p, 2 map sheets

ORAL PROGRAMME

Wednesday 31st August

8:00 - 9:00	Registration
9:00 - 9:30	Opening
	Session 1: <i>Fluids, deformation and metamorphism</i> Chair: Ernie Rutter, Albert Griera
9:40 - 10:10	<i>A hydromechanical model for lower crustal fluid flow</i> James Connolly (invited)
10:10 - 10:30	<i>Dislocation creep derived syn-deformational porosity development in highstrain shear zones: interplay between dislocation migration and selective dissolution by common metamorphic fluids</i> Marco A. Billia , Virginia G. Toy, Nick E. Timms, David J. Prior and Rob Hart
10:30 - 10:50	<i>Pressure solution cleavage organised infilling. Insights from the Mt. Catria site (Northern Apennines)</i> Stefano Tavani , Fabrizio Storti and Josep Antón Muñoz
10:50 - 11:10	<i>Friction of marble under seismic deformation conditions in the presence of fluids</i> Marie Violay , S. Nielsen, E. Spagnuolo, G. Di Toro and S. Smith

11:10 - 11:50 Coffee break

11:50 - 12:10	<i>Deformation of muscovite at low strain rates under hydrothermal conditions</i> Julian Mecklenburgh, Ernie Rutter and Katharine Brodie
12:10 - 12:30	<i>New conceptual model for how metamorphism and deformation interact in porous materials</i> John Wheeler , S. Llana-Fúnez and D. R. Faulkner
12:30 - 12:50	<i>The effect of hydrothermally generated talc on fault strength</i> Amy C. Ellis , Ernie Rutter, Kate Brodie and Julian Mecklenburgh
12:50 - 13:10	<i>A km-scale fluidised breccia in the Mesoproterozoic Mt. Painter Inlier of South Australia</i> Paul D. Bons , Anett Weisheit and Marlina A. Elburg
13:10 - 13:30	<i>Fluid-controlled dynamic opening and closing of fracture permeability at the crustal scale: a new numerical approach</i> Enrique Gómez-Rivas , Paul D. Bons, Philipp Blum, Daniel Koehn and Thomas Wagner

13:30 - 15:10 Lunch at the *Auditorio Príncipe Felipe* restaurant

	Session 2: <i>Earth surface processes and tectonics</i> Chair: Djordje Grujic
15:10 - 15:40	<i>River catchments of the Himalaya as self-correcting strain markers</i> Hugh Sinclair (invited)
15:40 - 16:00	<i>Tectonics and structural controls of fluvial network in the Duero Catchment, NW Iberia</i> Loreto Antón , A. Muñoz, G. De Vicente, A. Gomes and C. Ferreira
16:00 - 16:20	<i>The influence of fault segmentation on drainage network re-organisation and basin stratigraphy</i> Simon H. Brocklehurst , Emma Finch and Robert L. Gawthorpe
16:20 - 16:40	<i>3D geologic model for the Cenozoic evolution of the Tuz Gölü Basin (Central Anatolia, Turkey) based on seismo-tectonic analysis</i> David Fernández-Blanco and Giovanni Bertotti

17:00 - 19:00 Posters (*and beer*)

Thursday 1st September

	Session 3: <i>Microstructure of deformed rocks</i> Chairs: Elisabetta Mariani, Andre Niemeijer
9:00 - 9:30	<i>The Microstructural and Rheological Evolution of Shear Zones</i> Nicholas Austin (invited)
9:30 - 9:50	<i>Deformation and ultrafine recrystallization of quartz in pseudotachylite-bearing faults: a matter of a few seconds</i> Michel Bestmann , G. Pennacchioni, S. Nielsen, M. Göken and H. de Wall
9:50 - 10:10	<i>Thermometry of Quartz Mylonites: Importance of dynamic recrystallization on Ti-in-quartz re-equilibration</i> Djordje Grujic , Michael Stipp and Joe Wooden
10:10 - 10:30	<i>Linking fabric and texture development to three-dimensional strain evolution in deformed quartzite and granitoid conglomerate clasts</i> Dyanna M. Czeck , Eric Horsman, Terra N. D. Anderson and Basil Tikoff
10:30 - 10:50	<i>Rheomorphic shear zones in granites: examples from the Central Iberian Zone, Variscan Iberian Massif</i> Carlos Fernández , Guillermo Corretgé and Antonio Castro
10:50 - 11:10	<i>Linking titanium-in-quartz thermometry and quartz microstructures: strong evidence of continued vein formation during strain localization</i> Mike Härtel and Marco Herwegh

11:10 - 11:50 Coffee break

11:50 - 12:10	<i>Comparing microstructures from natural and experimental deformation in a high-porosity bioclast limestone</i> Ulrike Exner and Patrick Baud
12:10 - 12:30	<i>Porphyroclast rotation in polycrystalline aggregates: a numerical approach</i> Albert Griera , Paul D. Bons, Mark W. Jessell, Ricardo Lebensohn, Lynn Evans and Enrique Gómez-Rivas
12:30 - 12:50	<i>Influence of phyllosilicate mineralogy on the anisotropy of magnetic susceptibility</i> Tom Haerink , Rieko Adriaens, Ann M. Hirt, Timothy Debacker and Manuel Sintubin
12:50 - 13:10	<i>Dislocation creep of dry quartz</i> Rüdiger Kilian , Renée Heilbronner and Holger Stünitz

13:30 - 15:10 Lunch at *Auditorio Príncipe Felipe* restaurant

15:10 - 15:40	<i>The effect of CO₂-brine-rock interaction on the mechanical properties of intact rocks</i> Suzanne Hangx (invited)
15:40 - 16:00	<i>Quantitative microstructural analyses of natural gold alloys</i> Angela Halfpenny and Robert M. Hough
16:00 - 16:20	<i>Scanning Electron Microscopy combined with Focused Ion Beam and potential applications on the nanometre-scale and 3D study of microstructures of geomaterials</i> Luiz F. G. Morales and Richard Wirth
16:20 - 16:40	<i>Time lapse microstructural analysis of gold recrystallisation and coarsening</i> Dan Tatham , Elisabetta Mariani, Rob Hough, John Wheeler, Dave Prior and Andrew Cross
16:40 - 17:00	<i>Compaction related microstructure in chromitites from the Merensky Reef (Bushveld Complex, South Africa)</i> Zoja Vukmanovic , S.J. Barnes, S.M. Reddy, B. Godel and M.L. Fiorentini

17:00 - 18:30 Posters (*and beer*)

18:30 - 19:30 General Assembly

21:00 Conference dinner at *Hotel Tryp Oviedo*

Friday 2nd September

	Session 4: <i>Folding and faulting in rocks</i> Chair: Josep Poblet
9:20 - 9:50	<i>Shear zones and associated structures at the Variscan Front, South Wales</i> Richard J Lisle and Deepak C Srivastava (<i>invited</i>)
9:50 - 10:10	<i>The neutral lines in buckle folds</i> Marcel Frehner
10:10 - 10:30	<i>Lithospheric scale folding related magmatism in NW Iberia. Post Variscan magmatism in time and space</i> Gabriel Gutiérrez-Alonso , Javier Fernández-Suárez, Teresa E. Jeffries, Stephen T. Johnston, Daniel Pastor-Galán and Arlo B. Weil
10:30 - 10:50	<i>The structure of Western Cordillera Septentrional: transpressive deformation and strain partitioning in an island arc (Hispaniola)-continent (North America) oblique collisional setting</i> Pedro P. Hernáiz Huerta , F. Pérez Valera, M. Abad de los Santos, J. Monthel, P. Urien, A. Diaz de Neira, E. Lopera, M. Joubert and A. Pérez-Estaún
10:50 - 11:10	<i>Buttressing in the hangingwall of a Mesozoic normal fault (Asturian Basin, NW Spain); section constructed via photogrammetric methods</i> Hodei Uzqueda , J. Poblet, M. Bulnes, S. Martín and J.C. García-Ramos

11:10 - 11:50 Coffee break

11:50 - 12:10	<i>Structure and Geological History of the Carboneras Fault Zone, S.E. Spain</i> Ernest H. Rutter , Ray Burgess and Daniel R. Faulkner
12:10 - 12:30	<i>Fracture formation and development in a crystalline basement reservoir, central Yemen</i> Resi Veeningen , Bernhard Grasemann, Kurt Decker, A. Hugh N. Rice and Ralf Bischoff
12:30 - 12:50	<i>Kinematic constraints on lithospheric-scale oroclinal bending of the Ibero-Armorican Arc along the northern margin of Gondwana: a paleomagnetic and structural synthesis</i> Arlo Brandon Weil and Gabriel Gutiérrez-Alonso
12:50 - 13:10	<i>Evolution of the Extensional Parallel Folding and Faulting In the Northern Part of the Menderes Metamorphic Core Complex (Western Turkey)</i> Şener Üşümezsoy , Namik Aysal and Isak Yilmaz

13:30 - 15:10 Lunch at Auditorio Príncipe Felipe restaurant

	Session 5: <i>Crustal-scale deformation</i> Chair: Giorgio Ranalli
15:10 - 15:40	<i>The brittle-plastic transition during the seismic cycle</i> Claudia Trepmann (invited)
15:40 - 16:00	<i>A mesoscale constitutive model for rocks undergoing stress-driven melt segregation, applied to corrosion of lithospheric mantle</i> Benjamin K. Holtzman , Daniel S. H. King, David L. Kohlstedt and Mousumi Roy
16:00 - 16:20	<i>Rheology of granitoid fault rocks at the "brittle-to-plastic" transition: an experimental study</i> Matej Pec , Holger Stünitz and Renée Heilbronner
16:20 - 16:40	<i>Quartz veins as proxy for coupled fluid pressure and stress state evolution at the base of the seismogenic crust: examples from the High-Ardenne Slate Belt (Belgium, Germany, France)</i> Manuel Sintubin , Koen Van Noten, Hervé Van Baelen and Philippe Muchez
16:40 - 17:00	<i>Architecture of the orogenic mid-crust revealed by deep reflection seismic</i> Taija Torvela , Annakaisa Korja and Pekka Heikkinen

17:00 - 19:00 Posters (*and beer*)

POSTER PROGRAMME

GROUP A: TECTONIC PROCESSES

A01

Tectonic constraints on the uplift modes of erosive palaeosurfaces: study cases from the External Betics

Juan C. Balanyá, F. Moral, L. Barcos, M. Díaz-Azpiroz, I. Expósito, A. Jiménez-Bonilla, M. Rodríguez-Rodríguez

A02

Tectonic controls on local drainage evolution in semi-arid active foreland basin margins (Betics, southern Spain)

Manuel Díaz-Azpiroz, Miguel Rodríguez-Rodríguez, Fernando Pérez-Valera, Francisco Moral and Inmaculada Expósito

A03

Quantitatively structural control of the karst based on speleological cave survey data: Cabeza Llerosos massif (Picos de Europa, Spain)

Daniel Ballesteros, Montserrat Jiménez-Sánchez, Joaquín García-Sansegundo, Miguel Borreguero

A04

Marine terrace uplifting rates in the Cantabrian shore: contribution of U-Th speleothem dating

Montserrat Jiménez-Sánchez, H. Stoll, S. Giral, A. Aranburu, A. Moreno, M.J. Domínguez-Cuesta, A. Méndez-Vicente, D. Ballesteros, G. Pirla, B.R. Valero-Garcés, H. Cheng, L. Edwards

A05

Analysis of the transition diagenesis-metamorphism in the NE sector of the Cantabrian Zone (NW Spain)

Silvia Blanco-Ferrera, J. Sanz-López, S. García-López, F. Bastida, M.L. Valín

A06

Structural, petrographic and isotopic study of the Ziga peridotites (Western Pyrenees-Eastern Cantabrian Mountains): geodynamic implications

Irene DeFelipe, David Pedreira, Javier A. Pulgar, Eneko Iriarte, Miren Mendia

A07

The Ronda peridotites: an example of dual emplacement sense of the subcontinental mantle (Betic Cordilleras)

José Julián Esteban, Julia Cuevas, Jose María Tubía

A08

Primary coarse-granular lherzolites: the oldest lithospheric mantle in the Ronda peridotites (southern Spain)

José Julián Esteban, Jose María Tubía, Julia Cuevas, Néstor Vegas

A09

Constraining deformation events within the HP-HT units of the NW Iberia Variscan belt

Francisco J. Fernández, P. Castiñeiras, J. Gómez-Barreiro, P. Valverde-Vaquero

A10

Analogue rheological modelling of lithospheric orocline bending. Implications on the development of the Ibero-Armorican Arc

Daniel Pastor-Galán, **Gabriel Gutiérrez-Alonso**, Gernold Zulauf, Carlo Dietl, Friedhelm Zanella

A11

Age precisions for the Permian magmatism (Sallent area, central Pyrenees)

Lidia Rodríguez, J. Cuevas, J.J. Esteban, J.M. Tubía, S. Sergeev, A. Larionov

A12

Towards a rheological model for pluton emplacement: thermal constraints for the Late Miocene Monte Capanne pluton, Elba Island, Italy

A. Caggianelli, A. Lavecchia, **Giorgio Ranalli**, A. Dini, D. Liotta

A13

Rheological contrast at the continental Moho: effects of composition, temperature, deformation mechanism, and tectonic regime

Giorgio Ranalli, M. Adams

A14

The thermal state and rheological behavior of the lithosphere in the Spanish Central System and Tajo Basin from crustal heat production and thermal isostasy

Alberto Jiménez-Díaz, Javier Ruiz, Carlos Villaseca, Rosa Tejero, Ramón Capote

A15

Serpentine rheology and its influence on the mantle wedge dynamics

Ken-ichi Hirauchi, Ikuo Katayama

A16

Base of the seismogenic zone in NW Iberia

Sergio Llana-Fúnez, Carlos López Fernández

A17

Partitioning of lithosphere stretching and thinning at continental rifted margins between pre- and syn-breakup deformation: Norwegian margin study

John G. Watson, N. J. Kusznir, A. Roberts

A18

Ductile and brittle deformation structures of the Mäntsälä granodiorite batholith in southern Finland; observation at three scales

Marit Wennerström, Mira Markovaara-Koivisto

GROUP B: MICROSTRUCTURE OF DEFORMED ROCKS

B01

Frictional properties of Zuccale Fault rocks from room temperature to in-situ conditions: results from high strain rotary shear experiments

André Niemeijer, Cristiano Collettini, Chris Spiers

B02

Fault-related pseudotachylytes in the Barcelona Plain (NE Spain): Evidence of paleoseismic activity

Irene Cantarero, Gemma Alias, Anna Travé, Vinyet Baqués

B03

Microstructure and mineral fabric analysis of San Andreas Fault zone gouge from drill cores of the SAFOD borehole, Parkfield, CA

Manuel Kienast, **Luiz F. G. Morales**, Christoph Janssen, Hans-Rudolf Wenk, Erik Rybacki, Georg Dresen

B04

Developments of Dauphiné twins, fractures, and fine grains in a quartz grain under brittle-plastic transition zone

Jun-ichi Fukuda

B05

The effect of hydrothermally generated talc on fault strength

Amy C. Ellis, Ernie Rutter, Kate Brodie and Julian Mecklenburgh

B06

Seismic properties and microstructures of serpentinite mylonites

Tohru Watanabe, Yuhto Shirasugi, Katsuyoshi Michibayashi

B07

Flow stress history of a detachment system: combining recrystallized grain size, quartz CPO and deformation lamellae, Raft River (NW Utah)

Raphaël Gottardi, Christian Teyssier, Nick Seaton

B08

The evolution of the quartz c-axis fabric pattern and the strain paths in the Kazdağ (İda) Stack Antiform, Western Turkey

Şener Üşümezsoy

B09

The influence of grain size on the deformation of polyphase rocks

Joe Tant, Stephen J. Covey-Crump, Paul F. Schofield

B10

Microstructure evolution during the static recrystallization of cold-worked Carrara marble

Elisabetta Mariani, S.J. Covey-Crump, J. Mecklenburgh, J. Wheeler, D.J. Prior

B11

Microdeformation of Carrara marble

Alejandra Quintanilla-Terminel, J. Brian Evans

B12

Gypsum cement microstructures in fractures related with extensional event (Vilobí gypsum unit, Vallès – Penedès Basin, Miocene, NE Spain)

Mar Moragas, C. Martínez, V. Baqués, G. Alías, E. Playà

B13

Kinematics Of The Northern Betic Cordillera From Gypsum Fabrics (South Spain): Tectonic Implications

Fernando Pérez-Valera, M. Sánchez-Gómez, L.A. Pérez-Valera, A. Pérez-López

B14

Experimental deformation, partial melting, and compositional changes in perthitic K-feldspar at high pressure and temperature

Marianne Negrini, Holger Stünitz, Luca Menegon

B15

Changes in deformation mechanisms and neocrystallization in granite during a MT-LP deformation (Vivero Fault, NW Spain)

Marco A. López-Sánchez, S. Llana-Fúnez, A. Marcos and F.J. Martínez

B16

3D imaging and analysis of fracture networks, porosity and permeability in a reservoir dolomite, using micro-Computed Tomography

Maarten H. Voorn, A. Rath, U. Exner

B17

Comparison of the Brittle Deformation Characteristics of Darley Dale and Pennant Sandstones

Abigail Hackston, E. H. Rutter

B18

Diachronous SC geometries: an example from the Vepor Unit, West Carpathians

Zita Bukovská, Petr Jeřábek, Ondrej Lexa, Jiří Konopásek, Marian Janák

B19

A discrete characterization of the porosity evolution during gypsum dehydration based on an in-situ microtomographic heating experiment

Florian Füsseis, Christoph Schrank, Jie Liu, Benjamin Garnault, Klaus Regenauer-Lieb, Ali Karrech,

Sergio Llana-Fúnez

GROUP C: FOLDING AND FAULTING IN ROCKS

C01

Folds, gashes and saw-tooth structures in the south-central Pyrenees

Jesús Aller, F. Bastida, R.J. Lisle, N.C. Bobillo-Ares, C.O. Menéndez

C02

Reconstruction of thrust-related folds from superficial data: comparison of different balanced interpretations

Isabel Moriano, Josep Poblet, Mayte Bulnes

C03

Folded Variscan duplex in the Herrera Unit of the Iberian Range

Pablo Calvín, A.M. Casas

C04

Overlap of salt tectonics, thin-skinned tectonics and syntectonic sedimentation: Structure and kinematics of the Sierras Marginales in the Olvena area

Pablo Santolaria, A.M. Casas, A. Luzón.

C05

Anatomy of an intraplate strike-slip inversion belt: the Ubierna Fault System

Stefano Tavani, P. Granado, A. Quintà, E. Carola

C06

Geometric modelling and fracture prediction: examples from seismic, remotely sensed and field data

Tina Lohr, Jorge Ginés

C07

Structural modelling: from satellite interpretation to cross-section construction

Jorge Ginés, Mike Oehlers

C08

3D geological reconstruction of Puerta-Pareja fault-propagation fold (Loranca Basin, Central Spain)

Manoel Valcarcel, Josep Anton Muñoz, Ruth Soto

C09

Structural evolution of the Jabal Akhdar dome (Oman): insights from fracture and vein networks

Enrique Gómez-Rivas, Paul D. Bons, Daniel Koehn, Janos L. Urai, Max Arndt, Simon Virgo, Ben Laurich, Conny Zeeb, Lena Stark, Philipp Blum

C10

Single layer folding in non-coaxial conditions up to high strain

Maria-Gema Llorens, Paul D. Bons, Albert Grieria, Enrique Gómez-Rivas

C11

Tectonic evolution of the Sierras Interiores (South Pyrenean Zone, central Pyrenees)

Lidia Rodríguez, J. Cuevas, J.M. Tubía

C12

Relationship between cleavage and thrust-related deformation in the southern margin of the Pyrenean Axial Zone (Bujaruelo valley, Huesca)

Esther Izquierdo-Llavall, Antonio Casas-Sainz, Inmaculada Gil-Peña, Chiara Invernizzi

C13

Facing confrontation in coaxial deformation during the main Variscan tectonic event; SW Portuguese sector of Centro-Iberian Zone

Daniel Metodiev, José Romão, Rui Dias, António Ribeiro

C14

Structure and Geological History of the Carboneras Fault Zone, S.E. Spain

Ernest H. Rutter, Ray Burgess and Daniel R. Faulkner

C15

Ground-truthing in-situ seismic data against geological data: the Carboneras Fault Zone, S.E. Spain

Rochelle Taylor, **Ernest Rutter**, Kate Brodie, Daniel Faulkner, Stuart Nippres, Andreas Rietbrock, Christian Haberland

GROUP D: STRAIN IN SHEAR ZONES

D01

Testing transpression models in brittle shear zones compared with ductile deformation. A standardized procedure with contrasting approaches

Manuel Díaz-Azpiroz, Leticia Barcos, Carlos Fernández, Dyanna Czeck

D02

Protocol for testing the model of oblique transpression with oblique extrusion in ductile shear zones

Carlos Fernández, Manuel Díaz-Azpiroz, Dyanna Czeck

D03

Initiation and evolution of shear zone-related lozenges

Carlos Ponce, Elena Druguet, Jordi Carreras

D04

Finite strain analysis in quartzites; methods and markers

Alexis Soares, Rui Dias

D05

Application of shearband boudins analysis to understand ductile shear zones

João P. Sousa, Benedito C. Rodrigues, Jorge Pamplona

D06

Strain partitioning of Variscan deformation in the Peso da Régua – Vila Nova de Foz Côa region (Centro-Iberian autochthon): The Douro Flower Structure

Noel Moreira, Mauro Búrcio, Rui Dias, Carlos Coke

D07

Tomar-Badajoz-Córdoba shear zone in Abrantes region; the presence of a kilometric sheath fold?

Noel Moreira, Jorge Pedro, Rui Dias, António Ribeiro, José Romão

ABSTRACTS (*in alphabetical order*)

Folds, gashes and saw-tooth structures in the south-central Pyrenees

Jesús Aller¹, F. Bastida¹, R.J. Lisle², N.C. Bobillo-Ares³, C.O. Menéndez³

1 Departamento de Geología, Universidad de Oviedo, 33005 Oviedo, Spain

2 School of Earth and Ocean Sciences, Cardiff University, Cardiff, CF10 3YE, UK

*3 Departamento de Matemáticas, Universidad de Oviedo, 33007 Oviedo, Spain
aller@geol.uniovi.es*

In the Eocene turbidites of the south-central Pyrenees abundant metric size folds with cleavage developed during the Alpine deformation. They are close folds and range in shape from chevron to parabolic. These folds have associated veins. A common pattern of these inside a competent layer consists of a set of veins opening towards the stratigraphic bottom (bottom set) and another one opening towards the top (top set). The bottom set consists of curved veins and the top set consists of rectilinear or low curvature veins. This pattern usually appears on the normal limb of the folds, where the veins of the bottom have a concavity downwards. Frequently, the displacement of the vein edges gave rise to a step in the base of the bed. Its sense is such that the bedding plane steps up in the direction towards the hinge zone of the adjacent anticline. Where these steps show a regular spacing, they form a structure that we have named 'saw tooth structure'. In the scarce cases in which the veins appear in the overturned limbs, they are less well developed and the veins of the bottom set have concavity downwards. If the beds were to be unfolded, the concavity direction of the curved bottom veins would be opposite on the two limbs.

The different development of these structures on the two limbs of the folds, the different facing-direction of the steps of the saw-tooth structures and the different facing-direction of the concavity of the bottom veins on the two limbs if they are unfolded suggest that the development of these structures is contemporaneous with the folds. The more probable mechanism to explain the initiation of veins and saw-tooth structures is flexural slip. In a first stage, the slip along a bed boundary should involve a stress state with principal directions oblique to the bedding in zones adjacent to the boundary between layers. Favoured by a high fluid pressure, this stress state could generate small faults in the competent layer that form a high angle with the layer boundary. These faults formed a conjugate fault set with the bedding fault involved in the flexural slip. The existence of graded bedding probably favoured a better development of the fractures from the base of the bed than from the top.

Once the faults had initiated, they could have operated as obstacles to flexural slip and this could have given rise to a stress concentration on the steps produced. The stresses inside the competent layer should give rise to a propagation of the small faults as tension gashes in agreement with the orientation of the principal stresses inside the layer, producing a curved path for the fractures. A simple mechanical model produces the characteristics of the stress driving the growth and curvature of the gashes. The angular inclination of the propagation path of a fracture will be greater the lower the value of the forces acting in the direction longitudinal to the bed with respect to the forces acting in the perpendicular direction.

Tectonics and structural controls of fluvial network in the Duero Catchment, NW Iberia

Loreto Antón¹, A. Muñoz², G. De Vicente², A. Gomes³, C. Ferreira³

¹ Facultad de Ciencias, Universidad Nacional de Educación a Distancia (UNED), Madrid, Spain.

² Instituto de Geociencias, Departamento de Geodinámica, Universidad Complutense de Madrid, Spain

*³ Departamento de Geografia, Universidade do Porto e Centro de Estudos em Geografia e Ordenamento do Território (CEGOT), Portugal.
lanton@ccia.uned.es*

The Duero Basin, in northern Spain, is the largest of the intraplate cenozoic basins in Iberia. The basin shows a complex evolution from end Cretaceous to the early Cenozoic times as result of faulting and upbuilding of mountain belts and internal deformation affecting Iberian microplate during Alpine orogenic events.

To the west the Cenozoic basin is surrounded by the Variscan basement mostly composed by precambrian and paleozoic metamorphic rocks and Pre-variscan and variscan granitic rocks developed in a tectonically intricate zone predominantly deformed during the Variscan Orogeny and subsequently by the Alpine Orogeny. The Variscan basement shows a strong fracture pattern dominated by NNE-SSW strike-slip fault systems.

The development of the present fluvial systems is related to a change in the Duero Basin drainage, from endorheic to exorheic. Nowadays, the Duero river flows westwards through the Cenozoic Basin and enters in the area that configures the western fringe of the Basin, an elevated zone where the uplifted variscan basement crops out. The main morpho-structural features of this area are a rather flat relief mix together with a deep fluvial incision and a strong structural control of the drainage system by the fracture network. Main rivers as Duero, Tormes or Agueda can manage an incision up to 300–400 meters in the Spanish-Portuguese border.

Further West, the watershed has an asymmetric shape and reveals huge morphological differences between margins: the northern margin is larger, with long rivers and developed basins, while the southern margin, has narrow watersheds with shorter rivers, showing frequently, fluvial captures on the high plateaus. In this Lower Reach, the rivers longitudinal profiles that shows low concavity degree are located in the most uplifted tectonic compartments (Western Mountains and Central Plateaus) while longitudinal profiles with convex shape tends to increase upstream. This is a clear manifestation of the existence of two erosion cycles, well marked as we move to the watershed inland.

Changes in equilibrium conditions are reflected as changes in main trunk direction and variation in the concavity and steepness of longitudinal profiles. The analysis of more than 50 streams longitudinal profiles for the entire Basin evidence great differences in profiles shapes; whereas in the Cenozoic Basin profiles are close to equilibrium, to the west extensive bedrock segments along the active channel include knickzones of steep rapids and short steps, and V-shaped valleys are characteristics.

In this work we present the analysis of the channel network together with a well constrained geological and tectonic pattern, to analyze the role of tectonics in the evolution of the drainage in the area. Further studies in fluvial network evolution and its interplay with tectonics in the Duero Basin are currently under study though tectonic, geomorphology, surfaces dating and modeling approaches.

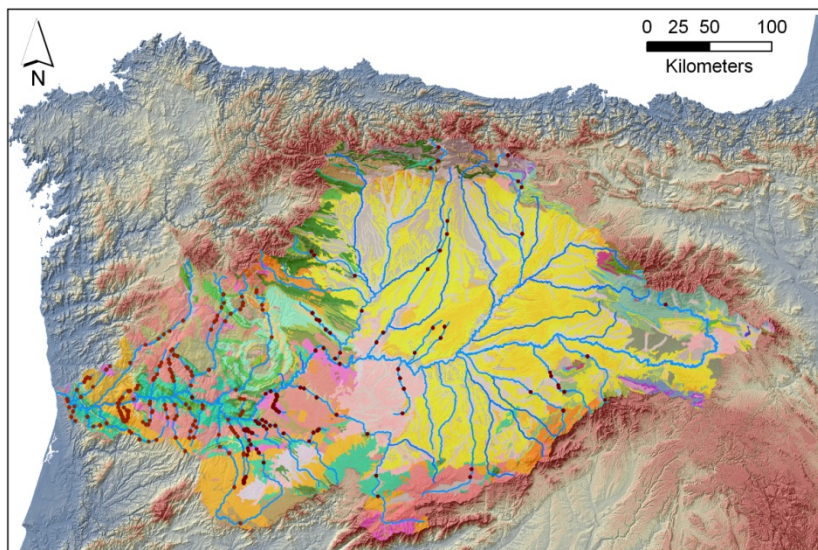


Fig.1. Duero catchment geological map. Main streams and knick points.

The Microstructural and Rheological Evolution of Shear Zones

Nicholas Austin

Imperial Oil

nick.j.austin@gmail.com

Evidence of localized strain is ubiquitous in deformed lithospheric rocks. Recent advances in laboratory deformation techniques, including the use of torsion experiments, have enabled the coupling of microstructural and rheological evolution to be investigated in experiments run to strains approaching those reached in many natural shear zones. Further, the increased use of electron backscatter diffraction to quantify crystallographic preferred orientation (CPO) has significantly increased understanding of CPO formation and evolution.

Laboratory data suggest that both the rate of grain size reduction and the stabilized grain size correlate well with the product of stress and strain rate (e.g. power). For energy to be conserved, the rate that work is done must be balanced by the rate of increase in internal energy plus the rate of energy dissipation. Assuming that the dominant mechanism for increasing the internal energy is an increase in grain boundary area, then these data suggest that the rate of grain size reduction is related to the rate that work is done on the system. As there is also a driving force for grain growth due to capillarity forces, the stabilized grain size will be determined by the balance of grain-growth rate and grain-size reduction rate, and is controlled by the product of stress and strain rate, as well as temperature. Consequently, recrystallized grain size is likely a paleowattmeter.

Additional complexities may arise in rocks composed of more than one mineral phase. Laboratory experiments suggest that, for rocks deformed at "high" strain rates, or which have "large" mean free spacing of the pinning phase, the final recrystallized grain size is well explained by competing grain growth and grain size reduction processes, where the grain-size reduction rate is consistent with the rate that mechanical work is done during deformation. On the other hand, when there is a "small" mean free spacing of the pinning phase, or if the sample is deformed at a "low" strain rate, the final grain size is controlled by the distribution of the pinning phase. CPO evolution and strength are also impacted by both the volume fraction and geometry of secondary phases. In samples with nominally the same grain size, spherical second phases lead to a strong CPO and promote weakening, whereas a similar volume fraction of elongate second phases leads to a weak CPO and promotes bulk strengthening.

The applicability of these laboratory observations has been tested with field-based observations made in the Morcles Nappe (Swiss Helvetic Alps). In the Morcles Nappe, calcite grain size becomes progressively finer as the thrust contact is approached, and there is a concomitant increase in CPO intensity, with the strongest CPO's in the finestgrained, quartz-rich limestones, nearest the thrust contact, which are interpreted to have been deformed to the highest strains. Combined, laboratory and field observations support the assertion that a rock's microstructure is strongly linked to its rheology, and thus may be used to provide insight into the distribution of strain observed in natural shear zones.

Tectonic constraints on the uplift modes of erosive palaeosurfaces: study cases from the External Betics

Juan C. Balanyá, F. Moral, L. Barcos, M. Díaz-Azpiroz, I. Expósito, A. Jiménez-Bonilla, M. Rodríguez-Rodríguez

*Department of Physical, Chemical and Natural Systems, Universidad Pablo de Olavide, 41013 Seville, Spain
jcbalrou@upo.es*

Betic External Zones comprise a continuous 80-110 km wide fold-and-thrust belt that extends from the west of the Gibraltar Strait to the southern end of the Iberian Cordillera. Made up by Mesozoic-Cenozoic palaeomargin sedimentary rocks, external units are completely detached above the Iberian Hercinian basement. Evidences of surface uplift from the Upper Miocene to Present are widely represented along the Betics. They are essentially based on the altitude of shallow marine deposits of Upper Miocene age and the current height of erosive palaeosurfaces probably generated near the absolute base level (Lhénaff, 1977, Ph.D. Thesis). In this study, we try to combine both criteria with time and space related deformation structures to better define the surface uplift modes in western external Betics.

West of the city of Granada, two segments can be distinguished in the southernmost external units according to their distinctive structural trend-line pattern and strain partitioning modes: 1) a western segment, convex to the foreland, where arc-perpendicular shortening was coeval to arc-parallel stretching; and 2) an eastern segment with a transpressive shear zone partially coinciding with the development of a concave-to-the foreland (recess) zone.

In the western segment, on both sides of the Ronda Basin, the structural revision of scattered relics found at different altitudes (800-1000 m) of an Upper Miocene (Tortonian ?) palaeosurface (Lhénaff, 1977) reveals that this erosive surface is affected by NW-SE trending normal faults. In the same sector, Upper Tortonian-Messinian shallow marine sediments are uplifted by the late growing of plurikilometric, NE-SW trending, open folds and related reverse faults. The NW-SE faults affecting the palaeosurface represent the later stages of a SW-NE arc-parallel extension that affected this sector from the Middle Miocene onwards.

The eastern segment starts at the Sierra de Peñarrubia with palaeosurface relics at an altitude of 600 m. This relief also has Upper Tortonian-Messinian shallow marine sediments on the top, and it is uplifted by an open antiform bounded by dextral strike-slip faults. The Sierra is cut-off by an antecedent stream that forms a water gap 100-200 m deep through the structure. Further East (Sierra de Huma), a portion of a comparable palaeosurface is identified at 1.150 m. In this range a major water gap (several hundred meters deep) is developed. A segmented (normal faulted) karstic plain is identified between 1.100 and 1.300 m in the upper part of the Torcal de Antequera Massif. This massif is bounded by dextral strike-slip fault zones and internally shortened by folds and reverse faults that have been active from the Upper Miocene to the Quaternary.

Both contractional and extensional structures are responsible for the uneven level of Upper Miocene palaeosurfaces in the western sector. Taken together, normal faults and open (double) plunging folds are responsible for the along-strike variations of structural relief altitude. Late stages of faulting systems and fold growing explain the different height of the palaeosurface fragments. In the eastern sector, first estimates of the structural uplift point to the efficiency of vertical extrusion and correlative relief generation in the transpressive case.

Quantitatively structural control of the karst based on speleological cave survey data: Cabeza Llerosos massif (Picos de Europa, Spain)

Daniel Ballesteros¹, Montserrat Jiménez-Sánchez^{1, 2}, Joaquín García-Sansegundo¹, Miguel Borreguero³

1 Department of Geology, Oviedo University, Spain

2 Institute of Earth Sciences Jaume Almera, CSIC, Spain

3 Société Suisse de Spéléologie, section Troglog, Swiss

ballesteros@geol.uniovi.es

The influence of Tectonics on speleogenesis has been qualitatively studied by several previous works based on 1) observations from bedrock outcrops, 2) geological maps, 3) geological cross-sections and 4) collection of joints and bedding plane measurements in caves and data projection on caves surveys. Cave survey data can be statistically analyzed and compared with the geometry of the massif discontinuities. The aim of this work is to establish quantitatively the influence of the structural factor in eight several vertical caves based on speleological cave survey data, joint and bedding measurements and stereographic projection. The caves considered in this study are situated in the Cabeza Llerosos massif, in the Picos de Europa (Cantabrian Mountains, N Spain). The length of the caves ranges from 500 to 4,400 m and the depths vary from 130 to 738 m. The methodology of work includes: 1) cave survey collection; 2) geological map and cross-sections with the cavities projection; 3) data collection (152 measurements) of bedding and joints in caves and near outcrops; 4) establishment of the families of joints and bedding by stereographic projection, 5) the definition of groups of cave passages from stereographic projection (based on their directions and dips) and 6) the comparison between bedding, families of joints and cave survey data by stereographic projection. Cabeza Llerosos massif is mainly formed by 1,000 m of carboniferous limestone affected by an NW-SE trending, sub-vertical and SW-directed thrusts and other faults which direction is SE-NW, SW-NE or N-S. The cave projections on the geological map and on the geological cross section are parallel to the trace of thrusts, others faults and bedding. Seven families of joints have been distinguished in all the area of study: J1) sub-vertical, J2) N63/68SE, J3) N29E/46NW, J4) N52E/72NW, J5) N129E/17NE, J6) N167E/57NE and J7) N180E/26E. The bedding is N30-55/60-80NE. Five groups of cave passages have been defined, but these groups are not represented in all caves. "A" group is formed by sub-vertical passages (shafts) and is represented by the 61 % of all the cave passages. "B" group is formed by N10W-N10E/3-20N galleries and correspond it with the 13 % of the passages. "C" group is defined by N20-70E/0-50NE passages and is represented by the 13 % of the passages. "D" group is formed by N125-145E horizontal galleries and includes the 6 % of the passages. "E" group is defined by N105-151W/38-65SW passages and is represented by the 3 % of the passages. "A" group is conditioned by the joint families J1, J3, J4 and J6, as well as their intersections. "B" group is controlled by the intersection between families J5 and J6. "C" is ruled by the intersection between families J1, J2, J5 and J7. "D" group follows the bedding and the "E" group is conditioned by the families J1, J2, J3 and J4. Therefore, the endokarst morphology is strongly controlled by the joints. Sub-vertical joints rule the 64 % of the cave passages and the intersections between sub-vertical and sub-horizontal joints condition the 26 %. The stratification forces only the 6% of the passages.

Deformation and ultrafine recrystallization of quartz in pseudotachylyte-bearing faults: a matter of a few seconds

Michel Bestmann¹, G. Pennacchioni^{2, 3}, S. Nielsen³, M. Göken⁴, H. de Wall¹

¹ GeoZentrum Nordbayern, University Erlangen-Nuremberg, Germany

² Department of Geosciences, University of Padova, Italy

³ INGV, Rome, Italy

⁴ Department Werkstoffwissenschaften I, University of Erlangen-Nuremberg, Germany

michel@geol.uni-erlangen.de

Tectonic pseudotachylytes, i.e. quenched friction-induced silicate melts, record coseismic slip along faults and are mainly reported from the brittle crust in association with cataclasites. The temporal and spatial association of fine-grained quartz with pseudotachylytes have been described within the literature for several locations and seems to be an important feature characteristic for seismic processes.

In this study, we document the occurrence of recrystallization of quartz to ultrafine-grained (grain size 1-2 µm) aggregates along microshear zones (50-150 µm thick) in the host rock adjacent to pseudotachylytes from two different faults within quartzite (Schneeberg Normal Fault Zone, Eastern Alps), and tonalite (Adamello fault, Southern Alps). The transition from the host quartz to microshear zone interior includes: (i) formation of high dislocation densities; (ii) fine (0.3-0.5 µm) polygonization to subgrains defined by disordered to well-ordered dislocation walls; (iii) development of a mosaic aggregate of dislocation-free new grains. The crystallographic preferred orientation (CPO) of quartz towards the microshear zone shows a progressive misorientation from the host grain, by subgrain rotation recrystallization, to a nearly random CPO possibly related to grain boundary sliding. Thus these ultrafine quartz aggregates appear to be typically associated with pseudotachylytes in nature. Microshear zones localized on precursory fractures developed during the stages of earthquake rupture propagation and the very initial stages of fault slip (Bestmann et al., 2011).

Based on thermal models we suggest that crystal plastic deformation of quartz accompanied by dramatic grain size refinement occurs during seismic faulting at the base of the brittle crust as a result of the high temperature transients (> 800°C) related to frictional heating in the host rock selvages of the slip surface. These localised high deformation temperatures made possible that the process of recrystallization, including recovery processes, could occur in a time lapse of a few tens of seconds.

REFERENCES

Bestmann, M., Pennacchioni, G., Frank, G., Göken, M., de Wall, H., 2011. Pseudotachylyte in muscovite-bearing quartzite: coseismic friction-induced melting and plastic deformation of quartz. *Journal of Structural Geology* 33, 169-186.

Dislocation creep derived syn-deformational porosity development in high-strain shear zones: interplay between dislocation migration and selective dissolution by common metamorphic fluids

Marco A. Billia¹, Virginia G. Toy¹, Nick E. Timms², David J. Prior¹, Rob Hart³

¹ Department of Geology, University of Otago, PO Box 56, Dunedin, New Zealand

² Western Australia Geothermal Centre of Excellence, Department of Applied Geology, Curtin University, Perth, GPO Box U1987, Western Australia, 6845, Australia

*³ Centre for Materials Research, Curtin University, GPO Box U1987, Perth, WA 6845, Australia
marco@geology.co.nz*

The micromechanisms by which fluids migrate through mylonites without brittle fractures is still poorly understood despite overwhelming evidence that ductile mid-crustal shear zones transmit large quantities of fluid. The static permeability of high-strain, ductile fault rocks is considered extremely low.

We recently investigated quartz microstructures of several fresh ultramylonite specimens from a 120 km long section of New Zealand's Alpine Fault zone. We employed secondary electron (SE) imaging of broken surfaces, confocal laser scanning microscopy (CLSM), electron backscatter diffraction (EBSD) and transmission electron microscopy (TEM) analyses of lamellae prepared using a focussed ion beam SEM (FIBSEM).

Quartz occurs both within mono-mineralic domains and within mixed quartz-feldspar-mica aggregate domains containing sigmoidal feldspar porphyroclasts up to 500 μm across. Grains are 2-1000 μm in diameter and exhibit a strong crystallographic preferred orientation (CPO) that we infer was imposed during dislocation creep. Grain boundaries and some subgrain boundaries are decorated with pores that commonly have bimodal size distribution and consistent, pseudo-tetrahedral morphology on a given crystal face. Grain boundary pores are the morphological expression of the interaction of high dislocation densities ($\leq 5 \cdot 10^9 \text{ cm}^{-2}$) in individual quartz grains, representing the pile-up of dislocations at grain and subgrain boundary surfaces, with dissolution on these high-energy sites by aqueous fluids during amphibolite facies metamorphism, deformation and subsequent exhumation.

Subgrain formation by progressive stacking of dislocations to form crystallographically controlled grain boundaries at high temperatures enhanced porosity by producing smaller, recrystallized grains that still contain dislocations on their boundaries, which are therefore still preferable sites for nucleation of new etch pits. However, partial late recrystallisation by grain boundary bulging at higher crustal levels produced subgrains without these high-stress sites that prevented dynamic porosity from developing.

Strong CPOs, together with preferential etching on low-index planes have the potential to exert a directional control on porosity generation and may cause an anisotropy in the dynamic permeability structure in highly deformed quartz-feldspathic crustal rocks. However, it is important that viscous grain boundary sliding (VGBS) also occurs to allow etching and for a permeable network to be maintained.

Analysis of the transition diagenesis-metamorphism in the NE sector of the Cantabrian Zone (NW Spain)

Silvia Blanco-Ferrera¹, J. Sanz-López², S. García-López¹, F. Bastida¹, M.L. Valín¹

¹ Department of Geology, University of Oviedo, Spain

² Department of Navigation and Earth Sciences, University of A Coruña, Spain

silvia.blanco@geol.uniovi.es

A tectonothermal study of the north-eastern sector of the Cantabrian Zone (Ponga-Cuera unit, Picos de Europa unit and the northernmost part of the Pisuegra-Carrión unit) using the conodont color alteration index (CAI) and the Kübler index (KI) methods shows a variation from diagenetic conditions at very low temperatures in the northern part up to anchizonal conditions in the southern part. A wide north-central area mainly has CAI values between 1 and 2, indicating a temperature interval from 50 to 80°C. This area went through two long periods of burial that were ended by compressive periods (Variscan and Alpine deformations) until exhumation events took place. The first burial for the Carboniferous rocks at the end of the Pennsylvanian is in accordance with the diagenetic CAI and KI values, while the second burial estimated for the Permian-Cenozoic cover is likely to have homogenized CAI values at around 1.5 by increasing the lowest previous values in most of the area. Variscan tectonic superimposition, in which thrusts were the dominant structures, had very little effect on the CAI values, and consequently must have been balanced by intense and fast erosion. Moreover, the southern area shows an increase in CAI values from 2 to 5.5, indicating palaeotemperatures of between 50 and 380°C. These values record a sharp transition from the diacaizone to ancaizone conditions associated with a high thermal gradient (about 95°C km⁻¹). The CAI isograde surfaces display W-E trending and are oblique to the basal thrust of the Picos de Europa unit and cut the Variscan (Gzhelian) structures. The diacaizone-ancaizone boundary (isograde of CAI = 4) is close to the diagenesis-anchizone boundary (KI = 0.42), which is located in the footwall of the basal thrust of the Picos de Europa unit. The southern high gradient may well be related to the diastothermal metamorphism developed close to the Carboniferous-Permian boundary in some areas of the Cantabrian Zone, coinciding with the beginning of an extensional regime. Furthermore, the highest observed thermal conditions are associated with conodont metamorphic recrystallization and related to fluid thermal transport from the Pisuegra-Carrión unit. The high thermal gradient, the isograde surface disposition and the fluid thermal transport are interpreted as being related to the presence of a thermal dome located in the Pisuegra-Carrión unit. The metamorphism associated with this dome cuts the two branches of the Asturian Arc, hence it postdates the closure of the arc. Local variations in the CAI values were produced as a result of Permian-Mesozoic hydrothermal activity. This activity also produced dolomitization and ore deposits in some areas. Alpine deformation hardly produced any changes in the previous thermal pattern; it only produced a northwards tilting of the structure and isograde surfaces.

A km-scale fluidised breccia in the Mesoproterozoic Mt. Painter Inlier of South Australia

Paul D. Bons¹, Anett Weisheit¹, Marlina A. Elburg²

¹ Department of Geosciences, University of Tuebingen, Germany

² Department of Geology and Soil Science, University of Ghent, Belgium

*School of Geology, University of KwaZulu-Natal, Durban, South Africa
paul.bons@uni-tuebingen.de*

An unusually large, >10 km² breccia zone can be found at Hidden Valley in the metamorphic Proterozoic basement of the Mount Painter Inlier, 600 km north of Adelaide, South Australia. Clast-size analyses indicate long-lived fluidisation processes as a result of structural fluid-flow focusing and exhumation.

The large Palaeozoic breccia zone is located at a major fault zone between Mesoproterozoic metasediments and metagranites. Its clasts, however, are a mixture of unmetamorphosed Neoproterozoic (Lower Adelaidean) cover-sediments, highly metamorphosed basement rocks and igneous lithologies of unknown origin. During the thick-skinned 500 Ma Delamerian Orogeny, the basement was folded in a large anticline, of which the axial fold-plane lies in the extension of Hidden Valley. A palinspastic reconstruction puts Hidden Valley about 2 - 3 km below the (now eroded) Adelaidean unconformity. Clasts in the breccia are derived from the lowermost 2-2.5 km of Adelaidean stratigraphy. Therefore, these clasts represent up to 5 km of vertical section and some clasts moved up to 5 km downward, relative to the host rock of the breccia.

The clast size distribution of the breccia was measured at map-, outcrop-, sample- and thin-section-scale. The size distribution follows a power law with a single exponent (fractal dimension) of about two from 1 mm up to 100 m. A small shift in the fractal dimension is only observed at the very smallest scale (<mm), and can be explained by corrosive wear.

The low fractal dimension, maturity of the breccia, roundness of the clasts, mixing of a large stratigraphic column and abundant rock flour matrix are typical features of a fluidisation process with wear abrasion during formation. Assuming a minimum fluidisation fluid-flow velocity of 5 - 8 m/sec for the mapped rock types this breccia would have formed within a few days using all the possible formation-water that can be provided. A more probable scenario is a continuous release of formation- and hydrothermal fluid during contemporaneous exhumation of the basement anticline. Focusing of the fluid along the anticlinal hinge zone and the major fault zone caused fluid-assisted brecciation at a certain level in the crust, starting in the Adelaidean cover and propagating down during exhumation. A long-lived fluidisation process acted like a conveyor belt and resulted in the unusual mixture of clast lithologies and their brecciation from the 100 m down to the mm-scale.

The influence of fault segmentation on drainage network re-organisation and basin stratigraphy

Simon H. Brocklehurst¹, Emma Finch¹, Robert L. Gawthorpe²

¹ School of Earth, Atmospheric and Environmental Sciences, University of Manchester, UK

² Department of Earth Science, University of Bergen, Norway

simon.h.brocklehurst@manchester.ac.uk

Landscape evolution in an extensional basin reflects a history of fault activity, drainage network evolution, and sediment transport and deposition. An integrated approach is needed in order to deconvolve climate, tectonic and relative sea-level change from the preserved stratigraphic record. The spacing of outlets and thus the supply of sediment within a rift is dependent not only on slope length, but also on the pre-existing drainage network and the evolving fault array.

A three-dimensional numerical model of erosion and clastic sedimentation is applied to investigate the effect of displacement on neighbouring normal faults on the development of drainage networks, including drainage capture and re-organisation, and the subsequent distribution of deposition. Material is eroded through a stream-power incision law and deposited using a modified diffusion algorithm. The initial topography is developed to steady state. This system is then perturbed by the introduction of a pair of propagating normal faults at varying displacement rates (1.0m/kyr - 2.0m/kyr), locations relative to one another (along strike, en echelon, or adjacent) and activity times. Additional two-stage experiments feature slower displacement during a rift initiation phase, followed by faster rift climax displacement.

When the faults lie along strike and propagate towards one another, a large proportion of the drainage network is routed through the narrowing gap between the faults. This large catchment may follow the same drainage pathway long after the faults have become connected. When the faults have an en echelon distribution, the relative separation of the two faults is a key control on the subsequent drainage network evolution; greater overlap reduces the drainage on the ramp between the faults, and increases the likelihood of internal drainage on the footwall of the downslope fault. When the relative timing of the two faults is altered, further modifications to network re-organisation and depositional geometries occur. If the upslope fault is active first, drainage re-directed around the fault tip has sufficient stream power to continue to cut across the downslope fault when it becomes active. However, if the downslope fault becomes active first, the drainage is directed around both fault tips in turn. The various drainage network histories are in turn reflected in the architecture of the stratigraphy deposited in the hanging walls, which is often different from that anticipated by consideration of the downslope fault alone. Two-stage experiments show strongly localised deposition in the immediate hanging walls of the faults, and reduced footwall incision, once the fault slip accelerates.

Diachronous SC geometries: an example from the Vepor Unit, West Carpathians

Zita Bukovská¹, Petr Jeřábek¹, Ondrej Lexa¹, Jiří Konopásek^{2,3}, Marian Janák⁴

1 Institute of Petrology and Structural Geology, Faculty of Science, Charles University, Albertov 6, 128 43 Prague 2, Czech Republic

2 Department of Earth Science, Faculty of Mathematics and Science, University of Bergen, Allégaten 41, N-5007 Bergen, Norway

3 Czech Geological Survey, Klárov 3, 118 21 Prague 1, Czech Republic

4 Geological Institute, Slovak Academy of Science, Dúbravská 9, P.O. BOX 106, 840 05 Bratislava 45, Slovak Republic

zita.bukovska@natur.cuni.cz

Small scale shear zones crosscutting an existing anisotropy at gentle to moderate angles are frequent phenomenon in deformed rocks. Such geometries are usually referred to as shear bands, C- a C'- bands, extensional crenulation cleavages, asymmetrical boudinage, asymmetrical folds or normal fault kink bands. Shear band geometries were for the first time described from the South Armorican shear zone (Berthé et al. 1979) and characterized as synchronous. In this study, we concentrate on evolution of shear bands developed in a detachment zone located in between two major units of the West Carpathians, the Vepor and Gemer unit. The studied area shows two main deformation fabrics - S1 and S2, which are subhorizontal to gently eastward dipping, with an eastward plunging lineation and form the geometry of SC bands, where S1 corresponds to S and S2 to C. Both fabrics have been examined by means of microstructural and microchemical analyses in order to characterize the evolution of these SC bands.

The S1 and S2 fabrics in orthogneiss and quartzite show recrystallization of quartz with distinct grain size, grain shape preferred orientation and c-axis patterns. In orthogneiss, the S1 is characterized by quartz aggregates with larger grain size (50-300 µm), while the crosscutting S2 cleavage contains much smaller grains (10 – 60 µm). The shape preferred orientation of quartz in the first and second microstructural domain is parallel to the S1 and S2 fabrics, respectively. In quartzite, the aggregates are characterized by microstructure with extremely large grain size (1-2 mm), which can not be correlated with the S1 fabric in orthogneiss, and probably represents an older pre-sedimentary microstructure. Using computer integrated polarisation microscopy method (Panozzo Heilbronner and Pauli, 1993) we have examined the c-axis patterns in both fabrics. These show either a higher-temperature Y-max or a single girdle with top-to-the west asymmetries within the S1 aggregates and a single girdle with top-to-the east asymmetries within the S2 cleavage.

Microprobe analyses of minerals forming S1 and S2 were performed in orthogneiss and schist with the peak metamorphic assemblage chlorite-chloritoid-kyanite. In orthogneiss, three generations of white mica are present. The first generation mica grains of probably magmatic are large and correspond to muscovite. These are overgrown by the second generation of small, phengitic white mica, which occurs in the S1 fabric. The third generation is muscovite, replacing the older white mica. This muscovite defines the S2 fabric and represents the major white mica in the orthogneiss. The chlorite-chloritoid-kyanite peak metamorphic assemblage in the schist clearly postdates the metamorphic foliation S1, as demonstrated by its transversal growth. This assemblage was subsequently affected by chlorite and muscovite-bearing cleavage S2. Monazite and xenotime occur in the vicinity of chloritoid and/or separately in the matrix. The ICP-MS dating of monazite yields the age of 96 ± 4 Ma that is interpreted to date the formation of S1 fabric. Previously published Ar-Ar age of 77 Ma obtained from white mica in these rocks (Janák et al., 2001) has been interpreted as exhumation age and most likely corresponds to the formation of S2 cleavage.

According to the quartz microstructures, metamorphic record and dating of monazite and white mica, we conclude, that the studied SC bands formed during two separate deformation events, which fit well to the overall tectonic scenario previously proposed for this area (Janák et al. 2001; Jeřábek et al., 2008).

Towards a rheological model for pluton emplacement: thermal constraints for the Late Miocene Monte Capanne pluton, Elba Island, Italy

A. Caggianelli¹, A. Lavecchia¹, **Giorgio Ranalli**², A. Dini³, D. Liotta¹

¹ Dipartimento di Scienza della Terra e Geoambientali, Bari University, Italy

² Department of Earth Sciences, Carleton University, Ottawa, Canada

³ Istituto di Geoscienze e Georisorse - CNR, Pisa, Italy

granalli@earthsci.carleton.ca

A thermo-rheological model of the post-emplacement history of the Late Miocene Monte Capanne pluton and surrounding rocks is presented. The principal aim of the work is to obtain temperature-time constraints to estimate the rheology, size and evolution of the tectonic aureole. The Monte Capanne pluton has a monzogranite composition and an overall concentric shell structure. The outer shell shows a remarkable porphyritic texture due to the presence of K-feldspar megacrysts up to 20 cm in length. The pluton is well suited for thermo-rheological modelling, owing to the good field exposures, the large amount of available data, and the simple geometry. In map view it has a broadly circular outline and in 3D the shape can be approximated by a flat truncated cone with a thickness of ~ 3 km and a diameter ranging from 8-9 km (top) to 11 km (bottom). The source region of the Monte Capanne monzogranite was mainly the hot lower continental crust with minor contributions from the mantle. This situation allows considering the Elba continental crust as a closed system.

The thermal model is based on 2D geometry with radial symmetry around the vertical axis of the truncated cone, assumes pure conduction, and takes into account the latent heat of crystallization. The numerical solution is obtained using the Stella© code implementing the 4th order Runge-Kutta algorithm. Starting from the results of previous studies, we assume that pluton growth was achieved incrementally by under-accretion (from top downward) of multiple magma pulses in a short time interval ($\sim 10,000$ yr) and that emplacement at ~ 6 km depth took place while the Elba continental crust was affected by rapid unroofing due to extensional tectonics and erosion.

Results of the thermal model, presented on contoured radial and vertical sections at different times, on T-t scatter diagrams and as P-T paths for various locations in and around the pluton, reproduce satisfactorily the geometry and peak temperatures of the narrow contact aureole. The incremental growth of the pluton in the short time interval of 10 kyr does not result in a pulsating change of temperature on T-t plots, apart from zones very close to the contact. At distances from 100 to 250 m from the contact, thermal peaks between 500 and 600 °C in the aureole are reached in a time range of 10-40 kyr. Within 250 m from the contact, the temperature is maintained above 450 °C for 100 to 200 kyr, depending on the structural level. The presence of residual melt inside the pluton is predicted for ~ 200 kyr from emplacement. Afterwards, the thermal perturbation related to magma emplacement in the upper crust is progressively attenuated and becomes negligible after 1 Myr.

The modelled thermal evolution provides the framework for a preliminary estimation of the time-dependent rheological behaviour of the crystallizing pluton and surrounding rocks. The temperature-induced transient softening of the latter has potential consequences on the structural history of Elba Island, and offers some insights on the post-emplacement tectonic evolution of similar plutons emplaced in the upper crust.

Folded Variscan duplex in the Herrera Unit of the Iberian Range

Pablo Calvín, A.M. Casas

*Departamento de Ciencias de la Tierra, Universidad de Zaragoza, Spain
Pablo_calvin@hotmail.com*

The Herrera Unit is located in the central sector of the Aragonese Branch of the Iberian Range (Zaragoza-Teruel). This unit constitutes the NE limb of a kilometric scale Variscan major anticline, with a predominant NW-SE to NNW-SSE trend and NE vergence. In its SW limb the Badules Unit crops out. The Datos thrust, a first order structure, superimposes the Badules unit onto the Herrera unit. Cambrian to Ordovician materials compose its hanging-wall, whereas Upper Cambrian to Devonian materials appear in its foot-wall. In this footwall a 4000 m thick series, essentially detrital, with Silurian and Devonian carbonate levels can be seen. South of the studied zone, the Lower Cambrian (Badules Unit) thrust over the Devonian (Herrera Unit).

The Herrera Unit is characterized by thin-skinned tectonics involving two detachment levels: the lower one is constituted by Precambrian shales, and the upper one by Upper Silurian shales. The Silurian level, more than 1000 m thick, separates two structural levels with different deformation styles.

In the Cambrian to Silurian materials that form the lowermost structural level, a duplex system characterizes the general structure, related to both detachment levels, with intermediate minor detachments. The East dipping thrusts could probably be the result of folded and tilted thrusts with eastward vergence, according to the general Variscan trend. This folding could be associated either with the late stages of the Datos thrust or represent the front of an antiformal stack. This structural configuration could also be explained by a backthrust system. A well developed cleavage (S1) affects the whole Cambrian to Silurian series and a second cleavage (S2) locally appears. The main system is an axial plane cleavage related to NNW-SSE folds, with a dominant East vergence and SSE plunge. Slaty cleavage appears in pelitic levels and fracture cleavage in sandstones.

Depending on the spatial relation with the thrust, the upper detachment level shows different deformation styles attending to cleavage type and fold geometry. In general, NNW-SSE crenulation cleavage appears due to a previous sedimentary planar anisotropy. The Devonian, upper structural level is characterized by E-verging, NNW-SSE thrust and fault-related folds with axial plane cleavage.

Fault-related pseudotachylytes in the Barcelona Plain (NE Spain): Evidence of paleoseismic activity

Irene Cantarero, Gemma Alías, Anna Travé, Vinyet Baqués

*Departament de Geoquímica, Petrologia i Prospecció Geològica, Universitat de Barcelona, Spain
I_cantarero@ub.edu*

Although the seismicity of the Catalan Coastal Ranges is broadly known, the presence of pseudotachylytes had not been described before in this region. These fault rocks are considered to be the only unambiguous indicator of seismic slip and therefore they give information about the processes that take place in the source of an earthquake.

The Barcelona Plain, one of the grabens formed during the Neogene extension in the Catalan Coastal Ranges, is characterised by a structure in blocks produced by segmented fault systems. Specifically, pseudotachylytes develop in the Enric segment (Badalona). The fault zone has a NE-SW striking and dips 55° SE. The footwall is constituted by a late hercynian granodiorite and the hangingwall by Triassic materials (middle and upper Muschelkalk facies). Deformation is localised in the footwall and generates breccias, cataclasites and pseudotachylytes.

Pseudotachylytes are related to cataclasites and calcite veins with crack-seal structure. They form very thin fault veins parallel to the weak foliation in cataclasites and, in the calcite veins, they develop at the contact between the calcite and the wall rock and also in the discontinuities between successive crack-seals. Locally, injection veins are also observed. Although it seems that deformation began with the formation of the cataclasites, followed with crack-seal formation and continued with pseudotachylyte formation, conflicting crosscutting relationships between these structures indicates their coeval origin. The synchronicity between pseudotachylytes, cataclasite formation and calcite precipitation indicates that frictional melting and pseudotachylyte formation occurred in a hydrated fault zone.

These three deformation structures follow three main orientations coherent with the geometry of Riedel shears, S (cataclasite foliation), P, R and Y and indicate a normal displacement of the main fault. P has a slip direction between 234 and 170 and a low dip (20°) and R is the conjugate system. P is defined by cataclasites, crack-seal veins and pseudotachylytes, R only by crack-seal veins and Y by crack-seal veins and pseudotachylytes.

Fault veins have a width up to 125 µm and have sharp and straight walls. Under transmitted light, pseudotachylytes display yellow-brownish colours whereas under polarised light they show a dark aphanitic matrix that contain subrounded clasts of quartz and feldspar. The study under the optical microscope points to the devitrification of the matrix. Previously to pseudotachylyte formation, the original paragenesis of the granodiorite (quartz, orthose, plagioclase and biotite) was altered. Biotites disappeared and chlorite and iron oxides precipitation took place in randomly oriented fractures. This fact conditioned the composition of the melt.

The recompilation of historical earthquakes in the vicinity of this fault segment between 1410 and 2009 show a maximum magnitude between 3 and 4. However, major earthquakes can occurred since the frictional melt is produced in earthquakes of at least 4.5 magnitude.

A hydromechanical model for lower crustal fluid flow

James Connolly

*Institute for Geochemistry and Petrology, Swiss Federal Institute of Technology, ETH Zürich
james.connolly@erdw.ethz.ch*

Regional metamorphism occurs in an ambiguous rheological regime between the brittle upper crust and ductile sub-lithospheric mantle. This ambiguous position has allowed two schools of thought to develop concerning the nature of metamorphic fluid flow. The classical school holds that metamorphic rocks are inviscid and that any fluid generated by devolatilization is squeezed out of rocks as rapidly as it is produced. According to this school permeability is a dynamic property and fluid flow is upward. In contrast the modern school, selectively uses concepts from upper crustal hydrology that presume implicitly, if not explicitly, that rocks are rigid or, at most, brittle. For the modern school, the details of crustal permeability determine fluid flow and as these details are poorly known almost anything is possible. Reality, to the extent that it is reflected by inferences from field studies, offers some support to both schools. In particular, evidence of significant lateral and channelized fluid flow are consistent with flow in rigid media, while evidence for short (104 - 105 y) grain-scale fluid rock interaction during much longer metamorphic events, suggests that reaction-generated grain-scale permeability is sealed rapidly by compaction; a phenomenon that is also essential to prevent extensive retrograde metamorphism. These observations provide a compelling argument for recognizing in conceptual models for metamorphic fluid flow that rocks are neither inviscid nor rigid, but have finite strength. The surprising result of this strength is that the steady state solutions for fluid flow in porous compacting media require that fluid expulsion is channeled into waves of fluid-filled porosity. The waves develop on a characteristic length scale known as the viscous compaction length, δ , that is also the length scale for lateral fluid flow. In this context, porosity refers to any hydraulically connected void space present on spatial scales $\ll \delta$. Thus, porosity waves may be manifest in nature as domains of fluid-filled fractures. Because δ is proportional to rock viscosity and consequently decreases exponentially with increasing temperature, the flow regimes of the classical and modern schools are recovered at high and low temperatures.

Linking fabric and texture development to three-dimensional strain evolution in deformed quartzite and granitoid conglomerate clasts

Dyanna M. Czeck¹, Eric Horsman², Terra N. D. Anderson¹, Basil Tikoff³

¹ Department of Geosciences, University of Wisconsin-Milwaukee, USA

² Department of Geological Sciences, East Carolina University, USA

³ Department of Geoscience, University of Wisconsin-Madison, USA
dyanna@uwm.edu

Strain gradients in deformed conglomerates provide an opportunity to relate quantified strain to fabric and texture development. Using deformed conglomerates, we studied quartzite and granitoid clasts in detail to analyze their differing small-scale structural responses to increasing bulk finite strain.

We analyzed the Seine Metaconglomerates, which are found along the Wabigoon-Quetico Subprovince boundary within North America's Superior Province and were deformed and metamorphosed to greenschist facies during granite-greenstone terrane development approximately 2.7 Ga. The metaconglomerates have a matrix of immature sand-clay size particles eroded from intermediate-mafic volcanic rocks and contain volcanic clasts with a range of felsic-mafic compositions, granitoid clasts largely of tonalitic composition, and quartzite clasts. Numerous structural features are consistent with a kinematic model of ductile transpression with oblique extrusion directions: subvertical foliations, a variety of lineation orientations, asymmetric dextral shear sense indicators on the subhorizontal plane, and primarily oblate strain shapes.

Strain analysis was conducted independently for each clast type using Rf/ϕ analysis, bootstrapping statistics, and a least squares solution method to combine two-dimensional ellipses into three-dimensional ellipsoids. Octahedral shear strain (ϵ_s) varied nonsystematically through the field area from 0.21-1.04 for granitoid clasts, 0.64-1.78 for felsic volcanic clasts, and 0.67-2.40 for mafic volcanic clasts. Unfortunately, quartzite clasts are too rare to produce quantitative strain measurements, but qualitative observations suggest that their strain magnitudes approximate strains measured for granitoid clasts. Based on these measurements and observations, within a given outcrop, clast competence hierarchy is quartzite > granite > felsic volcanic > mafic volcanic.

Quartzite clast microstructures including undulose extinction and subgrain formation suggest deformation was accommodated primarily by dislocation creep. In granitoid clasts, quartz microstructures including undulose extinction and subgrain formation suggest it dominantly deformed by dislocation creep, whereas feldspar deformation was accommodated primarily by fracturing with minor dislocation creep. Within the granitoid clasts, the mica shape fabric intensifies and grain linkages increase during deformation through a combination of intracrystalline strain and dissolution-precipitation processes.

Quartz lattice preferred orientation (LPO) differed between granitoid and quartzite clasts at comparable strains. In the granitoid clasts, the quartz LPO intensity increases at low to moderate strain with progressive deformation, but plateaus at moderate to high strain. However, the quartz LPO intensity in quartzite clasts does not vary systematically with increasing strain, suggesting the existence in some cases of a strong primary LPO that is not obliterated by the observed strains. The feldspar LPO in the granitoid clasts increases at low to moderate strain with progressive deformation, but stabilizes at moderate to high strain. These results suggest the quartzite clasts, which likely were derived from a variety of sources, had acquired primary LPO textures prior to their incorporation into the conglomerate. The granitoid clasts have no evidence of primary LPO textures, and the observed LPO is likely a result of the metaconglomerate deformation. The relatively high strains accumulated in the deformation were not sufficient to reset the primary LPO present in the quartzite clasts.

Structural, petrographic and isotopic study of the Ziga peridotites (Western Pyrenees-Eastern Cantabrian Mountains): geodynamic implications

Irene DeFelipe¹, David Pedreira¹, Javier A. Pulgar¹, Eneko Iriarte², Miren Mendia³

¹ Departamento de Geología, Universidad de Oviedo, Oviedo, Spain.

² Institució Milà i Fontanals, Consejo Superior de Investigaciones Científicas, Barcelona, Spain.

*³ Departamento de Mineralogía y Petrología, Universidad del País Vasco – E.H.U., Bilbao, Spain.
defelipe@geol.uniovi.es*

Cretaceous extension during the opening of the Bay of Biscay resulted in the creation of deep basins between Iberia and Eurasia, with exhumation of mantle rocks cropping out at present in several localities along the Pyrenean-Cantabrian belt. The westernmost outcrop of peridotites is located near the village of Ziga, close to the Paleozoic Basque Massifs. It has been traditionally associated with the Leiza fault, a major E-W oriented structure to the south of the Cinco Villas massif, along which other slices of high-grade metamorphic rocks crop out. In this work we present a detailed structural, petrographic, geochemical and isotopic study of the Ziga peridotites with the aim of gaining insight into the emplacement mechanism of these mantle rocks.

The detailed mapping reveals that the Ziga peridotites crop out as allochthonous blocks, together with fragments of acid and basic granulites, marbles, and basic subvolcanic rocks, embedded in a clayey matrix defining a highly deformed band just in the junction between the Leiza fault and another major structure, the Pamplona Fault, which shows a NNE-SSW orientation marked by the alignment of Keuper-facies salt diapirs. The deformation band has the same orientation of the Pamplona fault, and the mineralogical composition of the matrix is typical of the Keuper salt diapirs (kaolinite-montmorillonite, gypsum, muscovite, minerals of the chlorite group and quartz).

The ultramafic rocks are highly serpentinized lherzolites, consisting of primary crystals of olivine, pyroxene and minor amphibole; secondary antigorite and chrysotile as serpentine varieties; and calcite and minor aragonite as carbonate phases. Calcite occurs mainly as veins with crystals growing perpendicular to the fracture wall, crosscutting the primary rock fabric, but it can also appear filling holes as idiomorphic crystals or as a fine grain size mesh.

To check if these calcite veins can be related to low-temperature alteration of serpentinized ultramafic rocks in contact with seawater (ie. ophealcites), we analysed their carbon and oxygen isotopic signature. For comparison, we also analysed some ophealcites from the Col d'Urdach peridotites (French Western Pyrenees) whose submarine exposure is well documented by the presence of peridotite fragments in Albian-Cenomanian sedimentary breccias. Preliminary results (referred to PDB) show values of $\delta^{18}\text{O} = -4.74$ to -4.47 ‰ and $\delta^{13}\text{C} = -12.39$ to -9.79 ‰ for the Ziga veins, and $\delta^{18}\text{O} = -10.12$ to -4.04 ‰ and $\delta^{13}\text{C} = -5.24$ to $+1.30$ ‰ for the Col d'Urdach ophealcites. Three of four values of $\delta^{13}\text{C}$ for the Col d'Urdach samples lie in the range -0.15 to $+1.30$ ‰, typical of marine carbonates (in agreement with the field observations) and only one sample seems to reflect the presence of mantle-derived carbon ($\delta^{13}\text{C} = -5.24$ ‰). The very negative values of $\delta^{13}\text{C}$ found in Ziga, on the contrary, may require not only the presence of mantle-derived hydrothermal CO_2 , but perhaps also oxidation of methane released during serpentinization, pointing out to a deeper process. $\delta^{18}\text{O}$ results allow calculating the temperatures at which the veins formed. A preliminary estimation, considering the different inferred fluid compositions, seems to reflect similar values in the range 40 – 70°C .

Tectonic controls on local drainage evolution in semi-arid active foreland basin margins (Betics, southern Spain)

Manuel Díaz-Azpiroz¹, Miguel Rodríguez-Rodríguez¹, Fernando Pérez-Valera², Francisco Moral¹, Inmaculada Expósito¹

1 Departamento de Sistemas Físicos, Químicos y Naturales, Universidad Pablo de Olavide, Seville, Spain

2 Departamento de Geología, Universidad de Jaén, Spain

mdiazp@upo.es

Understanding how recent deformation events produced at active mountain fronts in convergent orogens control the resulting drainage systems is crucial to the knowledge of the influence that tectonics plays in earth surface processes and landscape evolution. Regarding hydro-morphology, foreland basins and neighbouring fold-and-thrust belts are characterised by drainage systems that, at a large scale, display an axial pattern in relation to the main relief uplift developed at the orogenic active front. Despite this general scheme, at a smaller scale and especially in areas with a gentle slope, it is expected that certain structures could generate local uplifts resulting in the formation of drainage subsystems that differ from the regional one. In this study, a local drainage system developed, under semi-arid climatic conditions, within the External Betic Zone (Cordoba Subbetics, Southern Spain) is analysed from hydrological, geomorphological and structural points of view.

The main hydrology and surface features of the study area are: (1) the regional drainage network is northwardly directed to the main foreland Guadalquivir basin. (2) Local drainage in the study area divides into two subsystems: the western part is a closed basin that hosts at the northernmost edge the El Conde playa-lake, which is deepest at its northeastern corner; whereas the eastern subsystem is open and the surface runoff is directed to the south-east (i.e., opposite to the regional drainage direction). (3) Hydro-morphological parameters of the El Conde playa-lake suggest that surface and subsurface runoff coming from the watershed is the main water input to the water body and that water loss by infiltration is negligible. (4) The drainage system shows incisions of several metres into its own alluvial quaternary deposits and/or into the rock basement, which occasionally result in the occurrence of hanging terraces.

Preliminary geological mapping of the studied area shows the presence of evaporites, shales and carbonates of Triassic age, together with marls of Cretaceous and Miocene age. Also, structural and geomorphological observations suggest that: (1) the contact between the Triassic and the Cretaceous formations is marked by a kilometre-scale deformation reverse zone with a rough NE-SW strike. (2) This zone produced a clay, gypsum-rich matrix tectonic *mélange*, including more rigid and competent blocks (gypsum, dolostones, limestones and sandstones) of different ages (Triassic to Miocene) and sizes (from centimetre- to hectometre-scale), that appear oriented (NE-SW and N-S) and boudinaged. (3) At the deformation front, some of these hectometre-scale, gypsum and dolostones blocks define a discontinuous NE-SW uplift ridge, which acts as a natural barrier to the northwardly directed runoff favoring, in a semi-arid climatic context, the formation of a playa-lake and also the southeastward directed drainage of the eastern part of the study area. (4) Moreover, some single water courses appear to be controlled by the orientation of the deformation front. (5) Drainage system incision could be produced by the uplift related to the reverse kinematics of the deformation zone and, locally, to metre-scale mud diapirs that have been observed breaking through quaternary alluvial deposits.

Testing transpression models in brittle shear zones compared with ductile deformation. A standardized procedure with contrasting approaches

Manuel Díaz-Azpiroz¹, Leticia Barcos¹, Carlos Fernández², Dyanna Czeck³

¹ Departamento de Sistemas Físicos, Químicos y Naturales, Universidad Pablo de Olavide, Seville, Spain

² Departamento de Geodinámica y Paleontología, Universidad de Huelva, Spain

³ Department of Geosciences, University of Wisconsin, USA

mdiaazp@upo.es

Comparison between complex transpression models and data from natural shear zones proves to be difficult, especially because multiple variables can combine in different ways to produce comparable results. To avoid this ambiguity, Fernández et al. (this volume) propose a standardized and objective procedure to constrain three main transpression parameters: obliquity (ϕ), kinematic vorticity number (W_k) and extrusion obliquity (u). This protocol was first defined to be applied to ductile shear zones where finite strain markers are common. However, transpression has been identified also in relation to upper crustal deformation zones where strain is often highly partitioned into several structural domains and discrete structures (folds and faults). Therefore, the protocol is adapted to these brittle shear zones, comprising six successive steps.

Step 1: In ductile shear zones, transpression obliquity (ϕ) is deduced from the location of the simple shear component, as the intersection between the shear zone boundary (SZB) and the vorticity normal section (VNS). The section of maximum fabric asymmetry recognised in the field represents a good proxy for the VNS. In brittle shear zones, the simple shear direction can be directly obtained from slickenlines in representative discrete faults. Steps 2-3: Comparison between the orientations of the finite strain ellipsoids (FSE) deduced from ductile shear zones and that resulting from the model is rather simple using lineations and/or the orientation of the X-axis of the FSE. This task is quite more difficult in brittle deformation, where a single FSE imposed on a shear zone produces discrete structures that accommodate different components of the bulk strain. Fault population data, fold analysis and, if it is an active zone, earthquake focal solutions can be combined to obtain the FSE for each set of structures, which must be further evaluated to estimate the bulk FSE. Steps 4-5: Ellipticity (R_s), orientation (angle θ) of the strain ellipse at the VNS and the shape of the FSE obtained by the model are compared with similar data deduced for the shear zone to determine a range of W_k values. These data can be determined in ductile shear zones if reliable strain markers are present. In brittle shear zones, the shape of the FSE can be approximated via balanced cross-sections, by the shortening across the shear zone (Z-axis), the upward extrusion (X-axis) and the lateral extension (Y-axis). In steeply dipping shear zones, the maximum horizontal stretching axis would correspond to the Y-axis, and it can be deduced from the orientation of fold-axes and/or the maximum horizontal extension accommodated by normal faults. Step 6: This step applies only for recent or active oblique convergent tectonic limits (as many brittle transpression zones are) where information about plate velocities is normally available. The geometric relationship between plate velocity vectors and the orientation of the deformed zone permits to further constrain ϕ and W_k . Currently, this protocol is being applied to a brittle transpressional shear zone developed in relation to a recess zone within the fold-and-thrust belt of the Betic Cordillera (southern Spain).

The effect of hydrothermally generated talc on fault strength

Amy C. Ellis, Ernest H. Rutter, Katharine H. Brodie, Julian Mecklenburgh

School of Earth, Atmospheric and Environmental Sciences, University of Manchester, U.K.

Amy.Ellis@postgrad.manchester.ac.uk

Previous research indicates that hydrothermal reactions generating phyllosilicate minerals, such as talc, may have significant impact upon strength and deformation behaviour in tectonically active settings such as oceanic spreading centres and large crustal fault zones. The interaction of the growth of frictionally weak hydrothermal minerals with progressive displacement on fault zones presents one possible explanation for anomalous weakness observed on low angle normal faults and the San Andreas Fault.

Experiments have been run to determine the frictional strength of hydrothermally generated talc grown as both a thin layer and interconnected network within serpentine gouge to compare with the frictional strength of a talc gouge. All experiments were run under hydrothermal conditions at 450°C and effective pressures ranging from 50-150 MPa. Talc was generated by the reaction: lizardite + quartz \rightarrow talc + H₂O, which has also been investigated as part of this study. This was followed by constant displacement rate deformation at approximately 4.6×10^{-4} mm s⁻¹, to determine the friction coefficient of each sample. Stress relaxation data was collected at the end of these experiments to assess low strain rate and creep behaviour.

Results for friction coefficients of talc and serpentine are comparable with previous studies, however a strength contrast is indicated between talc gouge material, hydrothermally generated talc veneers and talc grown within a pre-existing damage or gouge zone. Hydrothermally generated material is generally stronger at elevated effective pressures than gouge material. Talc grown within a serpentine gouge layer also behaves differently from a simple layer of talc.

Stress relaxation data indicates similar stress exponents for both talc and serpentine in solid and gouge forms, however talc grown within a serpentine gouge behaves differently, relaxing at an accelerated rate. This is attributed to the continued reaction of the gouge material to talc during the relaxation, permitting the material to deform at higher strain rates than would be expected, possibly via a creep mechanism. Microstructural study is underway to elucidate the active deformation mechanisms and in order to relate the generation of talc via reaction to the shear strain rate observed.

These results are significant for the description and explanation of fault zone weakening mechanisms and underline the importance of syntectonic reactions and the contribution made by incongruent pressure solution creep.

The Ronda peridotites: an example of dual emplacement sense of the subcontinental mantle (Betic Cordilleras)

José Julián Esteban, Julia Cuevas, Jose María Tubía

*Departamento de Geodinámica, Facultad de Ciencia y Tecnología, Universidad del País Vasco, apto. 644, 48080 Bilbao (Spain)
jj.esteban@ehu.es*

The Ronda peridotites (Betic Cordilleras) are exposed in three main massifs -Sierra Bermeja, Sierra Alpujata and Carratraca- and stand out by two main reasons: 1) they correspond to the largest outcrops of subcontinental mantle on Earth and, 2) the three metamorphic facies (garnet, spinel and plagioclase peridotites) defined by O'Hara (1975) for the ultramafic rocks coexist in them. In addition, the presence of graphite pseudomorphs after octahedral diamonds in garnet-bearing pyroxenites attests to peridotite extraction from depths of more than 180 km (Davies et al., 1993).

The Ronda peridotites are tectonically sandwiched between metamorphic sheets, grouped in the Alpujarride complex. The deformation related to the thrusting of the Ronda peridotites over these continental sheets is concentrated in ductile shear zones developed at high-temperature. Anhydrous mylonitic peridotites from the basal shear zone of Sierra Alpujata yield ca. 1100 °C and 1.4 GPa for the dynamic recrystallization event. The hot emplacement of the peridotites was related to partial melting in the underlying continental crust as evidenced by the existence of dynamothermal aureoles of felsic composition below the Sierra Alpujata and the Sierra Bermeja massifs. Both aureoles are composed of migmatites, granitoids and quartzo-feldspathic mylonites and show marked strain-gradients toward the contact with the overlying peridotites but differ significantly, as they are related to different pressure conditions and kinematics.

These dynamothermal aureoles can be considered as low viscosity shear zones formed at temperatures high enough, > 650 °C, to promote partial melting. Our results suggest that under such temperatures, ductile shear zones can experience a dramatic narrowing instead of the broadening postulated for increasing depth (and temperature) frequently.

At Sierra Alpujata, the aureole evolved from an initial eclogitic stage ($P > 1.7$ GPa; $T = 790$ °C) to low-pressure ($P < 300$ MPa) and high-temperature ($T \sim 600$ °C) conditions. This aureole reaches a maximum thickness of some 700 meters and is concordant with the overlying mylonitic peridotites. Minor "B-type" olivine intracrystalline slip, with the olivine a-axis perpendicular to the flow direction, was activated in this shear zone. Shear sense indicators from the mylonitic peridotites and quartzo-feldspathic mylonites indicate a consistent top-to-the ENE shearing.

The dynamothermal aureole below the Sierra Bermeja massif shows a thickness of 100 to 200 meters. The presence of chessboard microstructures and basal sub-grain boundaries in quartz reveals the activation of c-slip in quartz which points to high-temperature conditions during the deformation. Kinematic criteria indicate a top-to-the NNW shearing. This kinematic shift is linked to a remarkable pressure fall, as the Sierra Bermeja aureole was formed at similar temperatures but under much less severe pressure conditions, ca. 610 MPa, than the Sierra Alpujata aureole.

Different tectonic scenarios have been proposed to account for the extraction of these ultramafic massifs: extensional core complex, transpressional settings or back-arc settings. We consider that the field and structural constraints presented here do not support those models that merely propose an intense stretching of the lithosphere to explain the exhumation of the Ronda peridotites.

REFERENCES

- Davies, G.R., Nixon, P.H., Pearson, D.G., Obata, M. (1993). *Geology* 21, 471–474.
O'Hara, M.J., 1967. In: *Ultramafic and related rocks*: New York, John Wiley and Sons, 393–401.

Primary coarse-granular lherzolites: the oldest lithospheric mantle in the Ronda peridotites (southern Spain)

José Julián Esteban, Jose María Tubía, Julia Cuevas, Néstor Vegas

Departamento de Geodinámica, Facultad de Ciencia y Tecnología, Universidad del País Vasco, apto. 644, 48080 Bilbao (Spain)
jj.esteban@ehu.es

The Ronda peridotites, in the Internal Zone of the Betic Cordilleras (southern Spain), consist of several tectonic mantle slabs sandwiched within the continental crust. The relative chronology of the main textural domains of the Ronda peridotites is considered as one of the main tools for deciphering their structural and tectonic evolution. Early structural studies from the Ronda peridotites (Darot, 1973; Lundeen, 1976) and its counterpart in the Rifian belt of Morocco, the Beni Bousera peridotites (Reuber et al., 1982), agree in that the dominant porphyroclastic peridotites evolved from granular peridotites. The petrological zoning of the Sierra Bermeja massif (Obata, 1980) is in line with this view, as the spinel peridotites, of porphyroclastic type, come from older (and of higher pressure) coarse-grained garnet peridotites. The identification of a recrystallization front with granular peridotites along the contact between the spinel peridotites and the plagioclase peridotites (van der Wal and Vissers, 1996) has led most researchers to reject the previous textural sequence. According to the overwhelming current interpretation, the granular peridotites are considered as a secondary facies formed by static annealing of spinel peridotites of porphyroclastic type due to percolation of mantle melts through them.

The Carratraca massif, one of the less studied massifs of the Ronda peridotites due to its advanced serpentinization, consists from top to bottom of mylonitic garnet harzburgites and porphyroclastic spinel lherzolites. The spinel lherzolites show medium-grained porphyroclastic microstructures and a well-developed foliation. Lens-shaped bodies of foliation-free and coarse-grained granular lherzolites (globular enstatite > 1 cm) are found within the porphyroclastic peridotites frequently. It is worth noting that these granular lherzolites contain protogranular textures originated from garnet. The upper mylonitic harzburgites contain large elongate porphyroclasts of enstatite (5-10 cm long; $X/Z \geq 25$) strongly stretched by intracrystalline slip, which argues for the existence of coarse-grained granular peridotites as protoliths of the garnet mylonitic peridotites when the slip is restored.

All these structural overprinting relationships support that: 1) the oldest lithospheric mantle domain in the Ronda peridotites is formed by granular lherzolites originated within the stability field of the garnet peridotites and 2) the coarse-grained peridotites were present everywhere in the spinel and garnet metamorphic zones, before the formation of the porphyroclastic and mylonitic peridotites. Therefore, the current interpretation has to be improved, since it incorrectly proposes that the spinel porphyroclastic peridotites are the oldest domain and the granular peridotites represent a younger annealed domain. We consider that both interpretations can be reconciled by the incorporation of primary garnet equigranular peridotites as the oldest domain of the Ronda peridotites, which in turn lead us to propose the following structural evolution for the lithospheric mantle portion of the Ronda peridotites: primary granular peridotites → porphyroclastic peridotites → mylonitic peridotites → secondary granular peridotites.

REFERENCES

- Darot, M. (1973). Thèse 3^{ème} Cycle, Univ. Nantes, 120 p.
Lundeen, M.T. (1976). Ph.D. Thesis, Univ. Harvard, 177 p.
Obata, M. (1980). *Journal of Petrology*, 21, 533-572.
Reuber, I., Michard, A., Chalouan, A., Juteau, T. and Jermoumi, B. (1982). *Tectonophysics*, 82, 231-251.
van der Wal, D. and Vissers, R.L.M (1996). *Journal of Petrology*, 37, 23-43.

Comparing microstructures from natural and experimental deformation in a high-porosity bioclast limestone

Ulrike Exner¹, Patrick Baud²

¹ Department of Geodynamics and Sedimentology, University of Vienna, Austria

² Ecole et Observatoire des Sciences de la Terre Strasbourg, France

ulrike.exner@univie.ac.at

In porous granular sediments, strain localizes as tabular zones of grain rotation and fracturing, instead of forming discrete slip surfaces as in low porosity rocks. The mechanical properties of this mode of failure has been extensively studied in siliciclastic rocks, both in natural examples as well as in laboratory experiments. Depending on the porosity and differential stress, the material fails under dilatancy or compaction combined with a variable degree of shear. In contrast, only few field or experimental studies have been conducted so far on high porosity carbonates. Especially the occurrence and degree of mechanical twinning in addition to grain crushing, as well as the localisation of strain in compaction bands are still in discussion (Baud et al., 2009).

In this study, we performed triaxial deformation experiments on a Miocene carbonate grainstone (Leithakalk) from the Eisenstadt-Sopron Basin, Austria. Previous investigations on naturally occurring deformation bands in this rock (Rath et al., 2011) suggest an early phase of normal faulting, which results in the formation compactive shear bands essentially before the cementation of the rock. Ellipsoidal bioclasts show a reorientation within the deformation bands, which cannot be attributed to cataclastic features. Only after the generation of a blocky calcite cement coating the pore space, cataclastic deformation occurred adjacent to the pre-existing deformation bands.

As expected, the experimentally generated microstructures in the cemented, high porosity (28%) rock strongly deviate from structures observed in the natural deformation bands. Fracturing occurs (1) along uncemented grain contacts between bioclasts, or (2) within bioclasts with high microporosity. Within the bioclasts, microfractures show a characteristic roughness, reflecting the biogenic carbonate aggregates, whereas the cement crystals display planar fractures. Fragmentation of bioclasts occurs in broad zones of cataclastic grain size reduction. At low axial strain (< 1%), no localisation in distinct zones (neither perpendicular nor inclined to the shortening direction) can be observed.

Further experiments to higher axial strains and additional microstructural analysis of the crystal-plastic deformation of the calcite cement are expected to contribute to a comprehensive micromechanical model for high porosity carbonates.

REFERENCES

- Baud et al., 2009: Compaction and Failure in High Porosity Carbonates: Mechanical Data and Microstructural Observations. *Pure Appl. Geophys.* 166, 869–898
- Rath et al., 2011: Diagenetic control of deformation mechanisms in deformation bands in a carbonate grainstone. *AAPG Bulletin* 95

Rheomorphic shear zones in granites: examples from the Central Iberian Zone, Variscan Iberian Massif

Carlos Fernández¹, Guillermo Corretgé², Antonio Castro³

¹ Departamento de Geodinámica y Paleontología, Universidad de Huelva, Spain

² Departamento de Geología, Universidad de Oviedo, Spain

*³ Departamento de Geología, Universidad de Huelva, Spain
fcarlos@uhu.es*

The rheological behaviour of near-solidus magmatic systems is a matter of current debate. The term rheomorphism was introduced in the geological literature by Backlund (1937) to describe complex processes of transformation of rocks into a totally or partially fluid mass. The study of discrete shear zones appearing in Variscan granitic rocks of Puente del Congosto, Zarza de Montánchez and Cabeza de Araya (Central Iberian Zone) suggests the existence of phenomena of rheomorphism and fluidification of near-solidus magmatic systems. These particular structures are characterized by the following features: (1) they form tabular bodies, several cm width and tens of m length, with the appearance of intruding dykes, (2) previous markers (schlieren, granite contacts, magmatic foliation) show dilational to shear displacements ranging from several cm to a few dm, (3) the contacts with the host granites are sharp at the crystal scale, (4) there is no signs of plastic deformation in the crystals, and (5) the whole chemical composition is identical to that of the host granites. The only appreciable difference is in the texture, these tabular zones having for instance a bimodal crystal size distribution, while the host granite is essentially unimodal. These equivocal dyke-like structures, that we call rheomorphic shear zones, are very common in the studied plutonic complexes and they appear in two different situations: (1) associated with intra-magmatic shear zones (dilational or not), and (2) associated with purely dilatant structures in the near-solid magma. Both cases have been studied denoting that they show similar textural relationships and, consequently, may have a similar origin. A relevant observation is the common presence of clusters of several crystals in the host granitoid. These polycrystalline aggregates are often formed by plagioclase and biotite. We have used image analysis of electronic pictures (BSE, Z-contrast) to determine the crystal size distributions of the main phases (Qtz, Bt, Pl, Kfs) in both the dilatant and purely shear zones as well as in the host granitoid. The used techniques include measurement of crystal size distributions (CSD), directional statistics, shape analysis and the Fry method. The results indicate that these rheomorphic structures may be the result of fluidification by disruption of polycrystalline aggregates in a near solidus magmatic system. Magma from these rheomorphised zones may intrude as dykes into sinks tectonically generated in the more viscous, near-solid, host magma. These results may have implications for the understanding of intrusion and auto-intrusion of granitic magmas in the continental crust, particularly for the late processes related to the deformation of the already emplaced and nearly crystallised magma chamber or pluton.

REFERENCES

Backlund, H.G. (1937): Die Umgrenzung der Svekofenniden. Bull. Geol. Inst. Univ. Uppsala, 27: 219-269.

Protocol for testing the model of oblique transpression with oblique extrusion in ductile shear zones

Carlos Fernández¹, Manuel Díaz-Azpiroz², Dyanna Czeck³

1 Departamento de Geodinámica y Paleontología, Universidad de Huelva, Spain

2 Departamento de Sistemas Físicos, Químicos y Naturales, Universidad Pablo de Olavide, Spain

3 Department of Geosciences, University of Wisconsin, USA

fcarlos@uhu.es

Recognizing triclinic deformation paths in ductile shear zones is a difficult task. Objective criteria are needed first to identify such types of complex deformation regimes in nature, and second to constrain the values of the controlling parameters, mainly the obliquity angle (ϕ), the kinematic vorticity number (W_k), and the extrusion obliquity angle (u). In this work, a standardized procedure has been designed that exploits the method outlined by Czeck and Hudleston (2003), completed to take into account the complexities added by a localized nonvertical extrusion direction according to the theoretical model of Fernández and Díaz-Azpiroz (2009). The protocol includes considering information in five steps, which must be sequentially applied to a given natural case. Step 1: orientation of the vorticity-normal section, as a first approximation it can be considered as the plane with the maximum fabric asymmetry, thereby providing the range of possible ϕ values. Step 2: Orientation of the mineral and stretching lineations. Step 3: Orientation of the X-axis of the measured finite strain ellipsoid. Information from steps 2 and 3 are compared with the λ_1 patterns deduced from the theoretical model to obtain a range of W_k values. Step 4: Ellipticity (R_s) and orientation (angle θ) of the strain ellipse at the vorticity-normal section that is compared with theoretical R_s vs. θ curves to determine again a range of W_k values. The results of steps 2 to 4 are checked together and only those compatible combinations of ϕ , W_k and u values are considered. Often, more than one such combination yields compatible solutions. Step 5: To further constrain the result, the measured finite strain ellipsoid is plotted on a Flinn diagram against the theoretical shapes derived from the distinct combinations obtained from steps 2 to 4.

The procedure has been successfully applied to a few examples of natural ductile shear zones with differing amounts of available information. Cases with complete information –kinematic data, fabric orientation, determination of finite strain ellipsoid- like the Wabigoon-Quetico boundary, allow an acceptable testing of the model, yielding valuable and constrained knowledge on the vorticity and obliquity of the shear zone. In shear zones with more limited data –kinematic data, fabric orientation- as is the Southern Iberian shear zone, only two or three of the described steps can be applied, and broad ranges of W_k and u values are obtained. Even in this last case, the protocol guarantees an objective procedure to identify the triclinic nature of the shear zone, providing some helpful estimates of vorticity and obliquity.

REFERENCES

- Czeck, D., Hudleston, P.J. (2003). Testing models for obliquely plunging lineations in transpression: A natural example and theoretical discussion. *Journal of Structural Geology* 25, 959-982.
- Fernández, C., Díaz Azpiroz, M. (2009). Triclinic transpression zones with inclined extrusion. *Journal of Structural Geology* 31, 1255-1269.

Constraining deformation events within the HP-HT units of the NW Iberia Variscan belt

Francisco J. Fernández¹, P. Castiñeiras², J. Gómez-Barreiro³, P. Valverde-Vaquero⁴

¹ Departamento de Geología, Facultad de Geología, Universidad de Oviedo, 33005 Oviedo, Spain

² Departamento de Petrología y Geoquímica-Instituto de Geología Económica (CSIC), Universidad Complutense de Madrid, 28040 Madrid, Spain

³ Departamento de Geología, Universidad de Salamanca, 37008 Salamanca, Spain

*⁴ Área de laboratorios, Instituto Geológico y Minero de España, c/ La Calera 1, 28760 Tres Cantos, Spain
brojos@geol.uniovi.es*

We have analyzed the structural relationships between an overturned sequence formed by eclogite, migmatitic gneisses and metasedimentary gneisses at the eastern border of the Cabo Ortegal Complex (NW Spain). The high-quality outcrops along the Masanteo peninsula allow to unambiguously restore the pseudo-3D structure of the complex. This analysis was done using two general, detailed, cross-sections parallel to a 2,800 meter long shoreline trending N130E, and several perpendicular partial sections.

The main structure is a Variscan, southeast-facing antiform, overprinted by Alpine faults, which refolds a recumbent syncline and the associated high-grade structures. In detail, the structure has been restored using the main mylonitic foliation as the structural reference. This fabric is a gneissic foliation defined by a compositional layering, migmatitic or metasedimentary in origin, heterogeneously deformed by a mylonitic process. The main foliation was initially developed under eclogite- HP-granulite conditions and re-equilibrated under amphibolite facies conditions. During this process, lozenge-shaped structures were developed, that preserve less deformed rocks surrounded by anastomosing high-strain zones. These anastomosing shear zones locally pass to planar shear zones. Mylonitic high-strain zones usually present intrafoliar folds, rotated porphyroblasts, and small inclusions of mafic and calc-silicate rocks. Blocks of eclogite within the migmatitic gneisses occur frequently along the minor ductile detachments next to the major detachment at the boundary between the migmatitic gneisses and the massive eclogite unit of Cabo Ortegal. The detachment contains minor structures, such as asymmetric rootless folds, rotated porphyroblasts, sheath folds, complex mantled structures and oblique shear bands (C and C' types) developed in a phyllonite matrix. According to the quartz and omphacite fabric patterns, almost all shear sense criteria related to this tectonic event indicate flattening kinematics.

Towards the eastern boundary of the Masanteo peninsula, metasedimentary gneisses with a lower grade of metamorphism crop out. They are partially migmatized at the bottom of the sequence, where they are interlayered with garnet amphibolites and glandular orthogneisses. Unlike the underlying migmatitic gneisses, they lack eclogite blocks. These metasedimentary gneisses are also intensely deformed by the main foliation. Rootless sheath folds and asymmetric folds point to a wide range of directions, southeast to northeast, accordingly to the kinematics of the main foliation in the underlying migmatitic gneisses. Subsequently the main foliation is folded into a large recumbent syncline. This recumbent syncline was tectonically superposed over the underlying migmatitic gneisses and eclogite along a shear zone. This shear zone is interpreted as an extensional ductile detachment with a top to the northwest shear sense, contrary to the general thrusts kinematics (Marcos et al., 2002). The final present day anticlinorium structure is the result of a latter refolding of these high/medium-grade structures by upright folds with an axial-planar, crenulation cleavage developed under greenschist facies conditions.

The trace element geochemistry in zircon from an eclogite block within the migmatitic gneisses clearly indicates that eclogitization occurred during an Eo-Variscan episode that took place between ca. 403 Ma and 382 Ma, with a peak at ca. 390 Ma (U-Pb method using the SHRIMP-RG technique). Four zircon analyses aimed at oscillatory and soccer-ball zoning yielded 400 Ma, 8 zircon analyses in

oscillatory, sector and soccer-ball zoning yielded 390 Ma, and 5 analyses within sector and oscillatory zoning yielded 384 Ma). Preliminary U-Pb CA-ID-TIMS dating of felsic dioritic dykes indicate the presence of abundant Proterozoic inherited zircon, which has resulted in discordant points. So the age of intrusion remains unresolved. The least discordant data provides a lower intercept age of 475.02 ± 0.87 Ma in monazite, which should be considered as a maximum age for the intrusion of the dykes. The dykes are located within the migmatitic gneisses, between the eclogite unit and the extensional detachment. These felsic dykes are folded and overprinted by the main foliation that transects the folds, and they are sheared by the extensional detachment. We consider that they might have formed during assembling of the ultramafic units at the base of the HP-HT unit sequence.

Taking into account the geochronological data and the structural relationships between the exceptionally well-exposed lithological sequence of the Masanteo peninsula (Cabo Ortegal complex), we propose a tectonic evolution of the HT-HP units of the allochthonous complexes defined by the following main events:

D1 event: The imbrication of ultramafic, mafic and quartz-feldspathic gneisses that form the HP-HT units. This event took place before the intrusion of the dioritic dykes (i.e., after 460 Ma and before D2 deformation).

D2 event: Development of the main foliation under a general flattening regime. Tectonic thinning of the pile started during eclogitization at ca. 390 Ma and finished under amphibolite facies conditions. Rutile U-Pb cooling ages of ca. 382 Ma (Valverde-Vaquero and Fernández, 1996; Santos Zalduegui, 1995) constrain the exhumation rate for the eclogite, migmatitic and metasedimentary gneisses at ca. 4.9 mmy^{-1} , 3.9 mmy^{-1} and 1.4 mmy^{-1} , respectively.

D3 event: Development of large recumbent folds and related brittle-ductile thrusts during the emplacement of the HP-HT units (D3a) and the subsequent development of syn-collisional extensional detachments toward the opposite sense (D3b). D3 is well correlated with the D1 event in the footwall to the suture of the Variscan belt of northwest Spain (Pérez-Estaún et al., 1991), because the basal thrust of the Cabo Ortegal complex is cutting D1-folds developed in the footwall (Marcos and Farias, 1999).

D4 event: Horizontal shortening, with development of upright folds with an associated crenulation cleavage under greenschist facies conditions. This event created the large synclinoriums where the allochthonous complexes are preserved, as well as minor antiforms. This event can be correlated with the D3 event in the footwall to the suture.

D5 event: Alpine faults have mainly anticlockwise strike slip and normal components.

3D geologic model for the Cenozoic evolution of the Tuz Gölü Basin (Central Anatolia, Turkey) based on seismo-structural analysis

David Fernández-Blanco, Giovanni Bertotti

*Tectonic-Structural Geology Department, Vrije Universiteit, Amsterdam The Netherlands
d.fernandezblanco@vu.nl*

The Neogene Central Anatolian Orogenic Plateau (CAP), being relatively small when compared with its larger counterparts, as the Andean Altiplano or the Tibet, represents a great opportunity to study spatiotemporal mechanisms of plateau formation, which is the main goal of the ESF-sponsored Vertical Anatolian Movement Project (VAMP). This morphotectonic feature has a semi-arid and roughly-flat highland flanked by the Pontide and Tauride mountain ranges in the north and south, respectively. The Tuz Gölü Basin (TGB), located in the central sector of the CAP, is the biggest of several Neogene plateau-interior basins at an elevation of about 1.2-1.5 km. This elongated NW-SE trending depression is more than 100 km long and filled with a Neogene sedimentary sequence, several km thick. East and west boundaries of TGB are considered to be fault-terminations, with dextrally oblique normal movement that actively contributed to basin formation.

Seven seismic reflection lines located at the eastern and southern boundaries of the present Tuz Gölü Lake were conceded by Turkish Petroleum Corporation (TPAO) and interpreted in this contribution. Analysis of these seismic profiles shows that the Tuz Gölü Fault is not a basin-forming fault but only one of the several SW-dipping NW–SE-striking normal faults involving basement, as two analogous faults appear in the west, constituting the Sultanhanı Fault Zone. These two fault systems might have formed the eastern side of a NE-SW extensional zone that accommodated more than 5 km of Paleogene rocks and a minimum of 3.5 km of post-Paleogene sediments at its deepest points. An hitherto undiscovered compressional event sometime in the Late Miocene disrupted the extensional tectonics, accommodating in some areas horizontal displacements almost 2 orders of magnitude bigger than those accounted by the extensional phases. As our data shows, the present-day TGB is tectonically active and dominated by extension, possible continuation of the younger extensional tectonism that superseded the earlier phase of contraction and erosion. This is clearly revealed in the seismic lines by extensional inversion of contractional features, i.e. a roll-over anticline with a harpoon structure.

A regional 3D geologic model for the tectonic evolution of the Tuz Gölü Basin and surrounding areas is here proposed on the base of the study of sediment geometries and tilted blocks in depth-converted profiles in combination with the analysis of subsidence curves, isopach maps and a restored cross-section.

Structural Zonation at Río Atuel Valley, Mendoza province, Argentina

Natalia Fortunatti

1 Departamento de Geología, Universidad Nacional del Sur. San Juan 670 (8000), Bahía Blanca, Argentina.

2 INGEOSUR-CONICET

nfortuna@uns.edu.ar

Southern Central Andes at Mendoza province, Argentina, is characterized by a Permian-Triassic igneous basement that is unconformably overlaid by a thick Late Triassic-Tertiary sedimentary sequence. Both the basement and the sedimentary cover have been affected by Andean orogeny during Miocene to Pleistocene times and as a result, a thick-skinned fold-and-thrust belt was constructed. In the Atuel river valley area structural style was defined based on detailed surface survey and constrained with wells and seismic data.

Construction and interpretation of three East-West regional structural sections with 60 km length each one at Atuel river valley, between arroyo Malo and arroyo Las Ramaditas streams, were carried out. Through analysis of the age of deformed stratigraphic units simultaneously with regional tectonic framework, four sectors were defined:

- . Sector 1, outlined by Late Triassic-Early Jurassic sedimentary rocks known as Cuyo Group, partially exposed on the left hand of Atuel river valley. It is characterized by foreland-vergent thrust systems and hinterland-vergent thrust systems (or backthrust systems) defining triangle zones.

- . Sector 2, where Early Jurassic-Cretaceous sedimentary rocks outcrops located on the right hand of the Atuel river valley showed similar tectonic features than to Sector 1.

- . Sector 3, to the East of sectors 1 and 2, known as Loma del Medio High, where mesozoic sedimentary beds were surveyed with an increasing East-dipping attitude that leads to overturned strata. This stripe bounds sectors 1 and 4 on the left hand of the Atuel river valley.

- . Finally, Sector 4 involving Cenozoic synorogenic deposits (volcanic and volcanoclastic rocks). This sequence registered foreland basin infill and crops out at the Cuchilla de la Tristeza range, a broad asymmetric regional sinclorium.

All the defined sectors have a strong relationship with subsurface basement configuration, interpreted as a foreland-vergent tectonic wedges train. A regional basement structure with geometry of tectonic wedge can generate significant amount of structural relief, and explains major structural elements surveying at Sectors 1, 2 and 4 in the Atuel river valley (fault-related folds). Also, this seems to be a reasonable configuration in order to transfer shortening to sedimentary cover through several detachments, located at basement-sedimentary cover boundary, pelites or evaporites, where thrust system propagates in staircase trajectory related to ramps and flats. Sector 3 acquires its configuration by passive folding due to the development of successive basement tectonic wedges. Hinterland-vergent thrust systems or backthrusts located at Sector 1 and 2 were related to internal deformation of the hanging wall frontal basement wedge configuration. All tectonic structures surveyed at the sedimentary cover and interpreted for the basement are generated in piggyback fashion.

A structural zonation can be defined for Atuel river valley, southern Malargüe Thrust and Fold belt, in order to explain tectonic and geological features analyzed. The recognition of structural zonation for Central Andes in Argentina can be considered as an original tool for exploration of hydrocarbons and mineralized fields, applied to subsurface basement geometry interpretation.

Malargüe Fold and thrust Belt: new kinematic model at the Atuel river Valley, Mendoza province, Argentina

Natalia Fortunatti

1 Departamento de Geología, Universidad Nacional del Sur. San Juan 670 (8000), Bahía Blanca, Argentina.

2 INGEOSUR-CONICET

nfortuna@uns.edu.ar

Mountain building at Atuel river Valley (southern Central Andes, Mendoza province, Argentina) is related to Tertiary Andean orogeny that faulted and folded Permian-Early Triassic igneous basement (Choiyoi Group) and Late Triassic-Tertiary sedimentary cover, giving place to a thick-skinned fold-and-thrust belt known as Malargüe fold-and-thrust belt. At this particular site of Andean Mountain ranges, opposite-vergent thrust systems and triangle zones represents a common feature at deformed sedimentary cover, necessarily related to unexposed basement geometry.

Although this portion of Andean Mountain ranges has been interpreted as a hybrid between thick and thin-skinned styles, kinematic models involving tectonic inversion of normal faults and subsequent foreland deformation must be reviewed. Our study supports that west dipping, low angle reverse fault-tectonic wedge is the most reasonable geometry in order to achieve structural configuration surveyed for the Atuel river area. According to this, unexposed igneous basement is affected by a thrust that generates a leading horse, which propagates through a favorable horizon (basement-sedimentary cover interface, pelites or evaporites). As the fold grows in amplitude it can effectively transfers shortening to the stratigraphic upper levels due to foreland-vergent thrust systems while passively folds previous tectonic structures, related to an ancient foreland-vergent basement deformed block.

Several tectonic wedges are interpreted in the Atuel river Valley. Subsurface basement configuration was inferred with similar characteristics that outcropping Choiyoi Group shows at Bardas Blancas location (southern Central Andes, Mendoza province): basement-driven tectonic wedges show internal deformation related to thrusting towards the hinterland (backthrusts), which sprouts out in 'piggyback' fashion at the leading branch line of the hangingwall ramp.

Foreland-vergent low angle faults related to a wedge's leading horse internally deformed by a system of imbricate backthrusts is a valid kinematic model in order to achieve structural configuration surveyed at Atuel river valley, northern Malargüe fold-and-thrust belt, Mendoza province, Argentina. This kinematic model admits its application for successful resolution of tectonic problems at Central Andes in general and Malargüe fold-and-thrust belt in particular, offering an alternative solution relating opposite vergent low-angle faulting affecting sedimentary cover and basement.

A possible structural zonation at North Patagonian Andes thick skinned fold-and- thrust belt (41°-42° S), Argentina

Natalia Fortunatti

1 Departamento de Geología, Universidad Nacional del Sur. San Juan 670 (8000), Bahía Blanca, Argentina.

2 INGEOSUR-CONICET

nfortuna@uns.edu.ar

North Patagonian Andes between 41° and 42°S and 72° and 70°W, at Southwestern Argentina (Río Negro and Chubut provinces) has been object of an important research related to an heterogeneous stratigraphic record from Upper Paleozoic to Quaternary and its tectonic evolution.

Paleozoic medium-to-high-grade metamorphic and igneous rocks basement conforms the oldest unit of this area, affected by Gondwanian Orogeny (Upper Paleozoic). Mesozoic rocks are represented by a sedimentary sequence with tectonic-associated restricted outcrops, and the cordilleran Patagonian Batholith, a Jurassic-Cretaceous intrusive body with important regional significance. Cenozoic record is vinculated with Tertiary sedimentary and volcanic rocks of continental Ñirihuau Basin. Andean Orogeny affected all the described units, conforming a tectonic framework characterized from West to East by a thick-skinned fold-and-thrust belt, a foreland basin and the foreland.

Broadly analysis of major tectonic features in this portion of Central Andes shows a western side where pre-Tertiary units are affected by a foreland-vergent thrust system and a hinterland-vergent thrust system (backthrust system) with development of triangle zones (like El Bolsón Triangle zone), and an eastern side in which pre-mesozoic and Tertiary units again are faulted and folded by an oppositite-vergent thrust system. Tectonic major structures have a North-South to North-Southeast trend and are locally covered by Neogene volcanism.

This pattern is compared with regional tectonic framework defined by Atuel river Valley, at northern Malargüe fold and thrust belt, Mendoza province, also related with Andean orogeny. In this location for Central Andes a structural zonation was defined, in which each identified sector has a characteristic vergence of thrust system, related to subsurface basement geometry. Also, all the tectonics structures interpreted for the basement and surveyed at the sedimentary cover generates in piggyback fashion, conforming a kinematic model where basement driven tectonic wedges transfer shortening to sedimentary cover through low-angle faulting.

Regional tectonic framework analysis of North Patagonian Andes, in addition with new field and subsurface data, allow us to inferred that a structural zonation is developed related to basement geometry. Three regional structural cross-sections are in processed, in order to establish similarities or differences with Malargüe Thrust and Fold belt tectonic features, and prove the viability of a structural zonation generation associated with basement kinematic model.

The neutral lines in buckle folds

Marcel Frehner

*Geological Institute, ETH Zurich, Switzerland
marcel.frehner@erdw.ethz.ch*

The neutral line in a fold is a fundamental concept in structural geology. It divides areas of outer-arc extension from areas of inner-arc compression. Indeed, in natural folds so-called outer-arc-extension structures (e.g., layer-perpendicular extensional fractures) and inner-arc-compression structures (e.g., stylolites, enhanced foliation) can be observed.

In the past, folds have often been constructed kinematically from a given neutral line geometry using the tangential longitudinal strain pattern, for which a continuous neutral line along the fold has to be assumed.

In this study, a mechanical finite element model is used to numerically buckle single-layer folds with Newtonian and power-law viscous rheology. Two neutral lines can be distinguished, the incremental neutral line (zero-contour line of the layer-parallel strain rate) and the finite neutral line (zero-contour line of the finite layer-parallel strain), whereas the former develops first and migrates through the layer from the outer arc towards the inner arc ahead of the latter. Both neutral lines are discontinuous along the folded layer and terminate either at the top interface of the layer (for small shortening values) or at the bottom interface (later during the folding history). For a decreasing viscosity ratio between the folding layer and the surrounding matrix and for decreasing initial amplitude, the neutral lines develop later during the folding history and, for some cases, no neutral line develops. These results are similar for Newtonian and power-law viscous rheology.

The results of the mechanical single-layer simulations are discussed in light of interpreting fold-related structures, such as outer-arc-extension structures and inner-arc-compression structures. Particularly the initiation of brittle structures (e.g., outer-arc extensional fractures or inner-arc thrusts) depends on the momentary stress state within the folding layer. Therefore, such structures may be attributed to the incremental neutral line. On the other hand, enhanced foliation or stylolites in the inner-arc compressional field may be related to the finite strain and therefore to the dynamics of the finite neutral line.

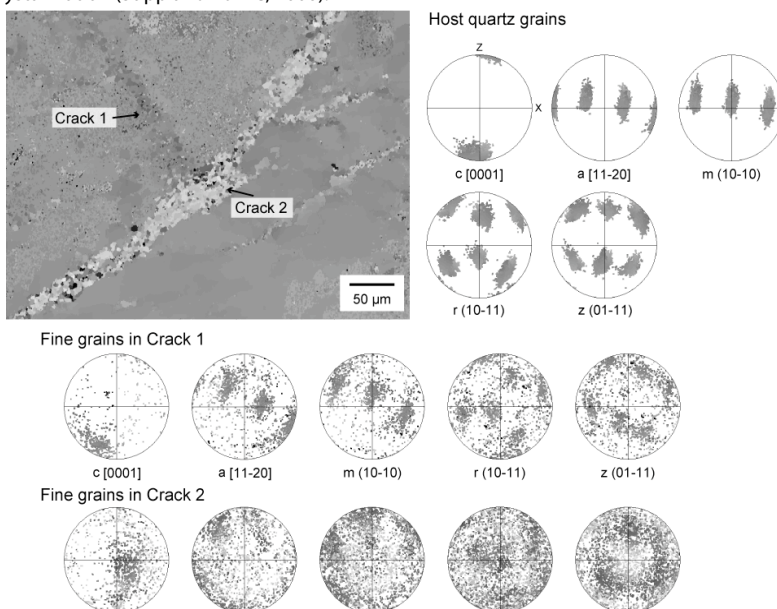
Developments of Dauphiné twins, fractures, and fine grains in a quartz grain under brittle-plastic transition zone

Jun-ichi Fukuda

Department of Earth Sciences, Tohoku University, Japan
j Fukuda@dges.es.tohoku.ac.jp

Under conditions where plastic deformation of rocks is dominated, changes in the mechanisms of dynamic recrystallization and the slip systems of quartz are indicative of deformation conditions of rocks: Dynamic recrystallization of quartz is changed from bulging, subgrain rotation to grain boundary migration, which depend on temperature, confining pressure, stress, water contents, etc. The slip systems of dislocation creep also have variations of basal<a>, rhomb<a>, prism<a> and prism[c]. Under brittle-plastic transition, changes in textures would be expected by changes in the above parameters. However, previous studies for natural samples are mostly for conditions where plastic deformation of rock is dominated, and studies for brittle-plastic transition zone are limited.

In this study, I focus on deformation of quartz and developments of textures under brittle-plastic transition zone, using granitoids in the Auke shear zone, Japan. The Auke shear zone gives relatively pure information of brittle-plastic transition, since its deformation was not strongly overprinted by former plastic deformations. Cataclasites are widely yielded and mylonites are partly seen in the investigated area. Also, pseudotachylytes develop from micrometre to several millimetre scales. Under an optical microscope, up to 3 mm large quartz grains are fractured and less than 10 μm fine quartz grains sometimes develop at fractures. Grain-size-reduction processes of quartz under brittle-plastic transition zone have been argued to be due to dynamic recrystallization, developments of cracks, and dissolution-precipitation, as investigated from experimental approaches (e.g., Vernooij et al., 2006). Also, developments of Dauphiné twins may promote dynamic recrystallization (Stipp and Kunze, 2008).



An area which includes a host large quartz grain and fine quartz grains less than 10 μm at fractures, was mapped by using electron backscatter diffraction (the IPF figure below). The host quartz grain shows a relationship of Dauphiné twins at a fracture (Crack 2), which can be seen in its crystallographic orientations of r (10-11) and z (01-11) planes. The crystallographic orientations of fine quartz grains are controlled by those of the host quartz grain at a fractured area (Crack 1), but show a distinct slip system of prism $\langle a \rangle$ at another area (Crack 2). In this presentation, I will also show changes of misorientation angles of host and fine quartz grains and angle/axis distribution. Then, I will especially discuss the grain-size-reduction processes of quartz related to dynamic recrystallization, crack developments, dissolution-precipitation and Dauphiné twins, and their dominations.

REFERENCES

- Stipp and Kunze, 2008. *Tectonophysics* 448 (1-4), 77-97.
Vernooij et al. 2006. *Journal of Structural Geology* 28, 1292-1306.

A discrete characterization of the porosity evolution during gypsum dehydration based on an in-situ microtomographic heating experiment

Florian Fusseis¹, Christoph Schrank¹, Jie Liu¹, Benjamin Garnault¹, Klaus Regenauer-Lieb^{1,2}, Ali Karrech², **Sergio Llana-Fúnez**³

¹ WA Geothermal Centre of Excellence, School of Earth & Environment, The University of Western Australia, Crawley, Australia

² CSIRO Earth Science and Resource Engineering, Kensington, Australia

³ Departamento de Geología, Universidad de Oviedo, Oviedo, Spain

florianfusseis@me.com

The dehydration of gypsum to bassanite at elevated temperatures is considered a model reaction for devolatilization in metamorphic environments, and experimental data are widely used to infer the mechanical effects of the reaction on a tectonic scale [1-3]. It is well known that the reaction will only proceed where the released water can be drained [4, 5]. Therefore the evolution of permeable porosity is critical for the process. Yet, due to experimental constraints, it was so far impossible to reveal the evolution of pore space during the experiment. Consequently, large-scale continuum-mechanic interpretations are poorly supported by discrete observations. This contribution presents the first four-dimensional dataset of the time-dependent evolution of porosity during gypsum dehydration collected in a Synchrotron X-ray tomograph.

We conducted a heating experiment at sector 2BM at the Advanced Photon Source (USA) to dehydrate an unconfined 2.3 mm diameter cylinder of Volterra Gypsum in situ. We used a purpose-built X-ray transparent furnace to heat the sample to 388 K for a total of 310 minutes and to acquire a three-dimensional time-series tomography dataset comprising nine time steps. The voxel size of 2.2 μm^3 proved sufficient to pinpoint reaction initiation and the organization of drainage architecture in space and time. We observed that dehydration commences across a narrow front, which propagates from the margins to the center of the sample in more than four hours. The advance of this front can be fitted with a square root function, implying that the initiation of the reaction in the sample can be described as a linear diffusion process.

Novel parallelized computer codes (6, 7) allow quantifying the geometry of the porosity and the drainage architecture from the very large tomographic datasets (20483 voxels) in unprecedented detail. We could determine the position, volume, shape and orientation of each resolvable pore and follow these properties over the duration of the experiment. We found that the pore-size distribution follows a power law with a nearly constant exponent at all times, and we use this relationship to infer the sub-resolution (i.e. sub-micron) porosity in the sample. Larger pores are generally more anisotropic and flake-shaped, often occurring en-echelon. With ongoing dehydration, pores coalesce and develop a preferred orientation with their longest axes sub-parallel to the long axis of the sample.

A percolation analysis of the time-series dataset confirmed the vertical axis as the most likely drainage pathway. This analysis also yielded a percolation threshold of 5% porosity and revealed that the porosity distribution homogenized within an hour after the reaction initiation front has passed. The analysis identified a volume of 4003 voxels ($\sim 8803 \mu\text{m}$) as representative elementary volume (REV) in the reacting domain.

REFERENCES

- 1 Heard and Rubey 1966, GSA Bull. 77, 741-760.
- 2 Ko et al 1997, JGR 102, B1, 825-839.
- 3 Stretton 1997, PhD thesis, Manchester
- 4 Llana-Fúnez et al in review, EPSL
- 5 Miller et al 2003, Tectonophysics 370, 241-251.
- 6 Liu et al 2009, G-cubed 10, 5.
- 7 Liu et al 2010, Advances in Geosciences 20

Structural modelling: from satellite interpretation to cross-section construction

Jorge Ginés, Mike Oehlers

*Fugro NPA Limited; Edenbridge, Kent, United Kingdom
j.gines@fugro-npa.com*

Geological modelling and cross-section construction are very important tools for presenting and communicating information about geological structures in any tectonic context. Satellite imagery and other remotely sensed data provide a reliable and accurate source of information, which acquires an added value in politically compromised countries or geographically challenging areas, where other sources of data may be scarce or non-existent.

The application of traditional photogeological methods to different satellite and remotely sensed data types is a well established procedure, applicable to geological mapping for mineral and hydrocarbon exploration. Optical and radar images are regularly used in the production of geological maps at regional and detailed scales and are typically combined with digital elevation models (DEM). DEM's provide quantitative structural information (e.g. precise dip and strike measurements and estimation of real unit thickness) which eventually is used in predicting the subsurface structure by construction of geological models and cross-sections

In this poster, we present a workflow that describes the systematic extraction of structural data in digital environments, and integrates them with the assistance of computer programs in order to construct precise 2D cross-section and 2.5D/3D geological models. Some examples and results are also shown from selected types of data, tectonic regimes and geographic locations, as well as a comparison between quantitative field and remotely sensed data.

Fluid-controlled dynamic opening and closing of fracture permeability at the crustal scale: a new numerical approach

Enrique Gómez-Rivas¹, Paul D. Bons¹, Philipp Blum², Daniel Koehn³, Thomas Wagner⁴

¹ Department of Geosciences, Eberhard Karls University Tübingen, Germany

² Institute for Applied Geosciences (AGW), Karlsruhe Institute of Technology, Germany

³ School of Geographical and Earth Sciences, University of Glasgow, UK

⁴ Institute for Geochemistry and Petrology, ETH Zürich, Switzerland

enrique.gomez-rivas@uni-tuebingen.de

There is strong evidence of non-constant fluid flow in the Earth's crust, for example huge veins and breccias that formed from fluids that were considerably hotter than their host rocks or veins formed by the crack-seal mechanism. In such systems flow is localised both in space (along fractures and high permeability beds) and time (i.e. in the form of fluid pulses). Most of the current conceptual and numerical fluid flow models are based on an assumed static system (e.g. a system with predefined constant permeability and boundary conditions). However, a direct consequence of localised flow in time is that the distribution of permeability and boundary conditions in the model are not static. The dynamics of fluid flow can only be understood when the reaction of the system to flow as a consequence of sudden opening and closing of hydrofractures is also incorporated in models (Miller & Nur, 2000; Bons & van Milligen, 2001). Conceptually, cyclic successions of the following processes take place in a dynamic flow system: (1) build-up of fluid pressure, (2) onset or re-activation of hydrofractures due to fluid overpressure, (3) fracture propagation, (4) fluid flow, (5) drop of fluid pressure and, finally (6) closing of fractures due to the precipitation of minerals from the fluids and/or to ductile flow of host rocks.

We have developed a new numerical scheme to simulate the rich dynamics of a self-organised system using the modelling platform Elle. Cyclic successions of the following processes are utilized to model large-scale dynamic fluid flow: (1) arrival of fluid batches from sources that increase fluid pressure, (2) dynamic update of fracture permeability due to fracture opening/closing depending on fluid pressure distributions, fluid/rock properties and external stresses and (3) Darcian fluid flow, which determines the pressure and hydraulic head distributions in the system.

With this numerical scheme we have developed series of simulations to understand the principles that operate in dynamic fluid flow systems. The results indicate that fluid flow at the crustal scale can operate as a self-organized system, in which fluid overpressure cause fast release of fluid batches that are rapidly transported upwards to regain equilibrium. There is a transition between two end-members depending on the closing rate of fractures due to mineral precipitation and flow of rocks. If the closing rate is very low, fractures do not close quickly and the system evolves towards a steady-state. This is the preferred scenario for extensive alterations in which fluids have enough time to invade host rocks from faults. On the contrary, if fractures can close quickly a self-organised pulsating regime can emerge. Such cases can account for localised alterations, like crack-seal veins or hydrothermal mineral deposits along fault zones.

REFERENCES

- Bons, P.D. and van Milligen, B.P. 2001. A new experiment to model self-organized critical transport and accumulation of melt and hydrocarbons from their source rocks. *Geology*, 29, 919-922.
- Miller, S.A. and Nur, A. 2000. Permeability as a toggle switch in fluid-controlled crustal processes. *Earth and Planetary Science Letters*, 183, 133-146.

Structural evolution of the Jabal Akhdar dome (Oman): insights from fracture and vein networks

Enrique Gómez-Rivas¹, Paul D. Bons¹, Daniel Koehn², Janos L. Urai³, Max Arndt³, Simon Virgo³, Ben Laurich³, Conny Zeeb¹, Lena Stark¹, Philipp Blum⁴

¹ Department of Geosciences, Eberhard Karls University Tübingen, Germany

² School of Geographical and Earth Sciences, University of Glasgow, UK

³ Structural Geology, Tectonics and Geomechanics, RWTH Aachen University, Germany

⁴ Institute for Applied Geosciences (AGW), Karlsruhe Institute of Technology, Germany
enrique.gomez-rivas@uni-tuebingen.de

Fault, fracture and vein networks in the Mesozoic succession of the Oman Mountains are a clear example of dynamic fracture opening and sealing in a highly complex thermal, hydraulic and mechanical system. Some of these rocks host large oil reserves in neighbouring areas and, therefore, unravelling the evolution of outcropping fracture networks in Jabal Akhdar is important to understand fracture distributions in the oil fields.

We carried out a detailed structural survey of faults, fractures and veins in the exhumed Jurassic and Cretaceous carbonates of the Jabal Akhdar dome to identify the tectonic events that took place in the area. We collected over 600 3D measurements of fracture and vein orientations, opening directions, striations on exposed planes, stretched crystals and fibres in veins, as well as stylolite orientations. Overprinting relationships between these structures enabled us to better constrain the tectonic evolution of the area and to recognize the main tectonic events at the sub-seismic scale.

Building on previous studies (e.g. Holland et al., 2009) our new data show that strike-slip deformation played an important role in the area, more than hitherto recognised. The strike-slip movement is recorded by subhorizontal striations on oblique slip and dip-slip normal faults and by abundant sets of conjugate en-echelon veins and steep stylolites. Many of these veins are confined to particular layers, which indicates the importance of mechanical stratigraphy in the limestone succession. In particular the E-W to NW-SE compression that can be observed throughout the Jabal Akhdar dome is compatible with segmented fault patterns observed in seismic profiles throughout oil fields in Oman and Abu Dhabi (e.g. Filbrandt, 2006). This compression event can be correlated with an oblique collision related to the the passage of the Indian continent along the Arabian Plate during the Santonian-Campanian. Strike-slip deformation in this area postdates top-to-South and top-to-NE layer-parallel shearing related to the obduction of the Hawasina and Samail ophiolite nappes, as well as seismic and sub-seismic scale networks of dip-slip to oblique-slip faults.

Our survey indicates that the Jabal Akhdar dome, with its unique outcrop conditions, forms an excellent natural laboratory to investigate the evolution of small to medium scale structures that cannot be observed in seismic studies.

REFERENCES

- Filbrandt, J.B., Al-Dhabab, S., Al-Habasy, A., Harris, K., Keating, J., Al-Mahruqi, S., Ozkaya, S.I., Richard, P.D. and Robertson, T. 2006. Kinematic interpretation and structural evolution of North Oman, Block 6, since the Late Cretaceous and implications for timing of hydrocarbon migration into Cretaceous reservoirs. *GeoArabia*, 11, 97-140.
- Holland, M., Urai, J. L., Muecher, P. and Willemse, E. J. M. 2009. Evolution of fractures in a highly dynamic, thermal, hydraulic, and mechanical system - (I) Field observations in Mesozoic Carbonates, Jabal Shams, Oman Mountains. *GeoArabia*, 14, 57-110.

Flow stress history of a detachment system: combining recrystallized grain size, quartz CPO and deformation lamellae, Raft River (NW Utah)

Raphaël Gottardi, Christian Teyssier, Nick Seaton

*Department of Geology and Geophysics, University of Minnesota, Minneapolis, MN, USA
gotta004@umn.edu*

The Raft River metamorphic core complex in NW Utah is bounded to the east by a Miocene detachment that localized in a Proterozoic quartzite which rests unconformably on Archean crystalline basement. Well-exposed sections of this mineralogically simple (quartz + white mica) quartzite allow detailed sampling of the approximately 100 m thick quartzite mylonite. The quartzite uniformly displays regime 2 dislocation creep microstructures and shows extensive recrystallization by subgrain rotation and grain boundary migration. Quartz crystallographic preferred orientation measured using EBSD (15 samples) shows symmetrical patterns indicative of dominant pure shear.

The recrystallized grain size concentrates narrowly between 20 and 30 microns in all samples, yielding flow stress estimates ranging from 47 to 62 MPa (from paleopiezometry, Stipp and Tullis, 2003). Oxygen stable isotope thermometry of quartz-muscovite pairs reveals a large thermal variation (more than 100°C, with from 485°C at the base to 345°C at the top) across the 100 m section (Gottardi et al., in press). Application of a quartz dislocation creep flow law (Paterson and Luan, 1990) yields strain rate estimates ranging from 10-12 to 5×10^{-14} s⁻¹. The microstructures and the lack of recovery processes reflect relatively high flow stress during detachment tectonics, irrespective of temperature, which suggests that temperature and strain rate self-adjusted to maintain near-constant stress conditions.

Throughout the detachment shear zone, deformation lamellae affect 20 to 50% of quartz grains in the mylonite. In thin sections cut perpendicular to foliation and parallel to lineation, deformation lamellae are oriented between 30 and 50° with respect to foliation and are nearly perpendicular to basal shear bands. Lamellae are straight to slightly curved, show up well in cathodoluminescence imaging, and appear to have formed late relative to quartz deformation-recrystallization. The spacing of deformation lamellae, which was evaluated using a universal stage, is a calibrated paleopiezometer (Koch and Christie, 1981). Lamellar average spacing was determined on photomicrographs by the intercept method on at least 20 grains per sample. The average spacing between lamellae ranges between 6.9 ± 1.4 and 11.3 ± 3.1 µm from the top to the base of the section. Using the Koch and Christie (1981) paleopiezometer we estimate the differential flow stress ranging from 53 to 20 MPa from the top to the base of the section. These values are slightly smaller and overlap with stress estimates based on recrystallized grain size. Using the same flow law parameters and a temperature estimate of 400°C, we obtain a strain rate ranging from 10-13 s⁻¹ (top of section) to 7×10^{-15} s⁻¹ (bottom of section).

Experiments on ionic material, metals and alloys show that deformation lamellae only develop at high differential stress and suggest that they form at the transition between dislocation creep ($1 < n < 5$) and exponential creep ($n > 5$) when the stress exceeds a critical stress value. Our study shows that microstructures and deformation lamellae developed during coaxial flow, under the same range of flow stress, while strain rate and temperature self-adjusted to maintain near-constant stress conditions. Deformation lamellae may have developed in the dislocation creep regime, when critical conditions were reached, probably during the latest cooling stages of the evolution of the shear zone when the system dropped below a critical temperature. Lamellae-based flow stresses increase upward, consistent with the final stages of ductile deformation in the detachment shear zone, as deformation migrated into the brittle detachment that overlies the mylonitic section.

Porphyroclast rotation in polycrystalline aggregates: a numerical approach

Albert Grier¹, Paul D. Bons², Mark W. Jessell³, Ricardo Lebensohn⁴, Lynn Evans⁵, Enrique Gómez-Rivas²

¹ Departament de Geologia, Universitat Autònoma de Barcelona, Spain

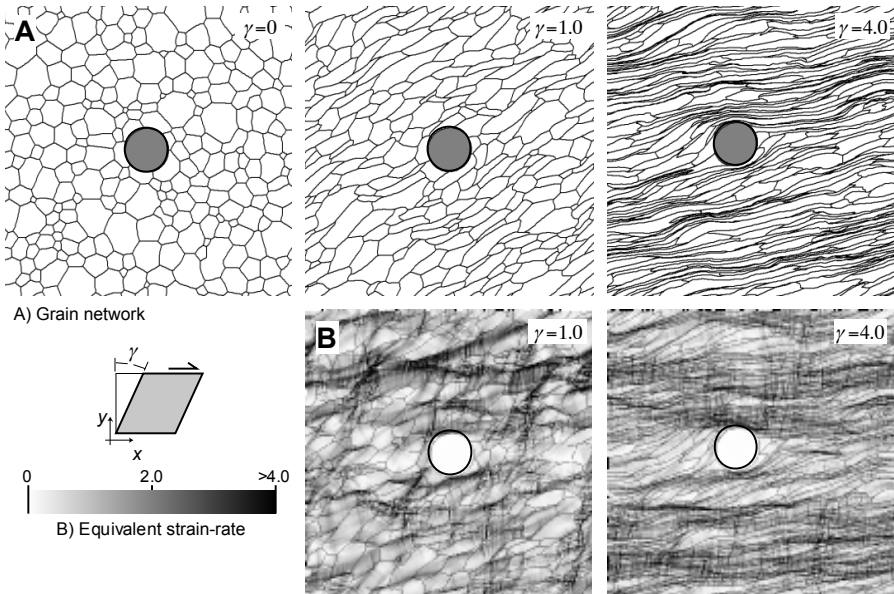
² Institut für Geowissenschaften, Eberhard Karls Universität Tübingen, Germany

³ IRD GET, Observatoire Midi Pyrénées, France

⁴ Materials Science and Technology Division, Los Alamos National Laboratory, USA

⁵ School of Geosciences, Monash University, Australia
albert.grier@uab.cat

Whether rigid inclusions, such as porphyroclasts and porphyroblasts do or do not rotate in a softer matrix during deformation has been debated for decades. Experiments and numerical simulations with viscous matrix rheologies show ongoing rotation of circular inclusions, whereas using Mohr-Coulomb plasticity results in non-rotation. As the rocks in which inclusions are found are normally deforming by dislocation creep, we used a full-field crystal plasticity approach to investigate the rotation behaviour of rigid circular inclusions. We show that the inclusion's rotation strongly depends on the anisotropy of the matrix minerals. Strongly anisotropic minerals will develop shear bands that reduce the rotation of inclusions. Inhibition of rotation can only occur after a significant amount of strain. Our results may help to explain why geological rigid objects often show evidence for rotation, but not necessarily in accordance with viscous theory that is usually applied to these systems.



Thermometry of Quartz Mylonites: Importance of dynamic recrystallization on Ti-in-quartz re-equilibration

Djordje Grujic¹, Michael Stipp², Joe Wooden³

¹ Department of Earth Sciences, Dalhousie University, Halifax B3H 4J1, Canada

² Department of Marine Geodynamics, Leibniz Institute of Marine Sciences, IFM-GEOMAR, Wischhofstr. 1-3, 24148 Kiel, Germany

*³ Department of Geological and Environmental Science, Stanford University, Stanford, CA 94305, USA
dgrujic@dal.ca*

Quartz mylonites from the Tonale Fault Zone in the Alps (northern Italy) have been investigated by the Ti-in-quartz geothermometer (TitaniQ) in order to test its applicability to measure deformation temperatures. The eastern part of the Tonale Fault Zone was contact metamorphosed by the synkinematic intrusion of the Adamello pluton, forming a ~800 m-wide mylonitic shear zone, with a synkinematic temperature gradient from ~280 °C at the frictional-viscous transition to ~700 °C at the pluton contact as derived from metamorphic mineral assemblages. Deformation microstructures from quartz mylonite samples, systematically collected across the mylonitic shear zone, display the entire range of dynamic recrystallization in quartz, which comprise bulging recrystallization (BLG), subgrain rotation recrystallization (SGR), and grain boundary migration recrystallization (GBM).

With regard to the trace element composition of quartz there are samples which are unaffected by contact metamorphism and Tonale shearing and those which show a resetting in trace element concentration. Ti and Al data in particular, show a sharp transition from samples with a decreasing concentration with decreasing peak synkinematic temperature to samples with a fairly constant concentration caused by pre-Alpine regional metamorphism. This shift corresponds exactly to the GBM to SGR transition at 540 °C. For all GBM samples, it was observed that TitaniQ registers the temperature at which quartz “locks in” its microstructure; i.e., when deformation and dynamic recrystallization ceases. Based on new SHRIMP zircon U/Pb dating of the Presanella tonalite (30.5 ± 0.5 Ma), we further ascertain that the time of contact metamorphism was very short, on the order of 1 Ma. The time of deformation at the particular peak synkinematic metamorphic conditions was actually much shorter than that. Therefore, the available time was insufficient to re-equilibrate the trace element composition of quartz by volume diffusion. The best explanation for the re-equilibration in the zone of GBM is an increased diffusivity along the migrating grain boundaries of the investigated quartz mylonites.

Hence, dynamic recrystallization by fast grain boundary migration in the zone of GBM was a very effective re-equilibration mechanism for Ti and other trace elements, while within the zones of BLG and SGR no re-equilibration of the Ti concentrations could be detected. Grain boundary migration recrystallization is likely one of the most important processes for the enhancement of diffusive equilibration during deformation and it is much faster than equilibration under static conditions by volume and grain boundary diffusion.

Lithospheric scale folding related magmatism in NW Iberia. Post Variscan magmatism in time and space

Gabriel Gutiérrez-Alonso¹, Javier Fernández-Suárez², Teresa E. Jeffries³, Stephen T. Johnston⁴, Daniel Pastor-Galán¹, Arlo B. Weil⁵

¹ Departamento de Geología, Universidad de Salamanca, Spain

² Departamento de Petrología y Geoquímica, Universidad Complutense, Madrid, Spain

³ Natural History Museum, London, United Kingdom

⁴ School of Earth and Ocean Sciences, University of Victoria, Canada

⁵ Bryn Mawr College, Pennsylvania, USA

gabi@usal.es

In most orogens, post-orogenic magmatism preferentially occurs in the upper (overriding) plate and has been interpreted to be caused by the break-off of the subducting plate and related asthenospheric upwelling. In contrast, post-orogenic magmatism in the Iberian portion of the Variscan belt occurred in the lower plate coevally with the development of a lithospheric scale fold known as the Ibero-Armorican Arc or orocline. U-Pb (zircon) crystallisation ages of 52 late-Variscan granitoid intrusions from NW Iberia (19 from new data, 33 from previous studies) constrain the lithospheric evolution of this orocline of the Variscan belt of Western Europe and allow assessment of the relationship between oroclinal development and magmatism in late-Carboniferous-early Permian times. The U-Pb ages, in conjunction with a range of geological observations, are consistent with the following sequence of events related to the behaviour of the lithosphere during the development of the aforementioned orocline : (i) oroclinal bending starts at 310-305 Ma producing lithospheric thinning and asthenospheric upwelling in the outer arc of the orocline accompanied by production of mantle and lower crustal melts; (ii) between 305 and 300 Ma, melting continues under the outer arc of the orocline (Central Iberian Zone of the Iberian Variscan belt) and mid-crustal melting is initiated. Coevally, the lithospheric root beneath the inner arc of the orocline thickened due to progressive arc closure; (iii) between 300 and 292 Ma, foundering of the lithospheric root followed by melting in the lithospheric mantle and the lower crust beneath the inner arc due to upwelling of asthenospheric mantle; (iv) cooling of the lithosphere between 292-286 Ma resulting in a drastic attenuation of lower crustal high-temperature melting. By 285 Ma, the thermal engine generated by orocline-driven lithospheric thinning/delamination had cooled down beyond its capability to produce significant amounts of mantle or crustal melts. The model proposed explains the genesis of voluminous amounts of granitoid magmas in post-orogenic conditions and suggests that oroclines and similar post-orogenic granitoids, common constituents of numerous orogenic belts, may be similarly related elsewhere.

Comparison of the Brittle Deformation Characteristics of Darley Dale and Pennant Sandstones

Abigail Hackston, E. H. Rutter

University of Manchester

abigail.hackston@postgrad.manchester.ac.uk

Triaxial tests have been performed on Darley Dale and Pennant sandstones as part of an ongoing project exploring the formation and sliding of faults under varied stress paths both in extension and in compression, such that mean-stress evolution can be varied. The tests are on both intact and pre-cut samples, with the saw-cuts at 35°, 45° and 55° to the length of the sample. For the saw-cut tests, constant confining pressure, constant mean stress and constant normal stress conditions were implemented.

Results can be displayed as Mohr diagram plots or in terms of various yield criteria (usually as a function of stress invariants, e.g. octahedral stress or the modified Lade criterion). Results have also shown that the friction angle (on a 2D Mohr plot) is different between compression and extension in Darley Dale sandstone, and that the fresh fracture angle in extension is also very low (approximately 16°). Darley Dale sandstone is considerably weaker than Pennant sandstone. The two rock types also form different fracture angles in intact samples. Darley Dale sandstone fractures at approximately 36° in compression, whereas Pennant sandstone fractures at approximately 31° under the same conditions. These differences are important for this project, as results have shown that the cohesive strength of Darley Dale sandstone is not sufficient for present purposes, as a material is required that will slide along saw-cuts rather than forming fresh fractures. Darley Dale sandstone forms fresh fractures when tested using angles of 55° and 45°, therefore the stronger Pennant sandstone is used for present tests, which focus on the effects of variations in pore fluid pressure and the presence or absence of fault gouge of different types, in addition to investigating frictional sliding behaviour on fresh sawcuts under varying loading conditions. The tests involving fault gouge consist of anisotropic and isotropic materials, so that stress refraction effects can also be investigated. Analysis of structures is performed on a macroscopic and microscopic scale, so the influence of micro-cracks or meso-cracks forming as a result of raising pore pressure sufficiently to induce hydraulic cracking can be studied.

Influence of phyllosilicate mineralogy on the anisotropy of magnetic susceptibility

Tom Haerincx¹, Rieko Adriaens², Ann M. Hirt³, Timothy Debacker⁴, Manuel Sintubin¹

¹ Geodynamics & Geofluids Research Group, Department of Earth & Environmental Sciences, Katholieke Universiteit Leuven, Celestijnenlaan 200E, B-3001 Heverlee, Belgium

² Applied Geology & Mineralogy Research Group, Department of Earth & Environmental Sciences, Katholieke Universiteit Leuven, Celestijnenlaan 200E, B-3001 Heverlee, Belgium

³ Institute of Geophysics, ETH Zürich, Sonneggstrasse 5, CH-8092 Zürich, Switzerland

*⁴ Geology & Pedology, Universiteit Gent, Krijgslaan 281-S8, B-9000 Gent, Belgium
tom.haerincx@ees.kuleuven.be*

The anisotropy of magnetic susceptibility (AMS) has been used as a petrofabric indicator since the early 1950s. Many studies have advocated a relationship with finite strain, and so AMS has been frequently used as a strain gauge. In these studies, AMS is used as an indicator of the preferred orientation of grains in a volume of rock. However, the measured anisotropy is defined by a combination of two effects: the intrinsic magnetic anisotropy of the minerals and the anisotropic distribution of the mineral grains, i.e. the rock fabric.

This work deals with the effect of mineralogical and chemical composition on AMS. As natural samples generally contain compositional variations, these effects must be qualitatively understood before one can use AMS as an indicator of a mineral preferred orientation for regional strain analysis. Samples were taken in homogeneous siltstone beds of the Plougastel Formation (Pridolian to Lochkovian age) on the Crozon peninsula (Brittany, France), the westernmost part of the Palaeozoic Armorican terrane. These rocks were subjected to contractional deformation at the beginning of the Carboniferous due to the closure of the Rheic Ocean, resulting in reverse faults and folds with associated axial-plane cleavage.

A comparison of low-field, room temperature AMS and low-field, low temperature AMS of 71 samples shows a temperature dependency in perfect agreement with the Curie-Weiss law, typical for paramagnetic material. The dominant paramagnetic nature of the samples is further confirmed by measurements of 30 samples with a high-field torque magnetometer that show a very good agreement between the high-field paramagnetic and the low-field susceptibilities. The paramagnetic mineralogy was further investigated by XRD measurements, with special focus on the phyllosilicates, generally the main paramagnetic AMS carriers in fine-grained siliciclastic rocks. This analysis shows a very consistent mineral content, with the presence of quartz, illite and/or muscovite, pyrophyllite and Fe-rich chlorite. However, the exact composition of the different samples is quite variable, with the total phyllosilicate content ranging from 10 % up to 38 %.

The results demonstrate a relationship between the degree of magnetic anisotropy and the phyllosilicate content. Assuming that the preferred orientation is fairly consistent for samples of the same, homogeneous lithology in one particular tectonostratigraphic context, such a relationship should be considered to correct AMS measurements for variation due to mineralogical composition, prior to its application as petrofabric indicator.

Linking titanium-in-quartz thermometry and quartz microstructures: strong evidence of continued vein formation during strain localization

Mike Härtel, Marco Herwegh

*Institute of Geological Sciences, University of Bern, Switzerland
mike.haertel@geo.unibe.ch*

Detailed microstructural examinations on mylonites from the Simplon Fault Zone (SFZ) in southern Switzerland revealed the transition of different recrystallization processes in quartz veins of the footwall, ranging from Grain Boundary Migration Recrystallization (GBM) over Subgrain Rotation Recrystallization (SGR) to Bulging Nucleation (BLG), from the rim towards the centre of the shear zone. GBM-microstructures can be recognized at distances of more than 4400 m from the centre and at around 1200 m distance they start to be progressively overprinted by SGR (in the northern part), producing a kilometer-wide mylonite zone comprising ribbon textures in the quartz veins. Near the centre of the SFZ, core-mantle-structures develop and bands of bulging grains transect older quartz ribbons. This microstructural sequence displays the cooling-related localization of strain from initial temperatures over 600 °C down to temperatures lower than 350 °C with respect to their dynamically recrystallized grain sizes. However, the age relations between all the quartz veins remained unknown and some microstructures do not fit into this pattern. The application of Ti-in-quartz geothermometry revealed highest temperatures of 535 ± 17 °C as formation temperatures of GBM-samples, which is lower than the expected formation temperature. The reason for this discrepancy is the continuous adjustment of Ti-concentrations in quartz, during dynamic recrystallization in the GBM-regime. Within the zone of SGR-affected mylonites a very wide spread of temperatures occurs, ranging from 376 ± 6 °C up to 509 ± 4 °C. Taking into account that SGR overprints former microstructures, but inhibits the readjustment of Ti-concentration in quartz, these temperatures are considered to display the formation temperatures of the subsequently precipitating quartz veins, following the localization of strain. These data allow us to differentiate between veins by their relative age relations and to follow the path of the inhomogeneous overprint of the old microstructures with ongoing strain localization during exhumation and cooling.

Quantitative microstructural analyses of natural gold alloys

Angela Halfpenny, Robert M. Hough

*Earth Science and Resource Engineering, CSIRO, Kensington, Western Australia
Angela.halfpenny@csiro.au*

Gold, due to its economic significance and variable properties is an important metal to understand. Much research has been performed to constrain the location and timing of gold deposition, although relatively few studies have focused upon the gold itself. This research focuses upon quantifying the crystallography and composition of naturally derived visible gold, with the aim of improving our understanding of how gold nucleates, crystallizes and deforms. The research is also interested in the mechanisms involved in gold modification after crystallization.

We have studied visible gold from quartz carbonate veins from lode gold deposits in Western Australia. In one example the free visible gold is only found within the veins and is occasionally intermixed with tetrahedrite whereas pyrite is hosted in the wall rock and has been deformed by the shear zone, although there are interactions between the gold and the pyrite at the vein margins.

The visible gold in the breccia veins occurs as aggregates of subhedral grains which vary in grain size from tens of microns to hundreds of microns in size and are located in the carbonate dominated vein material between the breccias clasts. Whereas the visible gold in the shear hosted veins occurs mostly as centimeter long veinlets with the occasional large aggregate. When large aggregates form they are intimately associated with tetrahedrite. The boundaries between the gold and tetrahedrite are extremely undulatory and the gold appears to be replacing the tetrahedrite.

The full crystallographic orientation of each gold crystal was measured using electron backscatter diffraction (EBSD) and chemical variations were measured using (EDS), both are scanning electron microscope (SEM) based techniques. The gold crystals contain $\Sigma 3$ twin boundaries, which are not always planar and exhibit weakly curved grain boundaries. The gold grains also exhibit a weak misorientation of the crystal lattice. Possible causes for this lattice misorientation could be due to deformation or replacement of Au atoms (Cu is $\sim 12\%$ smaller in atomic size, which leads to distortions in the crystal lattice when it replaces Au) or thermal alteration.

Measurements of the gold's composition by EDS show that there are no significant variations across each gold crystal at the 1% detection limit, this could indicate that the lattice variations are not due to significant substitution of Au atoms. The composition of the crystals has been measured at an average of 98% Au and 2% Ag. A thermally annealed microstructure would be characterised by straight grain boundaries and $\Sigma 3$ twins, which is not the case here, therefore we conclude that the original microstructure may have been representative of thermal annealing but has since been modified by plastic deformation.

The effect of CO₂-brine-rock interaction on the mechanical properties of intact rocks

Suzanne Hangx

*Shell Global Solutions, Kesslerpark 1, 2288 GS Rijswijk, the Netherlands
suzanne.hangx@shell.com*

One of the most promising ways of disposing of CO₂ is through Carbon Capture and Storage (CCS), entailing CO₂ capture at source, followed by long-term geological storage. Possible storage sites include depleted oil and gas reservoirs, saline aquifers and unminable coal seams. The former are particularly interesting and recognised as an important CCS route for countries with a major oil or natural gas production and transport infrastructure, such as the United States, Norway, United Kingdom and the Netherlands.

Long-term storage in depleted reservoirs is strongly dependent upon maintaining trap integrity, i.e., on maintaining caprock and fault integrity, as well as well bore integrity. Stress and strain changes accompanying reservoir depletion and/or CO₂ injection into an associated reservoir may lead to deformation-induced damage to wellbore, caprock, and fault-seal systems, particularly in the long term. The importance of CO₂-related creep effects, by enhanced microcracking and/or mineral dissolution-precipitation reactions, lies in their potential to cause reservoir rock compaction. In addition, chemical attack by CO₂ may modify the mechanical strength and transport properties of the caprock or may promote reactivation and/or leakage of sealed faults. Overall, geological storage of CO₂ in depleted oil and gas reservoirs is a complex matter, influenced by many, in their own rights complex, interlinked processes and mechanisms.

Over the past two decades, much research has focussed on elucidating some of the key questions, through geochemical as well as geomechanical modelling, and through experimental efforts. However, to date, very little experimental data exists on the effect of CO₂ on coupled chemical-mechanical processes occurring in reservoir and seal formations, and indeed on purely mechanical damage, for real rocks under in-situ conditions. Understanding them and obtaining site-specific data is important for (geomechanical and geochemical) numerical modelling efforts performed to assess upcoming CCS sites, as well as predicting the long-term fate of CO₂ in the subsurface. This presentation will focus on discussing the experimental work that has been done and is being undertaken to understand the effect of CO₂/brine/rock interaction on mechanical properties of intact rocks.

The structure of Western Cordillera Septentrional: transpressive deformation and strain partitioning in an island arc (Hispaniola)-continent (North America) oblique collisional setting

Pedro P. Hernaiz Huerta^{1,2}, F. Pérez Valera^{1,2}, M. Abad de los Santos^{1,2}, J. Monthel^{1,3}, P. Urien^{1,3}, A. Díaz de Neira^{1,4}, E. Lopera^{1,4}, M. Joubert^{1,3}, A. Pérez-Estaún⁵

1 IGME-BRGM-INYPSA Consortium for the SYSMIN Geothematic Mapping Project of the Dominican Republic

2 INYPSA Informes y Proyectos S.A., c/ General Díaz Porlier 49, 28001 Madrid, Spain

3 BRGM, Av. C. Guillemin, 45060 Orleans, France

4 IGME, c/ Calera 1, Tres Cantos 28760, Madrid, Spain

5 ICT Jaume Almera, CSIC, Lluís Solé i Sabarís s/n, 08028 Barcelona, Spain

phh@inypsa.es

The Cordillera Septentrional is a 15 to 40 km wide WNW-ESE oriented mountain range that runs parallel to the northern coast of the Dominican Republic. This range records the (oblique) subduction and collisional processes occurred between the Caribbean and North-American plates during Upper Cretaceous to Lower Paleogene times and a subsequent Upper Paleogene/Neogene to present intense left-lateral strike-slip tectonism, onset after collision. The Cordillera Septentrional is made up of volcano-plutonic and metamorphic complexes of Cretaceous to Lower Paleogene age that in turn make up the basement of large, Upper Paleogene and Neogene sedimentary basins resting unconformably on the former. Neogene to present transpressive deformation is partitioned into several main strike-slip faults or fault zones and coeval related folding that result in an important tectonic-controlled relief. The basement complexes outcrop in a NW-SE direction, slightly oblique to the dominant WNW-ESE structural fabric of the Cordillera and arranged in a right-hand en echelon pattern, associated with kilometric-scale restraining bends consistent with regional left lateral shearing.

The study focus on the structure of the western part of the Cordillera where three major tectonic domains (Altamira, La Toca and Puerto Plata, formerly described as blocks; de Zoeten and Mann, 1991; 1999), are recognized limited by the Camú, Río Grande and Septentrional fault zones. The Septentrional fault zone sets the boundary of the Cordillera with the Cibao basin although in these western transects the active trace of the fault is split in several segments displaced southwards into the basin with respect the mountain-front fault proper. The Camú fault zone runs parallel to the former several tenths of kms closer to the coast, southerly bounding the northernmost Puerto Plata domain. This fault has been recently mapped as a 3 to 10 km wide fault corridor made up of the mixture of decameter to kilometer scale fault bounded rhomboidal fragments of rocks and formations belonging to the neighbouring Puerto Plata and Altamira domains. Along the trace of the fault zone, positive flower structures coexist with negative ones; these last ones are filled by La Jaiba Fm of Lower-Middle Miocene age, thus postdating the age of the definitive strike-slip amalgamation of these domains. The Río Grande fault zone asymptotically joins the Septentrional and the Camú fault with a NW-SE direction and is conventionally considered to separate the Altamira and La Toca domains.

South of the Camú fault, the basement island arc complexes included in the Altamira (El Cacheal and Palma Picada complexes) and La Toca (Pedro García Complex) domains depict in cross section open to tight anticline or anticlinorium structures limited by subvertical and outwards verging faults. The overlying Paleogene (and Lower Miocene) turbiditic successions occupy the core of contiguous wide elongated sinclinatorium structures

North of the Camú fault, the Puerto Plata basement complex (PPBC) has a NW-SE orientation but in detail the internal structure of the complex shows quite a disorganized pattern as a result of

exhumation processes. The PPBC is partially overlaid by mélangé-type formations that typically host a varied mixture of blocks, including high-P metamorphic rocks (knockers).

Serpentine rheology and its influence on the mantle wedge dynamics

Ken-ichi Hirauchi^{1,2}, Ikuo Katayama¹

¹ Department of Earth and Planetary Systems Science, Graduate School of Science, Hiroshima University, 1-3-1 Kagamiyama, Higashi-Hiroshima, Hiroshima 739-8526, Japan

² High Pressure and Temperature Laboratory, Faculty of Geosciences, Utrecht University, P.O. Box 80.021, 3508 TA, Utrecht, The Netherlands
k-hirauchi@hiroshima-u.ac.jp

A variety of geophysical data suggest that the wedge beneath the forearc is cold and stagnant, while the wedge beneath the arc is hot and fluid. Recent tomographic studies revealed low V_p and V_s anomalies within the forearc wedge, indicating the occurrence of serpentinization. Serpentine minerals can be divided into the low- T (lizardite/chrysotile; liz/ctl) and high- T (antigorite) serpentine types, due to their temperature-dependent stability fields below $P = 2$ GPa. Revealing the effect of mantle wedge serpentinization on various geophysical phenomena, such as the downdip limit of great interplate earthquakes, seismic anisotropy, and slab–mantle decoupling, is now a topic of great interest, but not much attention has been paid to the rheology of the two serpentine types at high pressure ($P > 1$ GPa). In this study, we performed three series of shear deformation experiments under P – T conditions relevant to the mantle wedge corner (Katayama et al., 2009; Hirauchi et al., 2010a; Hirauchi and Katayama, submitted).

The one-layer or two-layer shear deformation experiments were conducted using a modified Griggs-type solid-medium apparatus at $P = 1.0$ GPa, $T = 200$ – 400°C , and at shear strain rates ranging from 10^{-5} to 10^{-4} s $^{-1}$. High-strain (γ up to 6) deformation of the two serpentine types resulted in plastic flow within individual grains via intracrystalline deformation, rather than cataclasis, with the development of a planar shape fabric. TEM observations revealed that the liz/ctl sample deformed by both (001) interlayer glide in lizardite crystals and grain boundary sliding of chrysotile nanotubes, whereas EBSD analyses showed that with increasing strain, the antigorite c -axis becomes oriented perpendicular to the flow plane. The contrasting amount of shear strain between the two layers after each experiment suggested that strain rates in liz/ctl are higher than in antigorite at a given pressure and temperature ($\dot{\gamma}_{\text{liz/ctl}}/\dot{\gamma}_{\text{atg}} = 5$ – 7).

Most of the textural and fabric features reported here are consistent with observations of deformed natural serpentinites thought to have been formed in paleo-subduction zones (e.g., Hirauchi et al., 2010b). The deformation style of liz/ctl under the above P – T conditions indicates that the downdip limit of great interplate earthquakes at the depth of the forearc Moho in cool subduction zones is explained by plastic (or superplastic) flow within individual grains via intracrystalline deformation. Based on the seismic properties in the experimentally deformed antigorite sample, we also suggest that the strong trench-parallel anisotropy beneath the forearc, characterized by the delay time of 1–2 s, is caused by a thin serpentinite layer, in which the (001) plane of antigorite is preferentially aligned with the plate interface as a result of simple-shear deformation induced by movement of the subducting slab. Finally, the significant difference in strength between liz/ctl and antigorite at our experimental conditions indicates that the distribution of serpentine species in the hydrated mantle wedge must be known to determine the degree of viscous coupling along the slab–wedge interface, at depths below the seismogenic zone.

REFERENCES

- Katayama, I. et al., 2009, *Nature* 461, 1114–1117.
Hirauchi, K. et al., 2010a, *Earth Planet. Sci. Lett.* 295, 349–357.
Hirauchi, K. et al., 2010b, *Earth Planet. Sci. Lett.* 299, 196–206.

A mesoscale constitutive model for rocks undergoing stress-driven melt segregation, applied to corrosion of lithospheric mantle

Benjamin K. Holtzman¹, Daniel S. H. King², David L. Kohlstedt³, Mousumi Roy⁴

1Lamont Doherty Earth Observatory, Columbia University, USA

2Department of Geosciences, Pennsylvania State University, USA

3Department of Geology & Geophysics, University of Minnesota, USA

4Department of Physics & Astronomy, University of New Mexico, USA

benh@ldeo.columbia.edu

Coupling between deformation and melt transport have long been recognized in field observations, and inferred to be important in the dynamics of crustal and lithospheric dynamics. We are studying these processes in closely knit experimental and theoretical approaches. Here, we present a mesoscale parameterization of the effects of stress-driven melt segregation (improved since its debut at the last DRT meeting, Liverpool, 2009). This constitutive model is comprised of two equations: (1) a simple homogenization (harmonic mean) of a material with horizontal (shear parallel) layers of varying viscosity (including mass balance for melt and the effect of melt on composite viscosity), and (2) an evolution equation for a single internal state variable describing the degree of melt segregation. At present, the evolution equation is relatively empirical, based directly on rheological and melt topological data measured in partially molten olivine rocks experimentally deformed in torsion. We use this model to explore the sensitivity of segregation rate to stress levels, permitted by the fact that the sample deformed in torsion experiences a range of thermodynamic conditions internally. The constitutive model is formulated for easy implementation in conjunction with common stress-, grain size- and temperature-dependent constitutive equations of elements in geodynamic models. Also, in order to illustrate possible consequences of stress-driven segregation in the Earth, we briefly present syntheses of results from studies of the lithosphere structure and evolution beneath the Colorado Plateau. In order to explore the possible kinetics of lithospheric corrosion by infiltrating melt, we implement the mesoscale constitutive model in a 1-D model of migrating melt in a deforming column, to explore the effects of stress-driven segregation on enhancing the rates of melt infiltration (work in progress).

Relationship between cleavage and thrust-related deformation in the southern margin of the Pyrenean Axial Zone (Bujaruelo valley, Huesca)

Esther Izquierdo-Llavall¹, Antonio Casas-Sainz¹, Inmaculada Gil-Peña², Chiara Invernizzi³

¹ Departamento de Ciencias de la Tierra, University of Zaragoza, Spain

² Área de Cartografía Geocientífica, IGME, Madrid, Spain

*³ Scuola di Scienze e Tecnologie, University of Camerino, Italy
estheriz@unizar.es*

The structure of the western part of the South Pyrenean Zone is mainly due to the superimposition of two coaxial tectonic stages: (1) the emplacement of the Larra-Monte Perdido fold-thrust system and (2) the emplacement of the Gavarnie thrust sheet. The Larra-Monte Perdido system is related to a local and scarcely developed cleavage, while the emplacement of the Gavarnie thrust sheet is coeval to the development of the regional cleavage domain that affects the western sector of the Axial Zone and northern part of the turbiditic South-Pyrenean basin. The coexistence of both cleavages in the same outcrop, or the deformation of the first cleavage during the second tectonic stage, has only been recognized occasionally.

The present study provides the accurate structural analysis of a single but a priori interesting outcrop that registers several superimposed tectonic stages during the alpine compression in the Pyrenees. The studied outcrop is located within the shear zone related to a thrust of the Larra-Monte Perdido system, in the southern part of the Bujaruelo valley. The thrust has a hectometric displacement and separates Eocene marls in the footwall from Paleocene-Ilerdian limestones in the hangingwall, the latter affected by a recumbent anticline.

The thrust zone is characterized by the development of a pervasive cleavage that affects both the marly turbidites and the limestones. The ductile deformation developed in these materials contrasts with the brittle deformation style of the thrust system towards western areas. In the eastern part of the outcrop cleavage has a dominant E-W to ESE-WNW strike, parallel to the general strike of the thrust plane, and dips shallowly to the North (average 20-25°). The strike of cleavage changes progressively towards the western part of the outcrop, where NW-SE-striking planes, with intermediate to gentle dips towards East, have been recognized. N-S to NE-SW-striking stretching lineations on ESE-WNW-striking cleavage planes developed frequently, and are subparallel to slickenfibres in calcite veins parallel to cleavage.

Cleavage, and extensional veins parallel to cleavage, are affected by NNE-SSW-striking folds, subparallel to the transport direction. Cleavage is also affected by NNW-SSE-striking folds, parallel to the regional folding coeval to the emplacement of the Gavarnie thrust. This second tectonic stage is also consistent with the development of a discontinuous, subvertical and E-W-striking cleavage, that appears only locally and cuts previous subhorizontal cleavage planes.

Preliminary fluid inclusions microthermometric analyses have been performed in two extensional veins from the outcrop: (1) an extensional vein coeval to the thrust displacement and (2) a vein parallel to cleavage. Homogenization temperature to liquid (Th) in two phase liquid plus vapour inclusions indicates a minimum average trapping temperature ranging from 191±15 to 93±11°C in different fluid inclusion assemblages, and points to a long thermal and deformation history for the studied outcrop.

Oblique megashear zones in the Precordillera (Central Andes, Argentina): the Rodeo-Talacasto Transpressional Belt

Silvia Japas, G.H. Ré, J.F. Vilas, S. Oriolo

*IGEBA, Universidad de Buenos Aires – CONICET, Argentina
msjapas@gl.fcen.uba.ar*

The Andean segment located between 28° and 33° S shows a strong anisotropic character as it is composed of tectono-stratigraphic units with different previous geological stories. They also show up major planar anisotropies that resulted from the accretion and amalgamation of different terranes (Ramos 1999). Therefore the deformation as a whole is strongly inhomogeneous.

Tectonic Fabric Analysis focused on the Central Andes from Argentina revealed two systems of conjugated megashear zones. The first system comprises left-lateral NNW and right-lateral NNE transpressional sets while the second one involves left-lateral WNW and right-lateral ENE transtensional sets (Japas 1998, Ré et al. 2001, Japas et al. 2002a and b, Ré and Japas 2004). One of these left-lateral NNW transpressional structures (Mendoza Norte, Ré et al. 2001) was lately confirmed as a NNW sinistral transpressional belt (Barreal-Las Peñas Belt, Cortés and Cegarra 2004, Cortés et al. 2005).

The Andean Precordillera is a North-trending, thin-skinned (Western and Central Precordillera) and thick-skinned (Eastern Precordillera) fold and thrust belt developed at the foreland of the Pampean flat slab. Between Rodeo and Talacasto towns, a set of thrust-controlled exposures of synorogenic Tertiary rocks are arranged in an en-échelon pattern following a NNW trend. Along this NNW belt, trends of Andean regional thrusts and folds change from NNE to NS/NNW as well as NNE-oriented outcrops of Palaeozoic sedimentary rocks are deflected counterclockwise. Furthermore, a NNW brachianticline (Loma Negra) developed at the eastern border of this Rodeo-Talacasto belt.

Preliminary structural fabric, kinematic and paleomagnetic data (work in progress) allow to define the Rodeo-Talacasto belt as the consequence of NNW sinistral transpression. According to both previous proposals (Cortés et al. 2005) and recent analogue models (Yagupsky et al. 2007), the structure of pre-Tertiary rocks would have controlled the development of this oblique belt.

REFERENCES

- Cortés, J.M. and Cegarra, M., 2004. *Asoc.Geol.Argentina, Serie D, Publ.Esp.*, 7: 68-75, Buenos Aires.
- Cortés, J.M., Pasini, M. and Yamin, M., 2005. 6th International Symposium on Andean Geodynamics (ISAG 2005, Barcelona), Extended Abstracts: 186-189
- Japas, M.S., 1998. *Rev.Asoc.Geol.Argentina* 53 (1) : 15. Buenos Aires.
- Japas, M.S., Ré, G.H. and Barredo, S.P., 2002. 15° Cong.Geol.Argentino, 1 : 326-331. El Calafate.
- Japas, M.S., Ré, G.H. and Barredo, S.P., 2002. 15° Cong.Geol.Argentino 1 : 340-343. El Calafate.
- Ramos, V., 1999. *Episodes* 22(3):183-190.
- Ré, G.H., Japas, M.S. and Barredo, S.P., 2000. *Asoc.Geol.Argentina, Serie D: Publ.Esp.* 5: 75-82. 10° Reunión sobre Microtectónica, Buenos Aires.
- Ré, G.H. and Japas, M.S. 2004. *GSA Annual Meeting, Abstract with Programs*, 36 (5). Denver
- Yagupsky, D.L., Cristallini, E.O, Zamora Valcarce, G. and Varadé, R., 2007. *Rev.Asoc.Geol.Argentina* 62 (1): 124-138. Buenos Aires.

The thermal state and rheological behavior of the lithosphere in the Spanish Central System and Tajo Basin from crustal heat production and thermal isostasy

Alberto Jiménez-Díaz¹, Javier Ruiz¹, Carlos Villaseca^{2,3}, Rosa Tejero^{1,3}, Ramón Capote¹

¹ Departamento de Geodinámica, Facultad de Ciencias Geológicas, Universidad Complutense de Madrid, 28040 Madrid, Spain

² Departamento de Petrología y Geoquímica, Facultad de Ciencias Geológicas, Universidad Complutense de Madrid, 28040 Madrid, Spain

³ Instituto de Geociencias, CSIC-UCM, 28040 Madrid, Spain

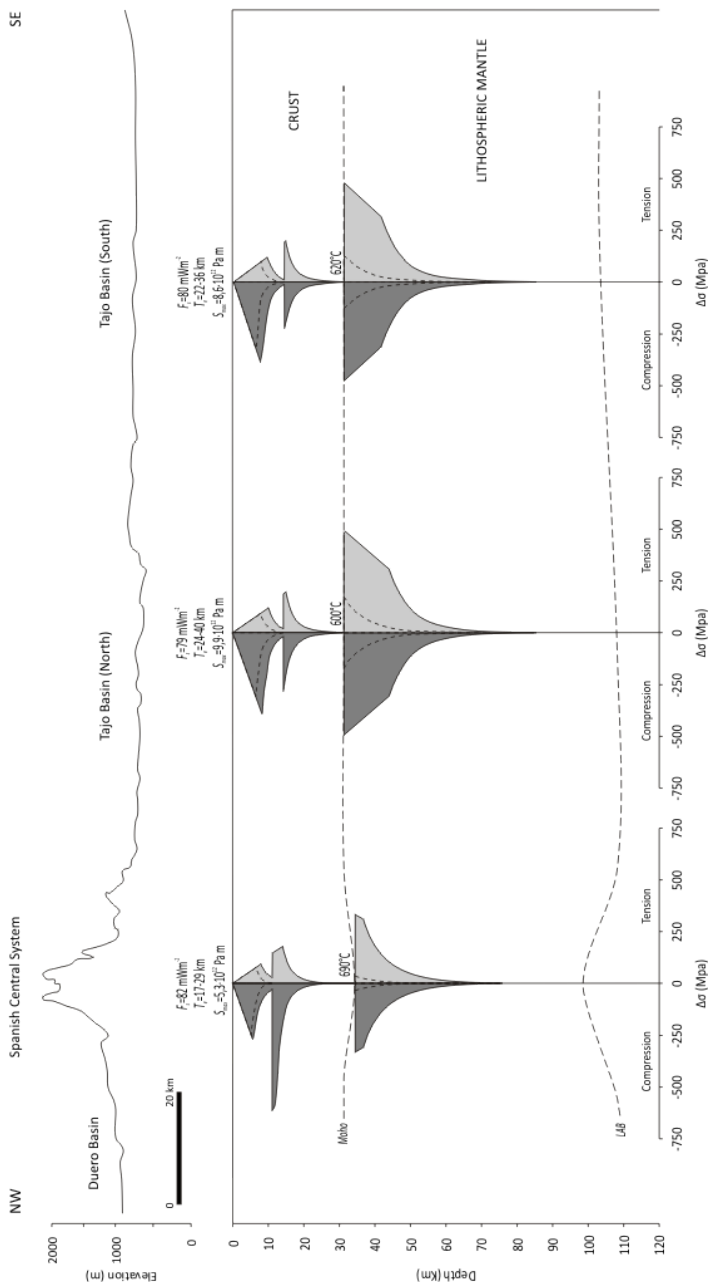
ajimenezdiaz@geo.ucm.es

The thermal state and the rheological behavior of the continental lithosphere depend on many factors. Due to the relationship between thermal and mechanical structure of the lithosphere, it is necessary to have an adequate knowledge of the thermal parameters, local heat flow and thermal structure, to reduce the uncertainty in strength estimates. For example, the amount and distribution of lithospheric heat-producing elements (HPE) and the values of the thermal conductivities of crust and mantle may affect the results substantially. Thus, the mechanical behavior and rheological stratification of the lithosphere in continental areas are largely a consequence of local conditions.

In this work is we model the thermal structure of the lithosphere of the Spanish Central System and the Tajo Basin, and their implications for lithospheric strength. The Spanish Central System constitutes the most prominent topographic elevation in the interior of the Iberian Peninsula, which corresponds to the main divide that separates two Cenozoic intracontinental sedimentary basins, the Duero Basin to the north and the Tajo Basin to the south.

We have used refined HPE values for obtaining new estimates of heat production rates, and we have used the relation between topography and thermal structure for calculate the best-fit surface heat flows. Moreover, we have implemented a temperature-dependent thermal conductivity (appropriate for olivine) for the lithospheric mantle for improve the calculations. In turn, the geotherms obtained in our thermal model, together with the implementation of a new rheological law for the upper lithospheric mantle (largely controlled by low-temperature plasticity of olivine-rich rocks), have improved estimations on strength and the effective elastic thickness of the lithosphere. All of this refines the thermo-mechanical models and lithospheric strength determinations of the study area, and will be presented and discussed in the DRT-2011 Meeting.

Figure 1. Results of thermal models and strength envelopes, calculated for a strain rate of 10^{-15} s⁻¹, plotted along a NW–SE transverse section of the area. Outer black line binds differential stress estimated for dry rock composition. Inner dashed line denotes differential stress for wet rock composition of the upper crust (quartzite or granite) and lithospheric mantle (peridotite). *F_s*: Surface heat flow. *T_e*: Effective elastic thickness for wet/dry rheologies. *S_{max}*: Maximum total lithospheric strength. Moho: crust-mantle boundary. LAB: lithosphere-asthenosphere boundary.



Marine terrace uplifting rates in the Cantabrian shore: contribution of U-Th speleothem dating

Montserrat Jiménez-Sánchez^{1,2}, H. Stoll¹, S. Giralt², A. Aranburu³, A. Moreno⁴, M.J. Domínguez-Cuesta¹, A. Méndez-Vicente¹, D. Ballesteros¹, G. Pirla¹, B.R. Valero-Garcés⁴, H. Cheng⁵, L. Edwards⁵

¹ Department of Geology, University of Oviedo, Arias de Velasco s/n 33005 Spain.

² Department of Environmental Geology and Georisks, ICTJA, Solé i Sabarís s/n, E-08028 Barcelona, Spain

³ Department of mineralogy and Petrology, University of Basque Country, Sarriena s/n, 48940 Leioa, Spain

⁴ Department of Geoenvironmental Processes and Global Change, IPE CSIC Avda. Montañana, 1005, 50059 Zaragoza, Spain

⁵ Department of Geology and Geophysics, University of Minnesota, Twin Cities, Minneapolis, Minnesota, 55455, U.S.A.

mjimenez@geol.uniovi.es

Previous research in the Cantabrian Coast (N Spain) based on U-Th dating of speleothems indicates uplift rates ranging from 0.03 mm/yr to 0.19 mm/yr. Here we present new geochronological data obtained in three caves of the Cantabrian Coast (N Spain) that constrain uplift rates for karstified surfaces identified as marine terraces.

El Pindal cave (Ribadedeva, Asturias) is located at 24 m a.s.l. in a karstic massif limited by a marine terrace at 50-64 m a.s.l. The cave shows an E-W trending, 590 m of horizontal development and the active level is located at 6 m a.s.l. The Deva River is interpreted as the former base level of the cave system. Several quartzitic gravel and sand alluvial levels deposited inside the cave are interpreted as the result of erosion of another marine terrace carved in quartzite bedrock (150-160 m a.s.l.) and located to the South. Several phases of precipitation of speleothems have also been identified; gravity processes, with roof fallen blocks and collapse structures in cave floor are also remarkable.

La Vallina cave (Porrúa, Asturias), opened at 70 m a.s.l., shows a NW-SE trending and 600m development, and an active level located at 35 m a.s.l.; the karstic massif is limited on top by a surface also interpreted as a marine terrace (90 m a.s.l.). Flowstone levels covering quartzite sands of fluvial origin can also be recognized, as well as several generations of speleothems.

Asnarre cave (Laga, Vizcaya) is located at 20m a.s.l., developed in a karstic massif also interpreted as a remnant of a marine terrace (50-60m), with a horizontal development of at least 50 m, parallel to the coastline. The first conglomeratic level consists of sandstones and ophiolite clasts deposited by fluvio-karstic processes, and fills up more than half of the phreatic conduct. Several cycles of conglomerate and speleothem silted up and fossilized the cave. No active level is known at present.

U-Th series dating (Alpha spectrometry and ICP-MS) constrain the ages of the oldest speleothems in the three caves. In Pindal Cave, four samples of flowstone yielded ages of 167 ± 3 ka, 200 ± 24 ka, 219 ± 25 ka and 230 ± 26 ka; an inactive stalactite (soda-straw) from a fallen block yielded an age of 295 ± 12 ka; one flowstone sample from La Vallina cave was dated 234 ± 20 ka; two flowstone samples from Asnarre cave gave ages of 292 ± 52 ka and 339 ± 116 ka. These results give a minimum age for the karstic systems development and for the marine terraces in which caves are developed.

Microstructure and mineral fabric analysis of San Andreas Fault zone gouge from drill cores of the SAFOD borehole, Parkfield, CA

Manuel Kienast¹, **Luiz F. G. Morales¹**, Christoph Janssen¹, Hans-Rudolf Wenk², Erik Rybacki¹, Georg Dresen¹

1 Helmholtz Centre Potsdam, GFZ German Research Centre for Geosciences, Germany

2 Department of Earth and Planetary Science, University of California, Berkeley, USA

Morales@gfz-potsdam.de

The NW-SE trending dextral San Andreas transform fault (SAF) separates the North American from the Pacific plate. Two locked segments to the NW and SE are separated by a creeping section close to Parkfield, CA (USA). The SE segment ruptured in 1857 during the Fort Tejon (Mw 7.9) earthquake, while the NW part ruptured in 1906 during the Mw 7.9 San Francisco earthquake. The apparent weakness of the SAF at Parkfield as revealed by fault normal compression and absence of frictional heat was a key motivation to launch and establish a joint fault drilling program, the San Andreas Fault Observatory at Depth (SAFOD).

In 2007 the last stage of drilling through the SAF was completed, recovering 50 m of continuous drill core from 2,8 km vertical depth. The recovered cores penetrate two actively creeping strands of the SAF at borehole measured depths of 3192 m and 3302 m, the southern deforming zone (SDZ) and the central deforming zone (CDZ), respectively.

The studied fault gouge and ultra cataclaste samples are located between 6 to 2 m and 0,3 m above the SDZ and CDZ, respectively, i.e. in close proximity to the sites of active deformation. The samples consist of elongated lithoclasts and fragments of quartz and feldspar in a clay-rich matrix. The lithoclasts contain microcrystalline quartz, variable amounts of cross-cutting calcite veins and cement in addition to minor amounts of clay minerals. Additionally, well rounded sandstone lithoclasts containing angular quartz and sericitized feldspar, mica, chlorite and calcite veins are present. The abundance of lithoclasts diminishes to zero with proximity to the deforming zones.

Microstructures reveal evidence for brittle fracture and solution-precipitation processes. Brittle deformation is evident by grain-size reduction, crack and seal episodes and fracture formation. Chemical processes include dissolution and precipitation of minerals, sericitization of feldspar and secondary cementation. Cathodoluminescence microscopy reveals at least three different generations of calcite veins confined to lithoclasts, showing dissolution seams, as well as crack and seal processes in K-feldspar. Some quartz grains exhibit Dauphiné twinning, suggesting episodes of high stress deformation during seismic events.

The clay-rich matrix shows an apparent < 1 mm wide foliation in the optical microscope. The preferred orientation of (micro) cracks, the sub-parallel trend of elongated lithoclasts and occasional parallel extinction of clay minerals constitute this foliation. However, a crystallographic preferred orientation (CPO) of clay minerals resulting from this foliation could not be confirmed by SEM and synchrotron texture analyses.

In the SEM clay mineral aggregates show equal amounts of edge to edge, face to edge and face to face contacts. Only in some areas, e.g. around quartz fragments, face to face contacts are dominant, defining a local preferred orientation. The random distribution of the clay fabric was confirmed by X-ray synchrotron texture analysis.

The observed microstructures reveal complex and heterogeneous deformation and annealing processes within the fine-grained SAFOD samples that require high resolution analytical techniques to be resolved.

Dislocation creep of dry quartz

Rüdiger Kilian¹, Renée Heilbronner¹, Holger Stünitz²

¹Geological Institute, Basel University, Switzerland, Bernoullistr. 32, 4056 Basel,

²Geological Institute, University Tromsø, Norway

ruediger.kilian@unibas.ch

The Truzzo granite in the Penninic Tambo nappe is subjected to heterogeneous Alpine deformation at amphibolite facies conditions. Small scale shear zones develop in undeformed volumes of granite which still exhibit magmatic structures. Along the strain gradient associated with the shear zones, magmatic quartz is recrystallized dynamically by grain boundary migration recrystallization and subgrain rotation. The dynamically recrystallized grain size ranges up to 750 μm , which is consistent with recrystallization at relatively low differential stresses (5 - 30 MPa). The presence of a monoclinic shape fabric and a crystallographic preferred orientation is typical for the deformation by dislocation creep.

Fourier-Transform-Infrared (FTIR) spectroscopy reveals very low water contents in the interior of recrystallized grains (in the form of discrete OH peaks and very little broad band absorption). The water content is in the range of values reported for dry Brazil quartz. Primary magmatic quartz grains contain fluid-inclusion-rich areas with a broad absorption band and higher water concentrations. Recrystallized grains are dry, and all fluid inclusion trails are clearly postkinematic. These measurements present the first data on strictly intragranular water contents of dynamically recrystallized quartz.

Deformation experiments have demonstrated that quartz with a very low water content is extremely strong and does not deform by dislocation creep at any realistic time scale at the inferred low values of differential stress. Only deformation experiments on wet polycrystalline quartz have produced flow laws that can be extrapolated to natural conditions, which yield satisfying results. This contrasts with our data of the dry quartz deforming by dislocation creep at relatively low differential stresses at natural strain rates. Contrary to the conventional concept of recovery, our data and observations also imply that quartz would be hardening as a consequence of grain boundary migration because fluid inclusions are expelled. The drainage of fluid inclusions indicates that water during deformation was at least present in the grain boundary region.

We discuss our data in the context of the effects of water on the potentially rate limiting factors of dislocation creep (e.g. glide or climb rate). We conclude that a transient introduction of water into the deforming grains during dislocation creep can explain our observations. The intragranular water concentrations which are rheologically effective in the naturally deformed Truzzo granite are much lower than those previously reported in the literature.

Shear zones and associated structures at the Variscan Front, South Wales

Richard J. Lisle¹, Deepak C Srivastava²

¹ School of Earth and Ocean Sciences, Cardiff University, UK

² Indian Institute of Technology, Roorkee, India

Lisle@cardiff.ac.uk

Numerous small shear zones in Lower Carboniferous carbonates of the Gower Peninsula and in coarse sandstones and conglomerates of Devonian age at Marloes Sands, Pembrokeshire provide evidence of the nature of localized deformation within low-grade metasedimentary rocks. These shear zones form conjugate pairs with the acute angle containing the maximum shortening direction can sometimes be shown to be simultaneously active. On Gower they have a thrust-like geometry in their relation to bedding, whereas in Marloes Sands the bedding contains the normals to the shear zones. The contrasting anisotropy due to the bedding at the two sites affects the geometry of the shear zones.

Associated structures reflect changing deformation mechanisms: pressure solution leading to spaced stylolitic cleavage and tension gash arrays, cataclastic deformation in high shear strain levels within the shear zones, and ductile deformation on the grain scale. Although there are instances of "light" shear zones where tension gash formation appears to have accompanied pressure solution, elsewhere there are cases of considerable volume changes. For example, "dark" shear zones which are devoid of mineralization represent a deviation from simple shear deformation.

Estimating the finite strain within shear zones, from cross-sections of brachiopods and clastic grains, is assisted where the strain markers can also be observed in the undeformed walls of the shear zone. Elsewhere, the inclination of the cleavage to the shear zone boundaries is a valid strain indicator only when the assumption of simple shear is made. To overcome this problem, a new method is devised that uses data from the cleavage and deformed passive markers (Fig 1). This technique also yields estimates of volumetric strains.



Fig 1: Shear zones, cleavage, tension gashes, and deformed early quartz veins. Such data can be used to determine finite strain and volume change. Marloes Sands. Pen for scale.

The structural features in the vicinity of the shear zone terminations indicate arcuate strain patterns and differential volume changes in the hanging- and foot-walls. These features closely agree with the results of finite element models of shear zone tips. The presence of these features is key to the consideration of the evolution of shear zones. Different scenarios are discussed.

Base of the seismogenic zone in NW Iberia

Sergio Llana-Fúnez, Carlos López Fernández

*Universidad de Oviedo, Geología, Oviedo, Spain
sllf@geol.uniovi.es*

The seismogenic zone of the continental crust is normally restricted to the upper crust. The overall strain is accommodated through the movement of a network of distributed pre-existing faults and/or discontinuities, ultimately controlled by the friction properties of the discontinuities. The thermal structure of the crust will determine the depth at which plasticity in quartz will take over as predominant deformation mechanism of the crust as a whole. For a continental crust with an average thickness of 30 km and an average heat flow at the surface of 60 mW /m² the transit between the friction- and plastic-dominated regimes can be estimated to be at around 13-15 km.

The continental crust in NW Iberia has such average thickness and heat flow and it is mostly made of crystalline rocks formed and deformed during the Variscan Orogeny. However, the base of the seismogenic zone, defined regionally as the depth at which 95% of the seismicity is accumulated, is located close to 20 km. There are several factors that can offset vertically this zone of mechanical transition, the presence of pressurised fluids will weaken the crust and would bring the transit from frictional to plastic behaviour deeper in the crust.

The distribution of seismicity in NW Iberia has another characteristic feature: the presence of earthquake swarms. The swarms have a tubular or pipe-like shape from the surface to around 12-15 km in depth, where they merge with background seismicity. The larger of the seismic swarms, around Becerreá, is sufficiently large (20 km diameter) as to rise the base of the seismogenic zone to around 13 km. The shallowing of the base of the seismogenic zone could be explained by local but sustained increases in temperature gradient through the crust. The rise of 7 km in the base of the seismogenic crust can be explained by a surface heat flow of 100 mW/m², a figure that is consistent with calculated local heat flow in some areas in Galicia with reported low temperature springs.

The Iberian Peninsula is currently under north-south compression. In NW Iberia this is reflected in the recent geological record by the development of minor conjugate sub-vertical fault systems striking NW-SE and NE-SW. The scattering of the seismicity indicates that the convergence and stresses associated are not sufficient to produce strain localization in discrete crustal-scale faults, so that stresses are relaxed in a number of small fractures distributed in the region. The lack of major heat flow anomalies that may be associated with intrusions suggests the migration of fluids through the upper crust following the intersection between the sub-vertical conjugate faults as the likely mechanism to explain the geometry of earthquake swarms, their distribution and a related shallowing of the base of the seismogenic zone.

Single layer folding in non-coaxial conditions up to high strain

Maria-Gema Llorens¹, Paul D. Bons¹, Albert Griera², Enrique Gómez-Rivas¹

1 Departament de Geosciences, Eberhard Karls University Tübingen, Germany.

2 Departament de Geologia, Universitat Autònoma de Barcelona, Spain.

gemallore@gmail.com

Folds and associated structures (e.g. axial plane cleavage) are widely used to unravel rock deformation. They are classical indicators of shortening direction and amount. However, fold geometries potentially contain much more relevant information on the kinematics of deformation and rock properties, such as viscosity contrast between layer and matrix or non-linearity of the viscosity. To extract this information from folds, it is necessary to quantify the relationship between all parameters that determine fold geometry and scale. Viscosity contrast between the competent layer and matrix (m) is generally seen as the main parameter that governs the fold patterns. However, non-linear rheology and deformation conditions (i.e. vorticity) are also crucial factors.

There are abundant cases of natural folds that developed under non-coaxial deformation conditions at high strain (i.e. in shear zones). The asymmetry of folds has been frequently used as shear sense indicators in these areas. Although numerical simulations of folding have become highly sophisticated in recent years, most of the present-day numerical models are restricted to folds that formed under coaxial conditions with layers oriented parallel to the shortening direction. Only limited numerical simulations of folding in simple shear have been done, but they did not systematically analyze development of folds with different rheologies (i.e. viscosity contrast between layer and matrix, non-linearity) and not up to high strain.

In this contribution we present series of 2-dimensional numerical simulations of single-layer folding under simple- and pure-shear conditions up to high strain. For this purpose, we use the software packages Elfe and Basil to simulate linear and non-linear viscous deformation.

The results show that fold geometries developed from linear viscous materials are similar for pure and simple-shear deformation conditions. The most noticeable difference is the refraction of foliation between competent layer and matrix. Foliation shows a more complicated refraction pattern in non-coaxial cases due to layer rotation.

Comparison of folds developed from linear and non-linear materials show that the effective viscosity contrast increases with non-linearity. This leads to the formation of folds with higher amplitudes and less thickening than in equivalent linear models. Fold envelopes are curved for all non-linear viscosities in simple shear, while they remain straight for linear cases, except at very high viscosity contrasts (>100). This is a clear effect of the enhanced effective viscosity contrast related to power-law viscosity.

The numerical simulations are compared with folded quartz veins from Puig Culip (Cap de Creus, Spain) in order to estimate the real amount of strain, the viscosity contrast, the stress exponent, and the boundary conditions during fold formation. The results indicate that the real strain of the folded quartz veins in this area can be up to 50% higher than the apparent strain. Viscosity contrast between the quartz veins and the surrounding meta-sediments varies from about 100 in the low strain zone to 50 at higher strains. This may be due to rheological changes with strain (strain softening) or to the difference in metamorphic grade.

Geometric modelling and fracture prediction: examples from seismic, remotely sensed and field data

Tina Lohr¹, Jorge Ginés²

1 ERC Equipoise Limited; Croydon, London, United Kingdom

2 Fugro NPA Limited; Edenbridge, Kent, United Kingdom

tinal@ercequipoise.com

Faulting and folding processes are producing a variety of fascinating geological structures we see today, from fault-propagation folds to relay-ramps, roll-over anticlines, or inverted listric faults. Kinematic modelling is an important tool that helps to understand and to reconstruct the generation of such structures. It also helps to predict likely areas of subordinate fracturing and folding that often develop due to the primary deformation. From outcrop examples it is known that there are numerous other aspects that play an important role in the generation of structures, e.g. lithology and therewith associated rheological contrasts, fluid content, temperature etc.

In this study we are focusing only on the geometric modelling and therefore we have chosen examples whose deformation can be largely described by kinematic modelling. Different structures are analysed from high-resolution seismic and outcrop data and subsequently modelled and compared. A variety of modelling parameters will be discussed and the implication they have for the range of uncertainties in predicting secondary structures.

Changes in deformation mechanisms and neocrystallization in granite during a MT-LP deformation (Vivero Fault, NW Spain)

Marco A. López-Sánchez¹, S. Llana-Fúnez¹, A. Marcos¹ and F.J. Martínez²

¹ Department of Geology, University of Oviedo, Spain

² Department of Geology, Autonomous University of Barcelona, Spain

malopez@uniovi.es

Deformation microstructures and neocrystallization are investigated with the increasing degree of strain in a granitic rock affected by the development of a crustal-scale extensional shear zone, the Viveiro Fault (VF). Light microscopy, SEM-BSE contrast images and EPMA techniques are used.

The Penedo Gordo granite, coarse-grained two-mica biotite-rich granite, is located at the hangingwall of the VF. A localized deformation in its eastern margin is observed, towards the core of the VF. The deformed zone consists of a set of narrow shear zones (mm to metric scale) heterogeneously distributed. Qualitatively, the granite samples were classified into five deformation degrees (I to V) based on a set of easily recognizable features. The observed matrix-porphyroblast relationships in the metapelites clearly indicate that the VF hangingwall developed a MT-LP metamorphism during its development. The inferred PTD path is almost an isobaric prograde path. Pseudosections for representative compositions fall in the range of 500-600°C and 390-450 MPa for $a_{\text{H}_2\text{O}}=1$.

The observed microstructures for the strained samples with grades I to IV indicate that dominant deformation mechanisms were: i) intracrystalline plasticity in quartz with BLG-recrystallisation (grades I to II) and SGR-recrystallisation (grades III to IV). ii) K-feldspars and plagioclases show solid-state deformation microstructures (eg. flame perthite, tartan twinning, patchy undulose extinction) in grades I to II. In grades III to IV cataclasis in feldspar is accommodated by mass transfer processes and metamorphic reactions dominate. New very fine albite-oligoclase grains crystallise at the rim as well as along fractures that affect large K-feldspar grains, sometimes accompanied by mica grains. Otherwise, K-feldspar precipitates along plagioclase fractures and other dilatational sites. Plagioclase with interstitial K-feldspar can also be observed. Plagioclase shows a pervasive sericitic alteration with the increasing of deformation.

The highly deformed samples (grade V) consist of a matrix mainly containing K-feldspar, plagioclase, quartz and micas with an average grain size below 15 μm . The samples usually show some quartz pods and small feldspar porphyroclast. Quartz pods disintegrate into polycrystalline aggregates, and the resultant grains are mixed into the surrounding matrix reaching its average grain size. In the matrix, the distribution of mineral phases tends to be homogenized (anticlustered distribution).

Similar feldspar microstructures, implying cataclasis accompanied by neocrystallisation, have been reported previously in natural rocks where the temperature was estimated between 250 to 400°C. In this study, petrological (regional) and structural (local) thermobarometry data, based on quartz dynamic recrystallization mechanism, indicate that temperatures during deformation reached 400-600°C, extending the temperature range previously reported. The microstructures of grade-V samples clearly indicate a change in the relative contributions of deformation mechanism during deformation with more participation of mass transfer processes. Fluids are clearly involved during deformation once the fracturing of feldspars starts.

Microstructure evolution during the static recrystallization of cold-worked Carrara marble

Elisabetta Mariani¹, S.J. Covey-Crump², J. Mecklenburgh², J. Wheeler¹, D.J. Prior³

¹ School of Environmental Sciences, University of Liverpool, UK

² School of Earth, Atmospheric and Environmental Sciences, University of Manchester, UK

*³ Department of Geology, University of Otago, New Zealand
mariani@liverpool.ac.uk*

In the Earth's crust and mantle syn-tectonic (dynamic) and post-tectonic (static) recrystallization of rocks can modify grain sizes, shapes and crystallographic orientations. This affects physical properties and anisotropies and is important for the interpretation of the mechanical behaviour of rocks in major fault zones along plate boundaries and geological terrains in mountain belts.

To improve our understanding of static recrystallization mechanisms, we carried out quantitative microstructural analyses of cold-worked and then annealed Carrara marble, using electron backscatter diffraction (EBSD) in a field emission gun (FEG) scanning electron microscope (SEM).

Initially samples were experimentally deformed to 8%, 17% and 27% strain, at 420 °C, 170 MPa confining pressure and a strain-rate of $3 \times 10^{-4} \text{ s}^{-1}$. Subsequent annealing was carried out at temperatures between 500 °C and 700 °C, and for periods from 3 hours to 35 days. The thirty two samples analysed show that, at all conditions, the strength of crystallographic preferred orientation (CPO) decreases with the progress of static recrystallization. This is linked with a progressive switch from e-twin to c-axis maxima, and may be interpreted as follows:

New recrystallized grains inherit CPOs from both twin and original old grains. If old grains have a c-axis maxima in the stress direction due to slip systems (other than e-twinning, e.g. basal $\langle a \rangle$) active during deformation, then the new grains will inherit it.

The c-axis maxima results entirely from dispersion of orientations around e-twin orientations, with the highest density around c, positioned centrally with respect to the three possible e-twin orientations.

Recovery and sub-grain rotation recrystallization of both parent and twin grains are active recrystallization mechanisms that form new pristine grains along grain boundaries and twin lamellae. These processes result in recrystallized grains with a distinctive misorientation angle distribution make-up, with predominantly high misorientation angle relationships with each other and both low and high angle relationships with their parent grains. The distribution of high misorientation angles is controlled by twinning relationships.

High energy, high angle boundaries are readily formed, leading to the onset of rapid grain boundary migration which, together with orientation pinning mechanisms, forms irregularly-shaped recrystallized grains.

Deformation of muscovite at low strain rates under hydrothermal conditions

Julian Mecklenburgh, Ernie Rutter, **Katharine Brodie**

*School of Earth, Atmospheric and Environmental Sciences, University of Manchester, Manchester. M13 9PL, UK
Kate.Brodie@manchester.ac.uk*

Layers of fine-grained layers of muscovite powder were hot-pressed between alumina sliding blocks at 700 °C and 200 MPa confining pressure and 100MPa pore pressure for 17 hours, to produce a compact, well-foliated polycrystalline starting material. The application of a high pore water pressure suppresses the dehydroxylation of muscovite, that otherwise restricts maximum temperature in experiments to about 500 °C. Nevertheless, the maximum test temperature is still restricted to 700 °C owing to the onset of breakdown reactions.

These synthetic shear zones were deformed at 600, 650 and 700 °C under constant differential stress or constant displacement rate down to shear strain rates of $2.5 \times 10^{-7} \text{ s}^{-1}$. A number of long (in excess of 1 month) stress relaxation tests were performed to access even lower strain rates. A further set of experiments were performed on single crystals placed between the sliding pistons with their basal planes parallel to the shear zone and the shear direction approximately parallel to the b axis under the same experimental conditions. At low strain rates the rheology changed from being represented by a power-law at high shear stresses and strain rates to being (near) linear-viscous at low strain rate and shear stresses. The transition occurred at strain rates less than $1 \times 10^{-6} \text{ s}^{-1}$ and at shear stresses less than 50 MPa. From our data at three different temperatures we now have obtained improved constraints on the temperature dependence of the near-linear viscous rheology. The flow law for the low stress near-linear viscous regime is:

$$\dot{\epsilon} = 10^{-1.67} \tau \exp\left(\frac{-105 \text{ kJmol}^{-1}}{RT}\right) \quad (1)$$

where $\dot{\epsilon}$ is the shear strain rate, τ is the shear stress in MPa, T is the temperature in K and R is the gas constant. The flow law for the high stress power-law regime is:

$$\dot{\epsilon} = 10 \tau^6 \exp\left(\frac{-300 \text{ kJmol}^{-1}}{RT}\right) \quad (2)$$

It is postulated that the near-linear viscous rheology represents deformation by the viscous glide of a low density of basal dislocations.

It has long been held that mica-rich rocks are mechanically weak under mid-crustal conditions, even when deforming by a power-law rheology. By extrapolating the high-temperature rheology to the lower strain rates characteristic of mica schist terrains and creep of phyllosilicate-bearing fault zones, mica-rich rocks are expected to be significantly weaker than predicted even by a power-law rheology. Given that mudstones, the protoliths of mica schist terrains, are the most abundant sedimentary rocks on the planet, these results have important implications for the strength of substantial portions of the mid-continental crust.

Grain size reduction of feldspar and pyroxene, phase mixing and strain localization in lower crustal shear zones (Lofoten, Northern Norway)

Luca Menegon¹, Holger Stünitz¹, Pritam Nasipuri¹, Henrik Svahnberg², Renee Heilbronner³

¹ Department of Geology, Tromsø University, Norway

² Department of Geological Sciences, Stockholm University, Sweden

*³ Department of Environmental Sciences, Basel University, Switzerland
luca.menegon@uit.no*

High temperature shear zones are common in the Anorthosite-Mangerite-Charnockite-Granite (AMCG) suite of the granulite facies Lofoten-basement of Norway, and typically consist of narrow structures (1 cm to 1 m in thickness) showing a mylonite-to ultramylonite transition from the shear zone boundary to the shear zone center or to one side of the shear zones. In this contribution we examine the deformation microstructures and synkinematic mineral assemblages of several shear zones developed from a mangerite (= monzonite) protolith.

The mineral assemblage in the host mangerite indicates anhydrous conditions (mesoperthite (plagioclase + K-feldspar) + clinopyroxene ± orthopyroxene), whereas the mineral assemblage in the shear zones consists of plagioclase + K-feldspar + quartz + hornblende + calcite + biotite ± clinopyroxene and indicates hydrated conditions. Hornblende-plagioclase geothermobarometry yields upper amphibolite- to granulite facies conditions during shearing (730-760°C, 0.55-0.8 GPa).

The mylonite consists of two distinct compositional domains: a pyroxene-derived aggregate and a feldspar-derived aggregate. The pyroxene-derived aggregate consists of the products of the following breakdown reaction: clinopyroxene + plagioclase ± K-feldspar ± orthopyroxene + H₂O + CO₂ → quartz + hornblende + calcite ± biotite. The reaction occurs in the undeformed protolith and progresses in the mylonite. Hornblende, quartz and calcite occur in extremely elongated polymineralic aggregates, where all the three phases have equant shape and homogeneous grain size (18-24 µm). In these layers, quartz has a very weak CPO with a c-axis maximum oriented at a low angle to the elongation direction. Overall, the microstructure suggests that the reaction products deformed dominantly by diffusion creep.

The feldspar-derived aggregate consists of fractured fragments of mesoperthite, surrounded by a bi-phase mixture of recrystallized plagioclase and K-feldspar. EBSD analysis indicates that the recrystallized grains originated as micro-fragments from fracture surfaces. In the recrystallized aggregate, plagioclase and K-feldspar show homogeneous grain size (26 µm), a very weak CPO (inconsistent with known slip systems), and the randomization of misorientation axes. Spatial distribution of K-feldspar and plagioclase shows a well dispersed aggregate and may serve as a tool to characterize diffusion creep deformation in phase mixtures. The dominant deformation mechanism is inferred to be diffusion creep.

In the ultramylonite the two compositional domains are indistinguishable and the degree of phase mixing is higher. Fractured fragments of mesoperthite are not preserved, the grain size of plagioclase, K-feldspar and quartz is further reduced (20 µm), and the main constituent phases do not show a CPO. Diffusion creep is interpreted to be the dominant deformation mechanism.

In summary, shear zone formation is invariably associated with a preliminary stage of cracking and fluid infiltration, which triggers syndeformational metamorphic reactions, strong grain size reduction, and activation of diffusion creep. Initial cracking at the estimated deformation conditions requires high differential stresses (in the absence of high pore pressures), and indicates a high strength of the lower continental crust at the onset of the deformation. A strain-dependent transition from dislocation creep to diffusion creep is not observed, and diffusion creep appears to be the dominant deformation mechanism in all compositional domains from the mylonite to ultramylonite stage.

Facing confrontation in coaxial deformation during the main Variscan tectonic event; SW Portuguese sector of Centro-Iberian Zone

Daniel Metodiev¹, José Romão¹, Rui Dias², António Ribeiro³

1 Department of Geology and Geological Mapping, National Laboratory of Energy and Geology, Lisbon, Portugal

2 Department of Geosciences and Évora Geophysical Center, Évora University, Portugal

*3 CEGUL and Department of Geology, Faculty of Sciences, Lisbon University, Portugal
daniel.metodiev@lneg.pt*

The SW sector of the Centro-Iberian Zone, which corresponds to the inner domain of the Iberian Variscides, is affected by a penetrative variscan progressive coaxial deformation. During the first and main Variscan deformation event (D1) the strong flattening in a NE-SW direction induces the pervasive folding of Cambrian to Silurian metasediments.

This deformation is more complex in the Cambrian metaturbidites of the Beiras Group, where the fold hinges can attain high plunges (70-80°) with a strong dispersion in their orientation. In the overlying quartzitic-shale layers of the Ordovician-Silurian succession the fold hinges (well exposed in the quartzites of the Armorican Formation) are sub-horizontal with a NW-SE direction. The folding event is coeval with a S1 cleavage which is the most penetrative structure at regional scale. This foliation is axial planar to the folds, which usually present an upright geometry giving rise to intersection lineations L1 with a low dispersion and sub-parallel to the fold hinges of the Ordovician-Silurian formations. However, in the Cambrian Beiras Group, L1 shows a strong dispersion. The contrast of the variscan deformation geometries between the Cambrian and Ordovician-Silurian metasediments is the result of the transient Sardinian deformation event. Considering the stretching lineations (X1) associated with the D1 Variscan event, they are always sub-perpendicular to the fold hinges of the Ordovician-Silurian formations, following the kinematic a axis. This behavior changes in the vicinity of the contact with the Ossa-Morena Zone, where X1 tend to be subhorizontal, following the kinematic b axis of the folds developed in the Ordovician-Silurian metasediments. This fact could be explained by the strong influence of the sinistral regional movement along the major Tomar-Badajoz-Cordova shear zone.

Spatially related with the main regional D1 folds are complex reverse faults which affect both limbs of the main Serra do Moradal-Fajão and Vila Velha de Ródão variscan synclines; such faults are also considered to be D1 variscan structures. The transport direction associated with these reverse faults is always sub-perpendicular to the fold hinges. The vergence of these reverse faults, as well as the facing of some second order related folds, is always towards the core of the first order regional folds; in the SW limb they are facing NE, while in the NE limb they have a SW vergence. This geometry induces a situation of confrontation in the inner domains of the orogeny during the main Variscan deformation event. Such geometry should be understood in the regional context. Indeed, the studied domain is developed between 2 first order asymmetric flower structures: the northern Douro and a southern one close to the boundary between the Ossa-Morena and Centro-Iberian Zones.

During the end of D1 the limits between the regional synclines are rejected by dextral (Sobreira Formosa) or sinistral (Ceira) shear zones. The existence of a tight confrontation area in the inner part of the SW sector of Centro-Iberian Zone suggests an inverse reactivation of syn-sedimentary faults of the Precambrian to Cambrian basement with NW-SE orientations. It conditioned the activity of the principal reverse faults during the Variscan orogenesis.

Gypsum cement microstructures in fractures related with extensional event (Vilobí gypsum unit, Vallès – Penedès Basin, Miocene, NE Spain)

Mar Moragas^{1,2}, C. Martínez¹, V. Baqués¹, G. Alías¹, E. Playà¹

¹ Dept. Geoquímica, Petrologia i Prospecció Geològica, Facultat de Geologia, Universitat de Barcelona, 08028 Barcelona, Spain

² Group of Dynamics of the Lithosphere (GDL), Institute of Earth Sciences Jaume Almera, ICTJA-CSIC, 08028, Barcelona, Spain

mmoragas@ictja.csic.es

Microstructural studies focused on gypsum cements precipitated along faults within evaporite host bodies are scarce. This is the main focus of this work, which has made it necessary to use concepts that are not typically applied to evaporite rocks and cements.

The Vilobí Gypsum Unit (Upper Burdigalian) is located in the Penedès half-graben, NE Iberian Peninsula. The half-graben is limited by ENE–WSW normal faults formed during the Neogene rifting stage of west Mediterranean area. The Vilobí unit consists of a succession up to 60 m thick of laminated to banded secondary (coming from anhydrite hydration) and primary gypsum that has been affected by two main deformation events: a ductile deformation represented by folds, millimetres to decimetres in size, which were produced during the early diagenesis, and a fragile deformation event related with the Neogene rifting. The later event affected the evaporite unit resulting in five sets of fractures of different time formation according to the cross-cutting relation (arranged chronologically from oldest to youngest):

- Set 1 (S1) consists of NE-SW trending extensional faults.
- Set 2 (S2) comprises a normal faults system with ENE-WSW trending.
- Set 3 (S3) formed by subvertical NW-dipping joints.
- Set 4 (S4) represented by NE-SW to ENE-WSW trending thrust faults.
- Set 5 (S5) comprises a SE-dipping system joints.

All fractures are refilled by gypsum cements with a large variety of deformation textures. It has been possible to observe direct relationship between main structures and microscopically observations of deformed samples. It could be established 4 stages of fracturing which reaffirm the chronology of precipitation and deformation defined at the outcrop scale.

- 1st Stage: Extensive context with active normal faults (S1 and S2). Antitaxial growths of fibrous gypsum cement indicating a shear sense in agreement with normal displacement, and incorporation of host-gypsum fragments and fish type crystals in shear zone.

- 2nd Stage: Tectonically stable stage with dilatation veins (S3) formation and precipitation of millimetre gypsum crystals.

- 3rd Stage: Compressive stage determined by outcrop indicators (S4), which represents reactivation of S1 and S2 faults. In that stage appear broken gypsum fibres and small gypsum fragments around irregular boundary of millimetre gypsum crystals.

- 4th Stage: Karstic regime in a relatively stable tectonic stage (S5). Megacrystalline gypsum cements precipitation with crystals up to 25 cm in size. These crystals show some indicators of small extensive stages as small oriented crystals (recrystallized) fragments in crystal boundaries, suggesting gentle tectonic reactivation events.

Minor deformations such as internal crystalline dislocations, grain contact and internal recrystallizations occur in millimetre gypsum crystals and megacrystalline cement.

Sulphur and oxygen isotope values indicate that gypsum cements were produced by sulphates-rich fluids which flow through the fragile structures after an interaction with host-gypsum rock. Consequently, it is significant that antitaxial growth of gypsum fibres in veins occurs in a host-rock with the same lithology, because this type of growth is common where the vein fill is different from the composition host-rock.

Scanning Electron Microscopy combined with Focused Ion Beam and potential applications on the nanometre-scale and 3D study of microstructures of geomaterials

Luiz F. G. Morales, Richard Wirth

*German Research Centre for Geosciences – GFZ – Telegrafenberg, 14473 Potsdam, Germany
luiz.morales@gfz-potsdam.de*

The recent development of scanning electron microscopy (SEM) systems integrated with focused ion beam (FIB) techniques has drawn the attention of material scientists for the new analytical possibilities at nanometre scale and in three-dimensions. Nevertheless, it was just in the last years that this technique was introduced in the study of minerals and rocks. The possibilities that emerge from the use of this tool on the study of microstructures, composition and crystallographic structure of geomaterials are remarkable. In these Dual Beam instruments, one has the combination of all capabilities of the FIB and the SEM in the same equipment. In addition to the standard SEM capabilities (secondary electron, back scattered, cathodoluminescence, EDX and EBSD detectors), the dual beam machines are suitable for TEM sample preparation, metal coating and orientation contrast imaging, as in a single FIB machine. In addition, high-angle annular dark field imaging (HAADF) using Z-contrast imaging in thin foils is possible, similarly as a TEM operating at low voltages. Through the mutual use of both guns, it is possible to generate 3D single images, 3D cross sectioning, 3D chemical analyses and 3D EBSD. Using the electron gun, the ion milling process can be better controlled and the preparation of very thin foils for HRTEM analyses (~30 nm thick) is possible. Of particular interest of the structural geology community is the possibility to study microstructures from μm to nm scale in three dimensions. This includes the observation and modelling of grain boundary network in 3D, microstructures in very-fine grained rocks (shales, ultracataclasites, ultramylonites), symplectites, myrmekites and metamorphic reaction rims. In addition, the possibility to make three-dimensional cross sections in thin-sections or directly in samples allows a better understanding on how the microstructures evolve with depth. The combination of the SEM/FIB allows the determination of crystallographic orientation in 3D, if the dual beam system is equipped with an EBSD camera. In this case, we first excavate a trench normal to the sample's surface with the FIB and polish it with different beam currents. After that we map the crystallographic orientation of the grains present in this surface. Subsequently we remove a thin layer (~0.1 μm) of this surface with the FIB operating at low beam currents and redo the crystallographic orientation map. By adding together the sequential EBSD maps in 2D we have a 3D representation of the grain orientation network. In addition to the CPO, we can also access the five parameters used to describe grain boundaries. Due the possibility to do 3D chemical analyses via EDX, it is also possible to quantify the volumes of individual phases in, for example, reaction rims in deformed rocks, which are particularly important for the quantification of metamorphic reactions. The use of FIB coupled with SEM imaging also allows the preparation of very small samples to be used for measurements of elastic properties under very high pressures in diamond cells, and possibly can be used for microsampling for isotope dating.

Strain partitioning of Variscan deformation in the Peso da Régua – Vila Nova de Foz Côa region (Centro-Iberian autochthon): The Douro Flower Structure

Noel Moreira¹, Mauro Búrcio², Rui Dias³, Carlos Coke⁴

1 Centro de Ciência Viva de Estremoz e LIRIO (Laboratório de Investigação de Rochas Industriais e Ornamentais da Escola de Ciências e Tecnologia da Universidade de Évora), Portugal

2 SOLICEL (Sociedade do Centro Industrial de Esteios de Lousa, Lda) e LIRIO, Portugal

3 Escola de Ciências e tecnologia da Universidade de Évora (LIRIO e Departamento de Geologia) e CGE (Centro de Geofísica de Évora), Portugal

*4 Universidade de Trás-os-Montes e Alto Douro, Departamento de Geologia e CGE, Portugal
nmoreira@estremoz.cienciaviva.pt*

Previous studies in Serra do Marão (Central-Iberian Zone autochthon; Coke, 2000) showed the juxtaposing of early Paleozoic sectors where the first and main Variscan deformation (D1) is incipient, with sectors where this deformation is quite pronounced. Kinematic criteria in the most deformed areas show that sinistral shear zones are pervasive; such a behaviour is compatible with the sinistral transpressive regime described for the most northern sectors of the of Central-Iberian autochthon (e.g. Ribeiro et al, 1990).

The structure displayed further east on Cambrian formations of Douro Group in Peso da Régua and Vila Nova de Foz Côa shows a similar alternation of wide less deformed areas with narrow bands emphasizing stronger Variscan deformation. These narrow bands, with a general WNW-ESE direction, show a close to isoclinal folding, with a penetrative cleavage; these folds, which have no vergence were associated with the sinistral shear zones. On the wide and less deformed areas, the folds are open, with WNW-ESE subvertical axial planes. The fold axis have a low dispersion and are subparallel to the intersection lineation L1, emphasizing the absence of transection on this sector.

In the northern sector of Peso da Régua area, it's clear an increase of deformation. The sinistral shear-zones are now predominant and the related folds are asymmetric with vergence to NNE quadrant. This sector makes the transition for the more deformed domains that usually characterize the Central-Iberian autochthonous.

So, the studied sectors are characterized by a structural pattern with a central domain with WNW-ESE open variscan folds subparallel to narrow sinistral shear zones; this domain is bounded to the north and south by major sinistral shears. Outside these boundaries the folds becomes asymmetrical with vergence to SSW on southern edge and to NNE in the northern one edge. Such geometry is possible to follow from the Serra do Marão to Vila Nova de Foz Côa near to the Spanish border.

Such structural pattern characterizes the axial zone of a flower structure, due to the sinistral transpressive regime in northern sectors of the Centro Iberian autochthon during the Variscan Orogeny. This structure is here named Douro Flower Structure.

The lateral continuity of this regional major D1 structure, that was possible to put in evidence by this work, is only interrupted by NNE-SSE Tardi-Variscan sinistral shear-zones (e.g. Manteigas-Vilariça-Bragança and Penacova-Régua-Verin faults). Such faults were reactivated during Alpine Orogeny, with the same sinistral kinematic component.

REFERENCES

- COKE (2000) – Evolução Geodinâmica do Ramo Sul da Serra do Marão; um caso de deformação progressiva em orógenos transpressivos. (unpublished PhD Thesis), Trás-os-Montes e Alto Douro University, Vila Real.
- RIBEIRO, A., PEREIRA, E. & DIAS, R. (1990) – Structure of Centro-Iberian allochthon in northern Portugal. In R. DALLMEYER AND E. MARTINEZ GARCIA (Eds.), *Pre-Mesozoic Geology of Iberia*, 220-236, Berlin: Springer-Verlag.

Tomar-Badajoz-Córdoba shear zone in Abrantes region; the presence of a kilometric sheath fold?

Noel Moreira¹, Jorge Pedro², Rui Dias³, António Ribeiro⁴, José Romão⁵

¹ Centro de Ciência Viva de Estremoz e LIRIO (Laboratório de Investigação de Rochas Industriais e Ornamentais da Escola de Ciências e Tecnologia da Universidade de Évora), Portugal

² Dep. Geociências da Escola de Ciências e Tecnologia da Universidade de Évora, CeGUL (Centro de Geologia da Universidade de Lisboa), Portugal

³ Escola de Ciências e Tecnologia da Universidade de Évora (LIRIO e Departamento de Geologia) e CGE (Centro de Geofísica de Évora), Portugal

⁴ Dep. Geologia (Fac. Ciências / Univ. Lisboa); CeGUL (Centro de Geologia da Universidade de Lisboa); Museu Nacional de História Natural, Portugal

⁵ LNEG-LGM, Unidade de Investigação de Geologia e Cartografia Geológica, Portugal
nmoreira@estremoz.cienciaviva.pt

The Tomar-Badajoz-Cordoba shear zone (TBCSZ) and the Porto-Tomar-Ferreira do Alentejo shear zones (PTFASZ) are two of the major variscan structures in the Iberian Massif. Their characterization is thus crucial to understand the geodynamic evolution of the Iberian Variscan Chain. These two major shear zones intersect in the Abrantes region (Ribeiro et al, 2007), which is regarded as a structural key sector. The sinistral of TBCSZ and the dextral of PTFASZ Variscan kinematics induced space problems and controls the structure of Abrantes region in the western segment of the TBCSZ.

Previous field-work this region (Gonçalves et al, 1979) reports a flower structure geometry with changes in the vergence change from SW in the western sector to NE in the eastern one of Abrantes region. However, latter studies along the TBCSZ emphasize the possibility of a kilometric sheath fold structure instead of the flower structure geometry that characterize most of the TBCSZ (e.g. Ribeiro et al, in press; Romão et al, 2010). Nonetheless, recent data, presented in this work, show a more complex structure in the Abrantes region resulting from two Variscan distinct deformation phases.

The first phase (D1) generate a penetrative foliation slightly dipping to SE, stretching lineation plunging to SE and macro- and micro-structural kinematic criteria indicating transport to NW. The D1 phase is evident in the syn-tectonic Granite of the Pedreira de Maiorga where flow structures, with c-planes, and thrusting kinematics to NW are observed. The L and SL tectonic fabrics are frequently observed in this granite and indicates tectonic stress during the magmatic cooling process. In the "Série Negra" (classic definition assigned to the neo-Proterozoic formations of the Ossa-Morena Zone) sheath folds are associated with D1 foliation. This foliation is characterized by rich green amphibole levels (actinolitic hornblende?) interspersed with rich alkali feldspar + quartz + plagioclase levels.

The second deformation phase (D2) produces isoclinal folding of the D1 foliation and generate an incipient cleavage, defined by microscopic textures of amphibole. Furthermore the D1 thrusting structures are also affected by D2 and shows, side by side, sinistral and dextral kinematic criteria. Therefore, in the Abrantes region the D1 should be associated with the genesis of a kilometric sheath fold, with transport to NW, while the D2, with isoclinal folding, obliterate the earlier structures.

REFERENCES

- Gonçalves, F., Zbyszewski, G., Carvalhosa, A. & Coelho, A. (1979) - "Carta Geológica de Portugal à escala 1/50000; folha 27-D - Abrantes". Serv. Geol. Portugal
- Ribeiro, A., Munhá, J., Dias, R., Mateus, A., Pereira, E., Ribeiro, L., Fonseca, P., Araújo, A., Oliveira, T., Romão, J., Chaminé, H., Coke, C., & Pedro, J. (2007) - "Geodynamic evolution of the SW Europe Variscides". *Tectonics*, 26, Art. Nº TC6009, doi: 10.1029/2006TC002058, 24 p.
- Ribeiro, A., Romão, J., Munhá, J., Rodrigues, J. F., Pereira, E., Mateus, A., Araújo, A., & Dias, R. (in press) - "Relações tectono-estratigráficas e fronteiras entre as Zonas Centro-Ibérica e Ossa-Morena do Terreno Ibérico e o Terreno Finisterra", In R. Dias, A. Araújo, P. Terrinha e J. Kullberg (Eds.), *Geologia de Portugal*, Livraria Escolar Editora.
- Romão, J., Ribeiro, A., Pereira, E., Fonseca, P., Rodrigues, J., Mateus, A., Noronha, F. & Dias, R. (2009) - Interplate versus intraplate strike-slip deformed belts: examples from SW Iberia Variscides. *Trabajos de Geologia*, V. 29, pp. 671-677, Oviedo, Spain.

Reconstruction of thrust-related folds from superficial data: comparison of different balanced interpretations

Isabel Moriano, Josep Poblet, Mayte Bulnes

*Departamento de Geología, Universidad de Oviedo, Spain
imoriano@geol.uniovi.es*

Several authors have proposed different methods to predict the subsurface geometry of thrust-related folds from shallow baseline data. Given certain bed dips of a backlimb, crest and forelimb of a fold model, we reconstructed the structure at depth as a fault-bend, a fault-propagation and a detachment fold following these methods and we checked that the resulting geological cross-sections were balanced. In addition, we modified the position of the surface dips so that the resulting fold models had different half-wavelengths and different structural relief and, therefore, allowing chevron folds and box folds to be constructed. In order to compare the different balanced interpretations, we elaborated several graphs in which various geometrical parameters (shortening, detachment depth and dimensions of the thrust ramp) are plotted versus the half-wavelength and the structural relief. We analyzed the evolution of the geometrical parameters with the rise in half-wavelength and with the rise in structural relief and we compared the value of the geometrical parameters depending on the type of fold interpreted.

Finally, several methods for the reconstruction of the deep geometry of thrust-related folds are applied to both natural and experimental examples of fault-bend folds. The full geometry of these examples is known, but we predicted their deep geometry assuming that only superficial data were available and, therefore, the structures could be reconstructed as fault-bend, fault-propagation and detachment folds. We utilized two groups of methods; to apply the first group of methods, the available baseline data were the superficial stratigraphic horizons not affected by thrusting, whereas to apply the second group of methods we employed a portion of the thrust and some deeper horizons. Eventually, we obtained a set of solutions that fit the baseline data. We calculated the deviation of the geometrical parameters measured in the reconstructions with respect to the true value measured in the natural or experimental folds analyzed.

Contribution to the study of recent tectonic movements: the application of the watershed of Ourika (High Atlas of Marrakech)

Mustapha Namous¹, Mostafa Amrhar¹, Bernard Delcaillau², Edgard Laville², Olivier Dugué²

*¹ Université Cadi Ayyad, Faculté des Sciences, Semlalia, BP 2390, 40000, Marrakech, Maroc,
² UMR, CNRS 6143 Morphodynamique Continentale et Côtière, 24 rue des Tilleuls, F14000 Caen, France
mustaphanamous@yahoo.fr*

The watershed of Ourika is a basin incised mountain slopes in the north-west of the High Atlas of Marrakech. This study is based on the evaluation of the index of slope failure rivers (Hack, 1973). The SLI (Stream Length Index), calculated on the entire drainage basin of Ourika, said segments of streams showing slope failures related to lithological factors (differential erosion) or tectonic (recent tectonic movements) (Delcaillau et al., 2010). The values obtained for the whole drainage pattern are shown in isovalue map of the entire watershed.

The results highlight three anomalous zones where rivers are breaks of steep slopes, two anomalous zone are located downstream of the basin, they are caused by lithological variations, the stream rivers cut into conglomerates upstream slope failures, and friable siltstones downstream. The third zone of anomalies is upstream of the basin and is concentrated along the Tizi n'Test fault zone, lithology is homogeneous along the knickzone, these result suggest the tectonic origin of slope failure and confirmed the reactivation of this fault system in the Quaternary period.

REFERENCES

- Hack, J., 1973. Stream-profile analysis and stream gradient index. U. S. Geological Survey Journal of Research 1, 421–429.
Delcaillau, B., Laville, E., Amrhar, M., Namous, M., Dugué, O., Pedoja, K., 2010. Quaternary evolution of the Marrakech High Atlas and morphotectonic evidence of activity along the Tizi N'Test Fault, Morocco. *Geomorphology* 118 (3-4), 262-279.

Experimental deformation, partial melting, and compositional changes in perthitic K-feldspar at high pressure and temperature

Marianne Negrini, Holger Stünitz, Luca Menegon

*Institutt for geologi, Universitetet i Tromsø, Dramsveien 201, N-9037 Tromsø, Norway
marianne.negrini@uit.no*

We performed (i) axial compression experiments on natural perthitic K-feldspar single crystals (compression normal to the {010} plane), (ii) shear experiments (on 10-20 μm grain size powder obtained from the same perthitic K-feldspar) and (iii) hydrostatic experiments (on powder and on single crystals). The experiments were carried out in a solid medium Griggs-type deformation apparatus at T of 900°C, confining pressures varying from 0.75-1.5 GPa and axial shortening ranging from 3 to 40% at a constant strain rate of $\sim 10^{-6} \text{ s}^{-1}$. Samples were deformed as-is and with added H₂O (up to 0.2 wt %).

Deformation in all single crystal samples is accommodated by shear fractures, where melt is present in variable amounts. The mechanical data for K-feldspar at 900°C and 1.0 GPa indicate flow stresses of 450-500 MPa (clearly below the Goetze criterion) and a marked decrease in peak strength with increasing confining pressure (flow stress at 1.5 GPa is 330 MPa, at 0.75GPa it is 680 MPa). The inverse normal stress dependence and peak stresses below the Goetze criterion indicate that along the cracks deformation is not friction controlled.

The single-crystal experiments contains less than 7vol% melt, distributed along cracks and shear zones oriented at 40° to σ_1 . EPMA analysis reveal an inhomogenous composition of the melt suggesting that the melt pockets along the cracks are not interconnected.

In experiments using powder (900C, 1.0 GPa conf. P) the melt fraction is higher and is distributed around single grains, which are completely homogenized (Ab21 An0 Or79), although the strength of the material is relatively high (100-150 MPa) and similar to the strength of deformed Labradorite (Stünitz and Tullis, 2001) where no melt was detected.

Zones of compositional homogenization have the same orientation as the conjugate cracks and are therefore related to the cracking processes. Homogenization is well visible in the fine-grained fragments of the gouges, which have an intermediate chemical composition between the K-feldspar (Ab8 An0 Or92) and the albite lamellae (Ab98 An1 Or1) of the starting material, indicating nucleation and growth of new grains.

The observations described above suggest that the deformation of feldspar at high pressure and temperature is promoted by a simultaneous formation of micro-cracks and melt formation. The formation of wet melt is accelerated by cracking as demonstrated by the different amounts of melt in hydrostatic and deformation experiments. Melt formation occurs faster at higher confining pressure, and weakens the faults which is demonstrated by the inverse dependency of peak-strength with confining pressure. The melt along the cracks accommodates the deformation by viscous processes (lubrication), but it does not produce very weak samples because at the low melt fraction of ~7% the melt pockets are not interconnected. The coalescence of the initial microcracks generate conjugate cracks in which the fine grained gouge undergoes chemical homogenization. The very fine fragments of the gouge act as nucleation sites. The deformation mechanism in the gouge may be dissolution-precipitation creep, demonstrated by the dissolution-precipitation processes.

Frictional properties of Zuccale Fault rocks from room temperature to in-situ conditions: results from high strain rotary shear experiments

André Niemeijer¹, Cristiano Collettini², Chris Spiers¹

¹ Utrecht University, Faculty of Geosciences, HPT Laboratory, The Netherlands

² Dipartimento di Scienze della Terra Università degli Studi di Perugia, Italy

niemeijer@geo.uu.nl

The Zuccale fault is a regionally-important, low-angle normal fault, exposed on the Isle of Elba in Central Italy, that accommodated a total shear displacement of 6-8 km. The fault zone structure and fault rocks formed at less than 8 km crustal depth. The present-day fault structure is the final product of several deformation processes superposed during the fault history. Here, we focus on a series of highly foliated and phyllosilicate-rich fault rocks that represent the basal horizon of the detachment. Previous experimental work on foliated, intact samples, sheared in their in-situ microstructural (foliated) condition, demonstrated a markedly lower friction coefficient compared to homogeneously mixed powdered samples of the same material. We concluded from these experiments that the existence of a continuous, through-going foliation provides numerous planes of weakness on which shear deformation could be accommodated. However, these experiments were performed under room-dry and room temperature conditions. Moreover, the question remains as to how foliation is formed in these rocks in the first place. In this study, we report results from a series of preliminary rotary shear experiments performed on 1 mm thick powders made from two fault rock types obtained from the Zuccale Fault. The tests were done under conditions ranging from room temperature to in-situ conditions (i.e. at temperatures of 250-350 °C, applied normal stresses up to 200 MPa and fluid-saturated). Samples consisting of calcite, talc, chlorite and kaolinite (sample ZF01) and of calcite, tremolite, hornblende, kaolinite, chlorite and quartz (sample ZF02) were sheared at sliding velocities of 1-300 $\mu\text{m/s}$ to displacements larger than 40 mm (i.e. $\gamma > 40$). Sample ZF01 was weaker than sample ZF02 at all conditions investigated. We attribute the lower strength of sample ZF01 to the weak talc present in this sample as opposed to sample ZF02 which contains mainly stronger hornblende as the phyllosilicate phase. Both samples showed some weakening with increasing temperature and displacement as well as pronounced velocity-strengthening behaviour, in agreement with previous work. The results suggest that phyllosilicate-bearing fault rocks can deform by stable, aseismic creep at low resolved shear stress and low shear rate conditions, where a continuous foliation may develop. We are presently characterizing the frictional properties of the different portions of the Zuccale fault under in-situ conditions to determine whether the foliation can be destroyed at higher sliding velocities, perhaps resulting in velocity-weakening behaviour. This has important implications for potential rupture dimensions in this geometrically complex fault zone.

Transtensional megashear zones in the Central Andes: the Hualilán Belt (Precordillera, Argentina)

Sebastián Oriolo¹, **Silvia Japas**², E.O. Cristallini³

1Departamento de Ciencias Geológicas, Facultad de Ciencias Exactas y Naturales, Universidad de Buenos Aires, Argentina

2 IGEBA, Universidad de Buenos Aires – CONICET, Argentina

*3Laboratorio de Modelado Geológico, IDEAN, Universidad de Buenos Aires – CONICET, Argentina
seba-sur@hotmail.com*

The Pampean flat-slab segment located between 27°–33° S in the Central Andes shows migration of deformation and magmatism due to the subduction of the Juan Fernández Ridge. It is also composed of several terranes that have amalgamated since Early Paleozoic times (Ramos 1999), so the interaction between previous anisotropies and the current tectonic regime gives rise to strongly heterogeneous deformation.

The Precordillera of San Juan is a thin- (Western and Central Precordillera) and thick-skinned (Eastern Precordillera) fold and thrust belt that was formed during the Tertiary Andean Orogeny. In the Hualilán Area, preliminary structural data and tectonic fabric analysis have revealed the presence of a set of WNW faults that divide the Sierra de la Mina into blocks, and strong WNW transtensional fabrics in the Lower Paleozoic and Miocene rocks that make up this range. WNW lineaments also control the drainage network and can be traced to the west in the Sierra de la Invernada. They would even represent the main boundaries of the swamp that develops in southeastern Hualilán.

According to previous works (Japas 1998, Ré et al. 2000, Japas et al. 2002a and b, Ré and Japas 2004), two systems of conjugated megashear zones can be defined in the Central Andes: left-lateral NNW and right-lateral NNE transpressional sets, and left-lateral WNW and right-lateral ENE transtensional ones. The Hualilán Belt would be equivalent to one of these left-lateral WNW transtensional megashear zones, which would have been controlled by pre-Tertiary structures as previous works have shown.

Further information obtained from deformation fabrics, structural, paleomagnetic and analogue modelling data (work in progress) will help to define the boundaries of the Hualilán Belt and its evolution linked to an oblique convergent margin. Therefore, they will put light on the relationship of the different transpressional/transtensional megashear zones that were already defined in the Pampean flat-slab segment.

REFERENCES

- Japas, M.S., 1998. Aporte del análisis de fábrica deformacional al estudio de la faja orogénica andina. Homenaje al Dr. Arturo J. AMOS. *Revista de la Asociación Geológica Argentina* 53 (1): 15.
- Japas, M.S., Ré, G.H. y Barredo, S.P., 2002a. Lineamientos andinos oblicuos (entre 22°S y 33°S) definidos a partir de fábricas tectónicas. I. Fábricas deformacional y de sismicidad. *15° Cong. Geol. Arg.*, 1: 326-331.
- Japas, M.S., Ré, G.H. y Barredo, S.P., 2002b. Lineamientos andinos oblicuos definidos a partir de fábricas tectónicas (segmento 22°S y 33°S). III. Modelo cinemático. *15° Cong. Geol. Arg.* 1: 340-343.
- Ramos, V., 1999. Plate tectonics setting of the Andean Cordillera. *Episodes* 22(3):183-190.
- Ré, G.H., Japas, M.S. y Barredo, S.P., 2000. Análisis de fábrica deformacional: El concepto fractal cualitativo aplicado a la definición de lineamientos cinemáticos neógenos en el Noroeste Argentino. *Avances en Microtectónica. Asoc. Geol. Arg. Serie D: Publ. Esp.* 5: 75-82. 10° Reunión sobre Microtectónica.
- Ré, G.H. and Japas, M.S. 2004. Andean oblique megashear zones: Paleomagnetism contribution. *GSA Annual Meeting, Abstract with Programs*, 36 (5).

Analogue rheological modelling of lithospheric orocline bending. Implications on the development of the Ibero-Armorican Arc

Daniel Pastor-Galán¹, **Gabriel Gutiérrez-Alonso**¹, Gernold Zulauf², Carlo Dietl², Friedhelm Zanella³

1 Departamento de Geología, Universidad de Salamanca, Spain

2 Institut für Geowissenschaften, Goethe-Universität, Frankfurt am Main, Germany

*3 Institut für Neuroradiologie, Goethe-Universität, Frankfurt am Main, Germany
gabi@usal.es*

The Western European Variscan Belt resulted basically from the collision between Gondwana and Laurussia during Devonian-Carboniferous times. This belt is characterized by the presence of a highly arcuate geometry known as Ibero-Armorican Arc. The evolution of the arc has been constrained paleomagnetically as an orocline that was generated from an almost initially linear belt in its core, the Cantabrian Zone, northern Iberia and took place in the uppermost Carboniferous, between ca. 310 and 300 Ma. Given the large scale of this plate-scale structure, it is bound to have had a profound effect on the whole lithosphere and consequently the effects of the involvement of the lithosphere should be recognized in structures and geological features of different nature and at different scales developed coevally with the orocline. In order to understand such process, nowadays, analogue modelling is the only reliable way to understand the lithospheric behaviour in 3D due to the computer calculating limitations for mathematical accurate 3D modelling.

In order to perform the modelling of the buckling process and its subsequent lithospheric delamination we have performed a two stage experiment in which, using the same materials and thermal boundary conditions, we have first simulated the buckling process in a thermo-mechanical apparatus (press). In this experiment we have obtained the resulting geometry after buckling an initially linear lithospheric segment. The second simulation was performed adding gravity to the previously obtained geometry, by means of a thermo-centrifuge machine, to test the possibility of lithospheric delamination where the mantle lithosphere had been previously thickened.

The first type of experiments show that during orocline buckling, regardless of the thickness of the different layers used or the strain rate, the mantle lithosphere is thickened in the core of the orocline and is thinned in the outer arc. Differences in the way the mantle lithosphere thickens are observed in relation with the initial lithospheric thickness considered. While the thickest mantle lithosphere thickens by generating a cone shaped mullion or a very tight conical fold, the thin mantle lithosphere thickens by conical and recumbent folding or is duplicated by thrusting in a similar way to subduction zones. On the other hand, the thinning in the outer arc is always obtained by radial tension fractures. Moreover, in some experiments strain was accommodated by dextral shear zones.

The subsequent centrifuge experiments reveal that delamination of the lithospheric thickening (root) with the analogue materials selected is possible and easy to get when the conditions were appropriate.

The new experimental results are in agreement with the models proposed about the expected lithospheric thickening under orocline bending conditions and provide new possible geometries for this thickened lithosphere that back up other simple digital models. Furthermore, the delamination of the selected materials to model the lithosphere behaviour is possible under analogue conditions and can explain the abundance of post-orogenic magmatic rocks in the core of the Ibero-Armorican Arc.

Rheology of granitoid fault rocks at the “brittle-to-plastic” transition: an experimental study

Matej Pec¹, Holger Stünitz², Renée Heilbronner¹

¹ Department of Geosciences, University of Basel, Basel, Switzerland

² Institutt for geologi, Universitetet i Tromsø, Tromsø, Norway

matej.pec@unibas.ch

Some of the largest earthquakes in the continental crust nucleate at the “brittle-to-plastic” transition at depths of ~ 10 – 20 km indicating that stresses can be released by rupture at elevated confining pressures and temperatures. In addition, experimental studies, field observations, and models predict that the strength of the lithosphere should be at its peak at these depths where the rocks deform by “semi-brittle” flow. Thus, the understanding of deformation processes taking place at these conditions is important for a better understanding of the seismic cycle and the rheology of faults in general.

We performed a series of experiments where crushed Verzasca gneiss powder (grain size $\leq 200 \mu\text{m}$) with varying water content (“pre-dried” and 0.2 wt% H₂O added) was placed between alumina forcing blocks pre-cut at 45° and weld-sealed in platinum jackets. The experiments were performed at 500, 1000 and 1500 MPa confining pressure, at temperatures of 300°C and 500°C and shear strain rates of $\sim 1.5 \times 10^{-3} \text{ s}^{-1}$ to $1.5 \times 10^{-5} \text{ s}^{-1}$ in a solid medium deformation apparatus (Griggs rig).

Samples deformed at 500 MPa confining pressure attain their peak strength around shear strains of $\gamma \sim 2$. Subsequently, samples weaken by $\sim 20 \text{ MPa}$ at 300°C and $\sim 140 \text{ MPa}$ at 500°C. We observe that the 300°C experiments are systematically stronger by $\sim 330 - 370 \text{ MPa}$ than the 500°C experiments. Furthermore, we observe a systematical stress increase with increasing strain rate.

At higher confining pressures (1000 and 1500 MPa) we observe that peak strength is reached at shear strains of $\gamma \sim 1 - 1.5$ followed by strain weakening to a stress lower than peak strength of ~ 60 at 300°C and $\sim 150 \text{ MPa}$ at 500°C. The strength difference between 300°C and 500°C samples is 270 – 330 MPa and does not increase with increasing confining pressure. The peak strength increase with a 500 MPa increase in confining pressure is modest (50 – 150 MPa at stress levels of 1200 – 1600 MPa) indicating that the rocks reach their maximal compressive strength.

Microstructural observations at different strains show the development of an S-C-C’ fabric with C’ slip zones being the dominant feature. At low strains, the gouge zone is pervasively cut by closely spaced C’ shears containing extremely fine-grained material ($< 100 \text{ nm}$ grain size). At peak strength, deformation localizes into less densely spaced, $\sim 10 \mu\text{m}$ thick C’ – C slip zones which most likely are amorphous and develop predominantly in feldspars. After peak strength the slip zones accommodate most of the displacement and we observe the formation of fine grained ($\sim 500 \text{ nm}$) Al-rich reaction products within the slip zones.

Quartz grains show the lowest degree of fragmentation and represent the rheologically strongest phase. Feldspar grains fracture more easily and are the weakest phase. The development of the bulk microstructure evolves with finite strain and does not show dependence on temperature.

CL observations, EDS maps and WDS microprobe data show changes in chemical composition in the slip zones indicating that mechanical disintegration of the grains is accompanied by transport of alkalis, producing a different mineral chemistry even at the short experimental time scale (~ 20 minutes to 30 hours).

Our results indicate that in “semi-brittle” flow, fracturing produces large amounts of extremely fine-grained material, which is a pre-cursor to probably amorphous material. Once a thru-going network is formed, viscous flow including mass-transfer processes within slip zones accompanies brittle deformation and at least in part controls the strength of the samples.

Kinematics of the Northern Betic Cordillera from gypsum fabrics (South Spain): Tectonic implications

Fernando Pérez-Valera¹, M. Sánchez-Gómez¹, L.A. Pérez-Valera¹, A. Pérez-López^{2,3}

1Departamento de Geología. Facultad de Ciencias Experimentales. Universidad de Jaén. Campus Las Lagunillas, s/n. 23071. Jaén.

2Departamento de Estratigrafía y Paleontología. Facultad de Ciencias. Universidad de Granada. Avda. Fuentenueva s/n. 08071. Granada.

3Instituto Andaluz de Ciencias de la Tierra (CSIC-Universidad de Granada). Avda. Fuentenueva s/n. 08071. Granada.

fperez@ujaen.es

The Betic Cordillera ends to the north forming an intricate mountain front over the Guadalquivir basin, where gypsum-bearing rocks, of Triassic origin (South-Iberian Germanic facies), are predominant along the main tectonic contacts. Nevertheless, Triassic rocks has been traditionally attributed to two lithostratigraphic units, the 'Subbetic Chaotic Complex' and the 'Olistostromic Unit', which are mapped undifferentiated with other Mesozoic rocks of Subbetic origin, or middle Miocene sediments. Other interpretations explain the geology of the area by means of lateral diapirs emplaced with a randomly distribution of blocks, inside of a limited accretionary prism.

A detailed analysis of the Triassic rocks shows structures from microscale to cartographic scale. Nice tectonic fabrics with consistent kinematic criteria contradict the classically admitted re-sedimentary (olistostromic) origin. Moreover, the cartographic structures that can be mapped consist in arc-shaped thrusts, limited by dextral transcurrent fault zones, all of them with a dominating direction of transport that ranges from E-W to ESE-WNW. In other cases, apparently disconnected outcrops of Triassic evaporites, together with other Subbetic rocks, outline hidden tectonic contacts that can be assimilate to the thrust or wrench fault zones.

In this work, a representative number of outcrops of Triassic rocks have been analyzed. Cataclastic and pseudoplastic fabrics are penetrative and show clear kinematic criteria, well preserved in gypsum-bearing rocks and/or lutites, in with scaly fabric is also developed. A collection of linear features has been found, these ones range from pervasive slickenlines in clay-bearing rocks to mineral lineation (stretching lineation) in gypsum mylonitic fabrics, pressure shadows and gypsum tails over rigid clasts. The fabrics indicate also sense of shearing with two main orientations: top to N 20 and to N 290, correlating respectively with the well known N-S and E-W folds developed over Jurassic and Cretaceous carbonated units cropping out south of the studied area. This fold sets can be observed also affecting to the lower Miocene sediments of the Guadalquivir basin.

We conclude that the previously considered chaotic or olistostromic unit of sedimentary origin corresponds to a tectonic *mélange* zone, forming an accretionary complex, where evaporites play a key role at the front of the Betic Cordillera with its foreland basin (Guadalquivir Basin). Kinematics data, obtain from outcrop-scale structures and more than 25 micro-tectonic stations, indicates that tectonic transport varies from top-to-the west along the middle Miocene towards top-to-the north until nowadays. Therefore, gypsum-bearing rocks became an inestimable tool to elucidate the kinematic regime of non metamorphic complex tectonic areas, since gypsum can be plastically deformed at low temperatures and pressures.

Initiation and evolution of shear zone-related lozenges

Carlos Ponce, Elena Druguet, Jordi Carreras

Dept. de Geologia, Universitat Autònoma de Barcelona, Spain.
carlos.ponce@uab.cat

Lozenges are ellipsoidal structures of country rocks completely surrounded by mylonites. They appear mainly in highly heterogeneous ductile deformation domains where shear zones abound, enclosing non-deformed or less-deformed rock. Lozenges have an elongate shape, with the long and short axis at a low and high angle to the shear zone average plane respectively. Their asymmetry can be used as a kinematic indicator if some caution is taken, especially when lozenges are developed in foliated rocks, as the anisotropy can induce kinematic and geometrical complexities (Carreras, 1997).

A typology of lozenges is needed to constraint the mechanical frame where the lozenge develops. Two criteria regarding the rheology of the host rocks can be considered: (i) homogeneity/inhomogeneity, and (ii) isotropy/anisotropy. Their combination gives rise to four different cases.

In both cases of inhomogeneous rocks, the lozenge appears due to the rheological contrast. The formation and development of the lozenge is mainly controlled by the competence contrast and by the initial shape of the body building up the lozenge, usually the relatively more competent rock. Strain localizes at the interface between different materials, with shear zones developing in the softer matrix, surrounding the non- or less-deformed competent object.

In the case of deforming homogeneous rocks, the initiation, development and evolution, and thus the final geometry of lozenges, are controlled by the geometry and kinematics of the bounding shear zones. However, for anisotropic homogeneous rocks, the presence of a previous foliation induces strain and kinematic partitioning and thus is responsible for a greater complexity with a variety of possible development mechanisms. Five processes that may lead to the development of lozenges are proposed on the basis of detail mapping and analysis of structures in the field study area (Cap de Creus, Eastern Pyrenees; Fig.1). The first two typically operate in both cases (isotropic or anisotropic rocks), while the last three models are more characteristic of anisotropic homogeneous rocks.

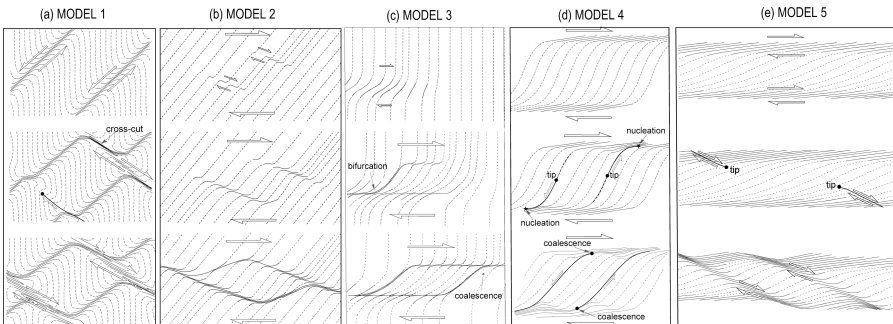


Fig. 1.- Models for the development of lozenges

(1) Intersection of two sets of differently oriented shear zones. The presence of conjugate shear systems (Williams and Price, 1990) can give rise to the typical millipede structures (Bell, 1981).

(2) Interaction and linkage of two overstepping sub-parallel shears throughout their curving propagation.

(3) Transfer of a shear zone to a parallel plane by propagating through the anisotropy.

(4) Linkage of individual shear zones of a dominant set throughout antithetic shears that propagate sub-parallel to the pre-existing foliation (Lister and Williams, 1979; Carreras, 2001).

(5) Development of extensional crenulation cleavages or shear bands on an already developed heterogeneous mylonitic fabric.

With progressive deformation, the geometry of the lozenge changes. The bounding shear zones tend to parallelize and this causes further lozenge elongation. The long and short axis rotates synthetically with the main shear sense (except for model 1), and therefore there is a decrease in lozenge asymmetry with respect to the shear plane. Consequently, the lozenge can experience rigid rotation and/or internal deformation. This internal deformation can be achieved either through folding and stretching, but also through foliation-parallel shearing in the case of foliated rocks.

REFERENCES

- Bell, T.H., 1981. Foliation development—the contribution, geometry and significance of progressive, bulk, inhomogeneous shortening. *Tectonophysics* 75, 273–296.
- Carreras, J., 1997. *Evolution of Geological Structures in Micro- to –Macro-scales*. Edited by S. Sengupta. Published in 1997 by Chapman & Hall, London.
- Carreras, J., 2001. Zooming on Northern Cap de Creus shear zones. *Journal of Structural Geology* 23, 1457–1486.
- Lister, G.S., Williams, P.F., 1979. Fabric development in shear zones, theoretical controls and observed phenomena, *Journal of Structural Geology* 1, 283–297.
- Williams, P.F., Price, G.P., 1990. Origin of kink bands and shear-band cleavage in shear zones: an experimental study. *Journal of Structural Geology* 12, 145–164.

Microdeformation of Carrara marble

Alejandra Quintanilla-Terminel, J. Brian Evans

*1 Department of Earth, Atmospheric and Planetary Sciences, Massachusetts Institute of Technology, USA
alequte@mit.edu*

Characterizing the strain localization, material heterogeneity, and mechanical anisotropy in rocks plays a critical role in the understanding of orogenic processes. By combining a high-resolution surface mapping technique with a split cylinder experiment, the local strain heterogeneities developed during deformation can be quantitatively measured. We have developed a micro-fabrication technique that allows us to deposit an axiscoordinated grid with marks spaced at ten micrometers intervals and have applied it to Carrara marble. A metal grid including a coordinated number system is deposited on the polished surface of a half cylinder of the rock sample. We then perform conventional triaxial mechanical tests in a Paterson Instruments machine on the composite samples of two half-cylinders. Images of the gridded surface before and after deformation are acquired using a digital microscope and the position of the grid markers is mapped using an edge detector algorithm. The micro-scale strain distribution is then computed in both 2D and 3D scale using an n point average technique, which provides resolution of strain heterogeneities at the same scale as strain predictions from FFT viscoelastic models. We present here the first exploratory experiments. The results show that the size of the strain heterogeneities depends on the deformation conditions and could be used to infer the mechanical history of naturally deformed rocks.

Rheological contrast at the continental Moho: effects of composition, temperature, deformation mechanism, and tectonic regime

Giorgio Ranalli¹, M. Adams²

¹Department of Earth Sciences, Carleton University, Ottawa K1S 5B6, Canada

²Department of Mathematics and Statistics, McGill University, Montréal H3A 2K6, Canada

The rheological contrast at the Moho can be an important factor in continental tectonics, as it affects the rheological stratification of the lithosphere, the possibility of horizontal decoupling and delamination, and the overall response of the lithosphere to tectonic stresses. Two commonly debated lithosphere rheological models (“jelly sandwich” vs. “crème brûlée”) depend in part on the occurrence and magnitude of a strength difference between lowermost crust and uppermost lithospheric mantle.

The strength difference at the Moho depends on several parameters, such as composition of lower crust and lithospheric mantle (including presence of volatiles), temperature, tectonic regime (compressional/extensional), and strain rate. The relevant deformation mechanisms can be brittle (Coulomb-Byerlee frictional law and possibly high-pressure failure) or ductile (power-law creep and low-temperature plasticity). We explore systematically the effects of composition and temperature on the strength difference, considering four possible compositions for the lower crust (felsic granulite, mafic granulite, wet diabase, dry diabase) and two for the lithospheric mantle (dry peridotite, wet peridotite). The rheology of the resulting eight compositional layerings is estimated as a function of Moho temperature, which is varied from 600 to 1500 K. The Moho temperature can be converted to surface heat flow if the thickness and composition of the crust are known. Compared to the effect of temperature, the effect of strain rate is relatively minor.

Excluding the case of very low temperatures, when the rheology of both lowermost crust and uppermost mantle is frictional brittle and therefore the strength contrast vanishes (a situation relevant to mature oceanic lithosphere), the strength of the uppermost mantle is usually higher than the strength of the lowermost crust (at the same strain rate). The strength difference is a strong function of composition and temperature. For a given compositional layering, it decreases with increasing temperature, from a maximum of the order of hundreds of megapascals to negligible values of a few megapascals or less. Consequently, small compositional contrasts (for instance, soft lower crust/soft lithospheric mantle, or hard lower crust/hard lithospheric mantle) and high Moho temperatures result in low or negligible strength differences at the Moho, while large compositional contrasts and low Moho temperatures result in high strength differences. In terms of bulk lithospheric behaviour, the former case corresponds to the “crème brûlée” model, while the latter corresponds to the “jelly sandwich” model. Neither model can be generalized to apply indiscriminately to the continental lithosphere.

Tectonic evolution of the Sierras Interiores (South Pyrenean Zone, central Pyrenees)

Lidia Rodríguez, J. Cuevas, J.M. Tubía

*Departamento de Geodinámica, Facultad de Ciencia y Tecnología, Universidad del País Vasco, 48080 Bilbao, Spain.
lidia.rodriguez@ehu.es*

The overall structure of the South Pyrenean Zone is dominated by thin-skinned tectonics with south-directed thrusts commonly detached along Triassic beds (Seguret, 1972). In the studied region of the Sierras Interiores, between the Tena and Aragon Valleys, a stratigraphic lacuna was developed from Triassic to late Cretaceous times. The stratigraphic sequence is formed from bottom to top:

- 170 metres of late Cenomanian to early Campanian massive limestones, that rest discordantly over the Paleozoic sequence of the Axial Zone.

- The "Marboré sandstones", a thick (400-600 metres) formation of Campanian to Maastrichtian age composed of marly sandstones, sandy limestones and sandstones with dolomitic cement showing a brownish tone.

- 130 to 230 metres of massive and light-coloured limestones of Paleocene age.

We have identified a deformational sequence with three main stages: 1) Thrust sheets with E-trending ramps were formed initially, from which more than 1 to 1.5 km of southward displacement can be established. Many thrust faults use the "Marboré sandstones" as detachment level. There also are, however, deeper thrusts that duplicate the basal Cenomanian limestones. 2) In a second step, asymmetric angular folds were generated, deforming the previous thrusts. The folds display horizontal and WNW-ESE trending axes, develop a N-dipping axial plane cleavage and have at least 500 m of wavelength. The thrust sheets duplicating the Marboré sandstones or the Cenomanian limestones are probably coeval, since they are both folded. 3) Finally, a second generation of minor thrust sheets is locally developed along the flat flanks of the folds. These structures, which accommodate the shortening of the late Pyrenean compression, are also detached along the "Marboré sandstones".

The main differences with previous interpretations on other sectors of the Sierras Interiores are the recognition of a second thrusting event younger than the folding and the consideration of the asymmetric folds as the evidence of a shortening event independent of any thrusting event, instead of being coeval structures (fault-propagation folds). Besides, the limited displacement of the "Marboré sandstones" seems to indicate that they cannot be longer regarded as a main detachment level at the regional scale. However, the deeper thrust that duplicates the basal Cenomanian limestones can be recognized all along the study area, which points out a great regional relevance (Rodríguez, 2011).

The tectonic evolution proposed here modifies the thinking about the basin dynamics in the South Pyrenean flysch, because the Sierras Interiores mark the poorly documented northern border of the turbiditic foreland basin that advanced progressively southwards from early Eocene time due to the migration of the deformation front.

REFERENCES

- Rodríguez, L. 2011. Ph. D. Thesis, UPV-EHU, Bilbao, 186 p.
Seguret, M. 1972. Ph. D. Thesis, USTLA, Montpellier, 155 p.

Age precisions for the Permian magmatism (Sallent area, central Pyrenees)

Lidia Rodríguez¹, J. Cuevas ¹, J.J. Esteban ¹, J.M. Tubía ¹, S. Sergeev ², A. Larionov ²

¹ Departamento de Geodinámica, Facultad de Ciencia y Tecnología, Universidad del País Vasco, 48080 Bilbao, Spain

² Centre of Isotopic Research, VSEGEI, 199106 St. Petersburg, Russia

lidia.rodriguez@ehu.es

Reliable ages about Permian volcanic events in the Pyrenees are limited and not yet well constrained. Only four dates were available in the nineties, a condition that has remained unchanged until nowadays. We present the first U-Pb SHRIMP age determinations on zircons extracted from the mafic dyke swarm intruding Devonian slates and limestones from the Sallent area (Axial Zone of the Central Pyrenees). The dated sample is an alkaline dolerite with intergranular texture made of euhedral to subhedral phenocrysts of plagioclase and interstitial pyroxene.

The Devonian rocks of the Sallent area are discordantly covered by Carboniferous and Permian sedimentary sequences. A voluminous volcanism with minor intrusive bodies, related to the opening of Stephanian-Permian troughs, is interlayered within early Permian sediments. This volcanism has been commonly divided in three main episodes in this area:

1.- The Midi d'Ossau episode, which produced peraluminous dacites and rhyolites, high-K calc-alkaline andesites and dacites (with U-Pb ages between 278-272 Ma) and low-K calc-alkaline andesites.

2.- The Anayet episode, which is represented by transitional to alkaline andesites of imprecise age but a Late Autunian to Saxonian extrusion time is postulated.

3.- The last volcanic episode is formed by homogeneous alkaline basalt with unconstrained age yet.

Only five zircons were obtained from 50 kg of the selected sample (Li-26), since the crystallization of this mineral is usually prevented in basalts due to very fast cooling. Zircon grains were analyzed on a SHRIMP-II SIMS in the Centre of Isotopic Research at VSEGEI (Saint Petersburg). Analyzed zircons are large fragments (>200 µm), probably obtained after crushing larger euhedral crystals and they have oscillatory zoning. High ²³²Th/²³⁸U ratios (0.59-1.00), common in zircon from basic igneous rocks, have been observed. In order to date the intrusion age five analyses were made in the central areas of these zircons. All analyses define a Concordia age of 259.2 ± 3.2 Ma (2σ - MSWD 2.1).

The 259.2 ± 3.2 Ma age presented here allows us to consider that this type of dykes could represent the last pulse of the Permian magmatism in the Pyrenees, as it provides the youngest reported age for such magmatic event. The interpretation as late, vanished magmatic pulses is also consistent with the occurrence of the analyzed rock as dykes and sills at a deeper structural level than the older Permian volcanic materials that crop out extensively in the Anayet and Midi d'Ossau sectors. Finally, although it is beyond the scope of this work, the age and the geochemistry of the Sallent dyke seem to mark the transition to the new geodynamic setting prevailing in the Pyrenees during the Mesozoic, which was responsible for the generation of the Triassic "ophites".

Structure and Geological History of the Carboneras Fault Zone, S.E. Spain

Ernest H. Rutter¹, Ray Burgess¹, Daniel R. Faulkner²

¹ School of Earth, Atmospheric and Environmental Sciences, University of Manchester, Manchester M13 9PL, UK

² Earth and Ocean Sciences, University of Liverpool, Liverpool L69 3GP, UK

e.rutter@manchester.ac.uk

The Carboneras fault zone (CFZ) is a major NE-SW trending tectonic lineament in SE Spain. Of Miocene through Recent age, it separates the volcanic Cabo de Gata terrain from the tract of uplifted metamorphic basement blocks and post-orogenic basins that comprise the Betic Cordilleras lying to the NW. We present the results of new geological mapping and age determinations, which constrain the geometry and geological history of the fault zone.

The CFZ consists of two main strands, about 100m apart, each containing several metres thickness of low metamorphic grade, clay-bearing fault gouge, formed in the uppermost 3 to 5 km of the crust. Outside the fault cores, there is widespread cataclastic damage done to the country rocks, plus some subsidiary fault strands. There is a striking lack of fault rocks derived from greater depths, posing the question of how a distinctly higher grade tract of metamorphic basement rocks (including migmatitic schists) has been incorporated at its present crustal level between the two main strands of the fault zone. Internal structures unequivocally demonstrate a left-lateral strike-slip pattern of movements developed over several millions of years during the Miocene, and stratigraphic constraints in basement rocks show that there has been little relative vertical displacement across the CFZ. The greatest movements are Langhian through Tortonian in age, but effects on Messinian and Pliocene rocks show that less intense movements have continued to the present day. Offsets of several km are seen on several fault strands, but the total offset on the CFZ is unknown. The two main faults strands are now known to cut pre-existing fault rocks and tectonic features, also formed under shallow crustal conditions.

The oldest freshly-deposited calc-alkaline volcanic rocks lying to the SE of the CFZ are 18.3 Ma in age (although reworked amphiboles in underlying sediments were dated at 21 Ma), and were originally deposited prior to the onset of fault movements. These rocks are now upended against the fault zone, and an 11 Ma unconformity within the volcanic sequence oversteps the southern strand of the fault zone. The youngest volcanic rocks are lower Messinian (6 Ma in age), step across the fault zone yet are cut by its youngest movements. On the north side of the CFZ the oldest post-metamorphic sedimentary rocks deposited are Serravallian in age (15 Ma) and a series of unconformities and deformation episodes affecting successive sedimentary formations attests to the relationships between fault movements and sedimentation.

The fault zone has acted as a conduit for subvolcanic rocks rising to the surface, and substantial tracts of the CFZ are decorated with andesitic intrusions, yet none of the eruptive material is preserved to the NW of the CFZ.

Overlap of salt tectonics, thin-skinned tectonics and syntectonic sedimentation: Structure and kinematics of the Sierras Marginales in the Olvena area

Pablo Santolaria, A.M. Casas, A. Luzón.

*Departamento de Ciencias de la Tierra, Universidad de Zaragoza, 50009-Zaragoza (Spain)
psotin@unizar.es*

The South Pyrenean Zone is classically divided into the Pamplona-Jaca Basin, the External Sierras and the South Pyrenean Central Unit (SPCU). From Late Santonian to Late Oligocene the thrust sheets which constituted the SPCU were emplaced following a footwall sequence in a thin-skinned tectonic style context where Triassic evaporites (Keuper facies) acted as the main detachment level. The curved/bended shape of the SPCU is due to different displacement of thrust sheets from high rates in the centre to relatively low rates at the edges, favouring important clockwise rotations at the western edge of the SPCU. This allows us to distinguish between a western area with N-S oriented structures and the central area, with ENE-WSW oriented structures

The studied zone is located to the south-east of the SPCU in the Sierras Marginales realm where a thinned (1200 m) Mesozoic-lower Cenozoic sedimentary sequence crops out. Specifically, it is located in the transition zone between N-S oriented structures and the ENE-WSW oriented structures. During the Early-middle Eocene the Sierras Marginales thrust sheet underwent a basinward/southward translation and during Eocene-Oligocene an internal deformation stage.

Detailed geological mapping and derived balanced cross-sections have been done to reconstruct both the structure in depth and kinematics supporting by syntectonic deposition related to alluvial fans.

The structure is characterized by km-scale thrust (and backthrust), with relatively important lateral continuity and small displacements. Thrust-related folds usually plunge eastward which accommodate low rates of shortening. These ENE-WSW thrust sheets are cut by NNE-SSW strike-slip faults and deformed (both folding and piercing) by rising Triassic evaporites. Kinematics derived from thrust geometry indicates a complex emplacement of the thrust sheets with presence of out-of-sequence thrusts, backthrusts, de-activation and re-activation of structures overlapping in time with evaporite migration and strike-slip movements which triggered probable vertical-axis rotations. This internal deformation stage took place subsuperficially as Late Oligocene syntectonic deposits record.

The geometrical and kinematic complexity of the studied sector is due to the overlap of several factors acting in a thin-skinned context: 1) a thinned Mesozoic-lower Cenozoic crust, 2) the southward migration of deformation from the innermost part of the SPCU to the Sierras Marginales realm which triggered salt tectonics, 3) the location between different orientation areas and 4) the extra load related to the sedimentation of denudated material coming from north. Quantifying the relative importance of each of these factors is not an easy task. Furthermore, it seems both the translational and the internal deformation stages are out of sync comparing with the centre of the Sierras Marginales. It points that deformation started in the centre of the SPCU and migrates laterally.

River catchments of the Himalaya as self-correcting strain markers

Hugh Sinclair & Rachel Walcott

*School of GeoSciences, University of Edinburgh, UK
hugh.sinclair@ed.ac.uk*

The majority of rivers that drain mountain ranges develop a simple plan-view catchment form where the length of the catchment, from the deformation front to the drainage divide of the range, is about twice its width (eg. Hovius, 1996). The Himalayas have been recognised as anomalous in this context, with many river catchments having much lower length/width ratios, with the long axis of catchments expanding parallel to the strike of the range. This has important implications for the distribution of erosion and sedimentation across the range, and hence, rock exhumation histories in the range and sediment fluxes to foreland basins.

This presentation will overview recent work that analyses the plan-view shape and the mean geomorphic slopes of river catchments at a range of scales from across the entire Himalayan Range. We observe that the Himalaya can be divided into three geomorphic domains: 1) A southerly domain that broadly coincides with the sub- and lesser Himalaya where catchments are elongate parallel to the mountain front; 2) A central domain that coincides with the Greater Himalaya and where catchments have a 2:1 ratio regardless of size; 3) A northerly domain that coincides with the Tethyan Himalaya where the smaller catchments have the standard 2:1 ratio, but where the larger catchments are significantly elongate parallel to the range. The northern and southern domains are also characterised by a large proportion of mean hillslopes below 25° whereas the central domain comprises hillslopes equal or greater than 25°; these hillslopes can be used as a proxy of erosion rates, and broadly coincide with thermochronological data on long-term erosion histories.

These observations are interpreted in terms of the horizontal strain history recorded by the catchments which elongate them parallel to the range (ie. as a strain ellipse) versus the vertical erosion history which attempts to return catchments to their more stable 2:1 ratio through fluvial/hillslope coupling (Perron and Dietrich, 2006). The propagation of thrust faults in the southern domain and their modification of catchment form through the deflection of channel networks has been well documented (eg. Gupta, 1997; van der Beek et al., 2002). The central domain is dominated by rapid erosion, and hence the strain history of catchments is obliterated. The northerly domain provides an interesting record whereby the degree of strain recorded by the catchments is scale dependent. The smallest, first order tributaries have standard 2:1 ratios, but as catchment size increases, so the degree of flattening increases; this is exemplified by the Indus and Tsangpo catchments. These large catchments are comparable to the Salween and Mekong rivers which Hallet and Molnar (2001) propose record distributed crustal strain at the corner of the Indian indentor.

If these interpretations of catchments as self-correcting strain markers is correct, the results imply that crustal deformation has been sustained and distributed across the Himalaya as would be expected for an actively deforming thrust wedge (cf. Avouac, 2003). We illustrate an example of ongoing deformation in the northern domain using structural, neotectonic and thermochronological data from the Indus Valley in Ladakh.

REFERENCES

- Avouac, J.P., (2003) Mountain Building, Erosion, and the Seismic Cycle in the Nepal Himalaya, *Advances in Geophysics*, 46, 10.1016/S0065-2687(03)46001-9
- Gupta, S., (1997) Himalayan drainage patterns and the origin of fluvial megafans in the Ganges foreland basin, *Geology*, 25, 11 – 14
- Hovius N. (1996). Regular spacing of drainage outlets from linear mountain belts *Basin Research*, 8, 29–44
- Hallet, B., and P. Molnar (2001), Distorted drainage basins as markers of crustal strain east of the Himalaya, *J. Geophys. Res.*, 106(B7), 13,697–13,709.
- Perron, T., Kirchner, J., Dietrich, W., 2009, Formation of evenly spaced ridges. *Nature* 460, 502-505 .
- van der Beek, P., B. Champel and J.-L. Mugnier (2002) Control of detachment dip on drainage development in regions of active fault-propagation folding, *Geology*, 30, 471-474

Quartz veins as proxy for coupled fluid pressure and stress state evolution at the base of the seismogenic crust: examples from the High-Ardenne Slate Belt (Belgium, Germany, France)

Manuel Sintubin, Koen Van Noten, Hervé Van Baelen, Philippe Muchez

*Geodynamics & Geofluids Research Group, Department of Earth & Environmental Sciences, Katholieke Universiteit, Belgium
manuel.sintubin@ees.kuleuven.be*

The High-Ardenne Slate Belt, part of the Rhenohercynian external fold-and-thrust belt at the northern extremity of the late Palaeozoic Variscan orogen (Belgium, France, Germany), exposes predominantly fine-grained siliciclastic metasediments, deformed in low-grade metamorphic, mid-crustal environments. In this respect, the slate belt serves as a fossil analogue of the low-permeability environment at the base of the seismogenic crust. Detailed structural, petrographical, mineralogical and geochemical studies of particular quartz vein occurrences enables the reconstruction of the temporal and spatial evolution of the permeability structure in this low-permeability environment in relation to fluid pressure, stress state, fracture and fault development, fluid redistribution and fluid-rock interaction.

A first type of quartz veins are bedding-perpendicular, lens-shaped extension veins that are confined to sandstone layers within a multilayer sequence. Vein arrays are very consistent at a regional scale. Fluid-inclusion studies demonstrate high (near-lithostatic) fluid pressures suggesting that the individual sandstone bodies acted as isolated high-pressure compartments. Hydraulic fracturing occurred during the compressional tectonic inversion (from extension to compression) in the earliest stages of orogeny. The vein fill shows a blocky character indicating crystal growth in open cavities. The typical lens shape of the veins suggests subsequent plastic deformation of cohesion-less fluid-filled cavities. This first type of quartz veins, exemplifying brittle-plastic deformation behavior below the brittle-plastic transition, is in contrast to contemporaneous bedding-perpendicular crack-seal veins observed in higher – upper-crustal – structural levels, reflecting pure brittle deformation behavior. In the latter setting, subsequent bedding-parallel veins materialize the completion of the tectonic inversion to an Andersonian compressional regime. Fluid-inclusion studies show that the bedding-parallel veins are formed at lithostatic to supralithostatic fluid pressures, typical for low shear-stress conditions during a compressional tectonic inversion.

The second type of quartz veins are discordant veins confined to an extensional low-angle shear zone in mid-crustal conditions. These very irregular veins transect a pre-existing pervasive cleavage fabric. They show no matching walls and again a blocky fill. Vein development is interpreted to be initiated shortly after an extensional tectonic inversion (from compression to extension) at high fluid pressures and low shear stresses, reflecting the late orogenic destabilization of the slate belt. The initial brittle parental extension cracks are subsequently affected by a steady-state, non-coaxial solid-state deformation in a creeping shear zone and evolve as plastically fluid-filled cavities at increasing shear stresses.

Extensive veining on a regional scale seems confined to particular periods of tectonic inversion, both at the onset and during the final stages of orogeny. These periods, characterized by sustained high fluid pressures and low shear stresses, turn out to be key moments for the redistribution of overpressured fluids in low-permeability environments at the base of the seismogenic crust due to the repeated regeneration of transient enhanced permeability structures. These veins indeed document a mixed brittle-plastic deformation behavior that is considered responsible for maintaining long-lived, along-strike permeability structures by means of steady-state plastic deformation of fluid-filled cavities. The creation and maintenance of these transient enhanced permeability structure is imperative to ensure a sustained fluid redistribution, fluid-rock interaction and (re-)mobilization of solutes.

Finite strain analysis in quartzites; methods and markers

Alexis Soares¹, Rui Dias²

1 Centro Ciência Viva de Estremoz e LIRIO (Laboratório Investigação Rochas Industriais Ornamentais, Escola Ciências Tecnologia, Universidade de Évora), Portugal

*2 Escola Ciências Tecnologia, Universidade de Évora (LIRIO e Departamento de Geologia) e CGE (Centro Geofísica Évora), Portugal
asoares@estremoz.cienciaviva.pt*

The strain quantification in tectonites is not a straightforward process; indeed, the geological structures could be obtained by different mechanisms. This diversity will be eventually reflected in the heterogeneous deformation of the rock fabrics that have been achieved by intra-, trans- and/or intergranular mechanisms. As the methods usually used in strain quantification studies (e.g. Normalized Fry-Erslev, 1988 and Rf/f -Lisle, 1985) have distinct sensitivities to these different mechanisms, they will usually give different values to the same rock sample. The full understanding of the real meaning of the strain results is thus a priority in structural geology studies.

In the Apúlia region (NW Iberian variscan autochthon), the lower Ordovician quartzites of the Armorican Formation are suitable for understanding the limitations of methodologies used in strains estimations. Indeed, concerning the deformation they have only been deformed by the first and main variscan tectonic event. In what concerns rheology, they are a very pure lithology, almost completely formed by quartz grains, which precludes viscosity problems. Moreover, as worm tubes of Skolithos type are frequent in these rocks, these fossils could also be used as strain markers for the bedding plane; indeed, in the undeformed state the Skolithos intersection with such plane have a circular to a low ellipticity shape.

As in each sample the strain was estimated in three perpendicular sections, the finite strain ellipsoid is possible to be computed (De Paor, 1990). The comparison between the different estimated strain values (Normalized Fry either in quartz grains or in Skolithos sections and RF/f also either in quartz grains and Skolithos sections) coupled with geometrical and kinematical field data, allow the establishment of different conclusions:

- Strain partitioning was an important process in the Variscan deformation of the Apúlia Ordovician quartzites;
- The strain intensity estimated using D parameter (Ramsay & Huber, 1983) is usually a valuable parameter of the deformation induced by the regional sinistral variscan transpression, which could be independently estimated using the deflection of the Skolithos (Dias & Ribeiro, 1991);
- The data obtained by the different strain methods / markers could in some cases be correlated with the deformation mechanisms that have been active, allowing a better understanding of the deformation history.

REFERENCES

- DePaor, D. (1990) - Determination of the strain ellipsoid from sectional data, *J. Struct. Geology*, 12, 131-137.
- Dias, R. & Ribeiro, A. (1991) - Finite-strain analysis in a transpressive regime (variscan autochthon, NE Portugal). *Tectonophysics*, 191, 389-397.
- Erslev, E.A., (1988)-Normalized center-to-center strain analysis of packed aggregates: *J. Struct. Geology*, 8, 201-209.
- Lisle, R.J. (1985) - Geological strain analysis. Pergamon Press, 99 p.
- Ramsay, G. & Huber, M. (1983) - The Techniques of Modern Structural Geology, Volume 1: Strain Analysis. Academic Press London.

Application of shearband boudins analysis to understand ductile shear zones

João P. Sousa¹, Benedito C. Rodrigues², Jorge Pamplona^{1,3}

¹ Centro de Investigação Geológica, Ordenamento e Valorização de Recursos, Universidade do Minho, Portugal

² Centro de Geologia da Universidade do Porto, Portugal

³ Departamento de Ciências da Terra, Universidade do Minho, Portugal
jpons@portugalmail.pt

The methodology used for the kinematic analysis of H-T ductile shear zones developed by Pamplona & Rodrigues (2011a), based on geometric analysis of boudins, proved to be a easy application tool.

The boudin analysis begins with the measurement of the Lb (boudin axis) orientation, as a fundamental element of the kinematic analysis in simple shear – Lb proved always to be perpendicular to a local displacement plane (Sx) that is defined as the plane that contains different lineations (e.g., stretching lineation in the host rock) and so, validates the orientation of the outcrop plane. The methodology also includes the measurement of several angular and dimensional parameters, some of them adapted from Goscombe and Passchier (2003).

The main objective of this study deals with the validation of the broad utility of this methodology in shear zones with different P-T conditions. It was studied a shearband boudin field on a Grt-St shear zone whose comparison with previous studies (Sil shear zone) had allowed the statement of several considerations.

Sil shear zone has three main shearband boudins generations: (i) pegmatite granitic dykes, quartz aluminous veins and milky quartz veins, with no geometric nor angular parameters able to discriminate these different lithologies;

Grt-St shear zone has three main shearband boudins generations: (i) granitic and pegmatite granitic dykes; (ii) foliated gray quartz veins; (iii) milky quartz veins, but with geometric distinction between them: milky quartz veins has higher values of L/W, angle $\text{Sn}^\wedge\text{Bbs}$ and angle Sn^\wedgec ;

The development of fold boudins, coeval boudinage and folding is enhanced at higher P-T conditions (Pamplona & Rodrigues, 2011b);

On both shear zones, the shearband boudins analysis has been approved as kinematic tool, with coherent sinistral kinematics at Sil shear zone and dextral kinematics at Grt-St shear zone.

These observations seems to point that the P-T conditions (the transition from Grt-St to Sil conditions) has strong effect on rheological contrasts between matrix and boudins (rigid bodies embed in a ductile matrix), drastically reducing this contrast.

The deformation conditions at ductile shear zones promote the development of shearband boudins trains. The analysis of shearband boudins allows the individualization of zones with sharp contrasts in the values of geometrical parameters, reflecting situations of strain partitioning.

The morphological development of shearband boudins is consistent on middle to lower crustal deformations conditions. However, at lower crustal conditions is greater the ability to the development of bilateral symmetric shearband boudins.

REFERENCES

- Goscombe, B.D., Passchier, C.W., 2003. Asymmetric boudins as shear sense indicators – an assessment from field data. *Journal of Structural Geology* 25, 575-589.
- Pamplona J., Rodrigues B.C., 2011a. Kinematic interpretation of shearband boudins: New parameters and ratios useful in HT simple shear zones. *Journal of Structural Geology*, 33: 38-50.
- Pamplona, J., Rodrigues, B.C., 2011b. Fold boudins: what is that? *Geophysical Research Abstracts*, EGU2011, 13:7465.

The influence of grain size on the deformation of polyphase rocks

Joe Tant¹, Stephen J. Covey-Crump¹, Paul F. Schofield²

¹ School of Earth, Atmospheric and Environmental Science, University of Manchester, UK.

² Department of Mineralogy, Natural History Museum, UK.

Joseph.tant@postgrad.manchester.ac.uk

It is well established that grain size has an influence upon the deformation of rocks. Previous studies into grain growth kinetics have focused on monophase rocks. However, polyphase rocks (rocks with more than one phase, i.e. minerals or pores) are much more common. Studies using synthetic polyphase rock analogues and computer simulations have been carried out but experimental studies using real minerals are lacking. This research is an experimental investigation of the grain growth kinetics of two-phase rocks and for the implications on the deformation of polyphase rocks in the grain size sensitive regime.

Grain size plays an important role in determining rock strength throughout the lithosphere, particularly at higher temperatures where diffusion processes become significant. Under such conditions rocks become weaker with finer grain size, thus if grain size is reduced by recrystallization during deformation then potentially the overall strength of the rock will decrease, leading perhaps to strain localization. Whether or not weakening occurs depends upon the rate of grain growth following the initial recrystallization. In monophase rocks the processes of grain size reduction by recrystallization and grain size increase by grain growth tend to balance and so there is no overall reduction in strength. However, in polyphase rocks the grain growth stage can be restricted or even stopped by the presence of second phases.

In this study we synthesise two-phase rocks of calcite and halite by hot isostatic pressing powder mixtures of different volume proportions. The grain growth behaviour of calcite is well understood whereas the grain growth characteristics of halite are less well known and current experiments are aimed toward establishing the grain growth kinetics of monophase halite samples. Initial polyphase experiments are designed to investigate the influence of volume proportion, the relative grain sizes of the phases, and their spatial distribution (contiguity) on the grain growth kinetics under isostatic conditions. The experiments are performed in a tri-axial deformation apparatus at ~200 MPa confining pressure and at temperatures between 300-700 °C. Once the grain growth kinetics have been characterized, deformation experiments will be undertaken in order to investigate how they impact on the mechanical response of the sample as a whole. A complementary set of deformation experiments will also be carried out at the ISIS neutron facility, Rutherford Appleton Laboratory to examine how grain size influences the stress and strain partitioning between the individual minerals.

Time lapse microstructural analysis of gold recrystallisation and coarsening

Dan Tatham¹, Elisabetta Mariani¹, Rob Hough², John Wheeler¹, Dave Prior³, Andrew Cross¹

¹ School of Environmental Sciences, University of Liverpool, U.K.

² CESRE, CSIRO, Australia.

*³ Department of Geology, University of Otago, New Zealand.
tatham@liverpool.ac.uk*

Recent observations of gold nuggets, and visible gold in veins, have been shown to preserve an internal polycrystalline structure that is characteristic of thermal annealing. Thermal annealing, via post depositional heating of natural gold accumulations, might be sufficient for recrystallisation to occur, forming larger grains (and masses), and to develop polycrystalline gold structures as are observed in high grade accumulations in ore deposits. Little is known about the gold itself in these settings and quantitative microstructure is a key and novel aspect that will open new frontiers to the current understanding of gold deposits.

Recent advances in data acquisition speeds for electron backscatter diffraction (EBSD) in field emission gun scanning electron microscopy (FEG-SEM), together with in-situ heating stage technology, now permit the collection of fully quantified microstructural data in real-time during in-situ recrystallisation and grain coarsening experiments, with good spatial and temporal resolution. This allows microstructural changes to be observed and quantified at all stages during high-temperature experiments.

In the example here, we have studied the microstructural evolution of Au/Ag and Au/Ag/Cu alloys (with up to 30% cold rolling strain) through recrystallisation and grain coarsening up to 700°C. The alloy compositions mimic the composition of natural gold in crustal rocks. These studies allow not only to make direct comparisons to microstructures observed in natural gold samples and interpret them in terms of their thermal history, but also to assess the fundamentals of grain-scale microstructure development during recrystallisation of gold at elevated temperatures.

Anatomy of an intraplate strike-slip inversion belt: the Ubierna Fault System

Stefano Tavani¹, P. Granado¹, A. Quintà¹, E. Carola^{1,2}

¹ *Geomodels, Departament de Geodinàmica i Geofísica, Facultat de Geologia, Universitat de Barcelona, 08028 Barcelona, Spain*

² *CIUDEN, C/II Avenida de Compostilla 2. 24400 Ponferrada. Spain*

stefano.tavani@ub.edu

The Ubierna Fault (Basque-Cantabrian Basin, Spain) has been considered for years as the contractive mountain front of the Pyrenean Belt in the Cantabrian area, resulting from the inversion of a Mesozoic extensional fault system. An integrated study of macro and mesostructural deformation patterns, seismic cross sections and aerial images, has revealed a strike-slip Cenozoic tectonic framework. During the Eocene to present day deformation, this fault and the Ventaniella Fault located to the south acted as right-lateral slightly transpressive elements forming a 120 km long and 15 km wide overstep area, named Ubierna Fault System, where the cumulative right-lateral displacement exceeds 15 km.

The Cenozoic tectonic framework of the Ubierna Fault System includes right-lateral reactivation of deeply-rooted WNW-ESE striking inherited extensional faults, development of negative and, mostly, positive flower structures, branch faults, strike-slip duplexes, and releasing and restraining bends. NNW-SSE striking normal faults and joints are produced by the WNW-ESE right-lateral strike-slip motion.

The extensional elements are well developed and deformation progression implied their incorporation into the strike-slip system as right-lateral faults (forming part of strike-slip duplexes). NE-SW striking contractional horsetail terminations resulted from the inversion of inherited deeply-rooted extensional transversal elements. The abundance of flower structures striking WNW-ESE and paralleling the main strike-slip faults, together with the overall uplift of the overstep area, testifies for a slight compressional component.

To the north of the Ubierna Fault System deformation degree is strongly reduced and the Mesozoic extensional structures are largely preserved. Right-lateral tectonics is testified by kinematic data collected along the major WNW-ESE extensional faults, by the development of restraining bends and by the diffuse development of extensional structures striking NNW-SSE that, in many cases, include pull-apart basins cored by diapirs. At a regional scale, the Ubierna Fault System represents the southern segment of a Cenozoic transpressional belt, which emanates from the Pyrenean Orogen and penetrates for tens of kilometres into its foreland basin. To the north of the Ubierna Fault System, the transpressive belt incorporates the western portion of the Basque-Cantabrian Basin and the Asturian Massif area. Lateral transition between this transpressive belt and the dip-slip belt located to the east, occurs across an area experiencing along strike-shortening, which developed to in order to accommodate the eastward extrusion of the transpressional belt.

Pressure solution cleavage organised infilling. Insights from the Mt. Catria site (Northern Apennines)

Stefano Tavani¹, Fabrizio Storti², Josep Anton Muñoz¹

¹ Geomodels, Departament de Geodinàmica i Geofísica, Facultat de Geologia, Universitat de Barcelona, Spain

² Dipartimento di Scienze della Terra, Università di Parma, Italy

stefano.tavani@ub.edu

In an outcrop located in the leading syncline of the Mt. Catria Anticline (Northern Apennines, Italy), unusually pervasive pressure solution cleavages developed in the well-layered marly limestone of the Scaglia Rossa Formation, due to the buttress effect of a steeply-dipping reverse fault. Cleavages are stratabound and at an high angle to bedding. Joints striking perpendicular to both cleavages and layers provide natural sections showing the cross-sectional morphology of cleavages. Variable cross-sectional width of insoluble material, cleavage length and stylolitic teeth amplitude allow to recognise different cleavage generations, and to infer the cleavage formation sequence. From this sequence it arises that newly developed cleavages tend to form in the areas between highly spaced cleavages, almost in the middle of the pre-existing cleavage-bounded lithons. These observations support an organised infilling process. Similarly to what observed for joints, the presence of a pressure solution cleavage can alter the state of stress in the surrounding rock volume, inhibiting the development of new cleavages in its vicinity.



Ground-truthing in-situ seismic data against geological data: the Carboneras Fault Zone, S.E. Spain

Rochelle Taylor¹, Ernest Rutter¹, Kate Brodie¹, Daniel Faulkner², Stuart Nippres², Andreas Rietbrock², Christian Haberland³

¹ University of Manchester, Manchester M13 9PL, Great Britain

² University of Liverpool, Liverpool L69 3GP, Great Britain

³ GFZ, 14473 Potsdam, Germany

Rochelle.Taylor@manchester.ac.uk

The Carboneras fault zone (CFZ) is a major NE-SW trending tectonic lineament in SE Spain. Of Miocene through Recent age, it separates the volcanic Cabo de Gata terrain from the tract of uplifted metamorphic basement blocks and post-orogenic basins that comprise the Betic Cordilleras lying to the NW. The CFZ consists of two main strands, about 100m apart, each containing several metres thickness of low metamorphic grade, clay-bearing fault gouge, formed in the uppermost 3 to 5 km of the crust. Outside the fault cores, there is widespread cataclastic damage done to the country rocks, plus some subsidiary fault strands.

The excellent exposure of the fault rocks and their protoliths makes them particularly well suited to verifying the results of in-situ seismic investigations. Seismic methods are widely used to investigate fault rock structures, but commonly in regions that are less well exposed than the CFZ. Two high resolution seismic reflection/refraction transects were carried out in river valleys cutting the fault zone, and tomographic sections have been constructed. Samples of fault rocks and their protoliths were also collected for laboratory measurements of acoustic wave velocities. Inevitably, the shallow seismic investigations are strongly affected by the cracking on a range of scales that has been done to the country rocks during fault motions, whereas the small samples used for laboratory acoustic measurements are relatively pristine. Despite this, of course, there is still marked sensitivity of velocity to pressure at low pressures as small cracks are progressively closed. To reconcile the results obtained using the two approaches requires the effects of crack damage to be superimposed upon the laboratory seismic data. To assess the density of macroscopic cracks, outcrop crack lengths were measured in the field and from photographs. Assuming crack length follows a power law relation to frequency, this fixes a small portion of the power spectrum, which is then extrapolated to cover the likely full range of crack sizes. The equations of Budiansky and O'Connell linking crack density to elastic moduli were used to calculate modified acoustic velocities, and the effects of the wide range of crack sizes were incorporated by breaking the distribution down into bins of limited range of crack density. In this way it has proved possible to reconcile the laboratory and field velocity measurements.

The seismic tomography results show particularly well the location of steeply-dipping fault cores and the decoration of fault zones with intrusive igneous material, and these correlate well with the results of geological observations.

Architecture of the orogenic mid-crust revealed by deep reflection seismic

Taija Torvela^{1,2}, Annakaisa Korja², Pekka Heikkinen²

¹ Department of Geology and Petroleum Geology, University of Aberdeen, UK

² Department of Geosciences and Geology, University of Helsinki, Finland

taija.torvela@helsinki.fi

During orogenesis, the crust is thickened considerably. The thickening leads to partial melting and, consequently, rheological weakening of the middle and lower crust and leading to mid-crustal flow. The extension and the collapse of an orogen are intimately associated with these processes. How much the mid-crust is weakened, and how the weakening and the resulting crustal flow affect the crustal architecture are subject to debate. In the field, large-scale ductile extensional features are difficult to recognise due to the lack of sharp contacts, extensive recrystallisation, and the often poor geomorphological expression of gently dipping structures. Furthermore, deep seismic reflection data analysis traditionally focuses on the large-scale acoustic contrasts. Being relatively acoustically homogeneous, the internal architecture of the partially molten mid-crust has, therefore, attracted little attention in seismic data analysis. A detailed study of seismic data can, however, potentially reveal crucial information about the architecture of the mid-crust and the distribution of the deformation within it.

A high-resolution deep seismic reflection survey FIRE (Finnish Reflection Experiment) was carried out in 2001-2005 in Finland. The survey consists of four FIRE seismic profiles with a total length of 2135 km. The data have been pre-stack depth-migrated in absolute amplitude. In the southern part of the survey, the profile FIRE 2A images an exposed granulite facies core complex representing the middle crust of the Svecofennian orogeny (~1.89-1.87 Ga). By applying an instantaneous meta-attribute calculated on the seismic data, the middle crust reveals an unexpected architecture consisting of mega-scale, penetrative S-C' structures. The structure implies that the mid-crust was pervasively weakened and extended during and after the orogeny. The seismic interpretation is correlated with field data, constraining the timing and the direction of the extension. The field and the subsurface architectures indicate a presence of extensional shear zones, but also penetrative distribution of the deformation between the shear zones, mid-crustal flow, and extension within the entire mid-crust.

The brittle-plastic transition during the seismic cycle

Claudia Trepmann

*Department für Geo- und Umweltwissenschaften, Ludwig-Maximilians-Universität München, Germany
claudia.trepmann@lmu.de*

Earthquakes result from stress release by brittle failure. Their nucleation requires unstable frictional sliding on a fault plane with velocity softening. C. Scholz introduced the terms schizosphere for the seismogenic zone, where earthquakes can nucleate, and plastosphere for the zone, where stresses can reach the brittle strength, but unstable sliding is prevented by velocity hardening. The transition between these two regimes likely occurs above the so-called brittle-plastic transition, where maximum lithospheric differential stresses are predicted. The brittle-plastic transition depends on the strain rate, which increases rapidly during a large earthquake. Brittle failure is then transiently possible in materials that respond by thermally activated viscous creep at lower strain rates. Creep in the plastosphere during stress relaxation after quasi-instantaneous coseismic loading is believed to be one of the causes for the decelerating surface deformation observed by geodetic measurements after large earthquakes.

Here I will address the record of peridotites at conditions that correspond to those prevailing just below the base of the seismogenic zone in oceanic lithosphere. While the microfabrics of naturally deformed peridotites provide the integral record of many superimposed episodes of the geologic history, laboratory experiments allow specific stages to be isolated and studied separately. Noteworthy, in the present context of transient deformation, the laboratory experiments can be performed at near-natural strain rates, favouring a direct comparison between experimental and natural microfabrics. The comparison of microfabrics generated in deformation and annealing experiments on natural peridotites with those observed in shear zone peridotites from the Western Alps reveals an amazing resemblance. Core-and-mantle microstructures – which elsewhere have been interpreted as indicators of steady state dislocation creep – can form during short-term high stress deformation in the low-temperature plasticity field and subsequent recrystallization at low stresses. Grain size reduction appears to be controlled by the initial deformation stage at high stress, while growth of grains occurs during subsequent creep – rendering conventional paleopiezometers inappropriate. In recrystallized aggregates, a crystallographic preferred orientation of new grains can be predominately controlled by the replaced host grains – thus not necessarily indicating the activated glide system. The superposition of microfabrics attributed to different deformation regimes does not necessarily reflect changing temperatures, as commonly invoked, but short term changes in stress and strain rate. Wherever natural rock microfabrics indicate deformation at high stress (a combination of brittle failure and low-temperature plasticity) followed by creep and annealing, this may reflect a stress cycle experienced in the uppermost plastosphere beneath a nearby fault ruptured in a major earthquake. Regarding the frequency of earthquakes in tectonically active regions and the time exhumed mantle rocks require to pass through the uppermost plastosphere, the microfabrics may have recorded more than one such cycle. Perhaps steady state should be regarded as the exception rather than the rule when interpreting such natural microfabrics.

The evolution of the quartz c-axis fabric pattern and the strain paths in the Kazdağ (İda) Stack Antiform, Western Turkey

Şener Üşümezsoy

*Istanbul University, Department of Geological Engineering, 34320 Avcılar, Istanbul, Turkey
aysal@istanbul.edu.tr*

The Kazdağ stack antiform was build up by the south-eastward thrusting of the tectonically surging batholithic gneisses over the antiformal stack of the amphibolite, marble, gneisses and metadunite thrust units. More than 100 samples were collected along the five traverses which parallel to stretching lineation and crossing the Kazdağ stack antiform and measured in universal table for quartz-c axis fabric. The relation between the quartz-c axis fabric and the strain pattern were calculated. The evolution of the quartz-c axis fabric variations and related strain patterns changes along the traverses let us to understanding the strain path during the thrusting and the streaking of the Kazdağ. The four types quartz-c axis fabric pattern can be distinguish. The central Y maxima's product of the prism $\langle a \rangle$ slip under the strong constrictional deformation, the elliptic central Y maxima is also product of the prism $\langle a \rangle$ slip under the dextral constrictional deformation. The few samples show typical double maxima which typically product of the rhomb $\langle a \rangle$ slip under the flattening strong dextral deformation. Asymmetric dextral single girdle fabric show strong flattening deformation condition during the over thrusting events. The combined basal $\langle a \rangle$ slip in addition to the rhomb $\langle a \rangle$ slips resulted in the formation of the asymmetric dextral single girdle fabric.

Evolution of the Extensional Parallel Folding and Faulting In the Northern Part of the Menderes Metamorphic Core Complex (Western Turkey)

Şener Üşümezsoy, Namik Aysal, İsak Yilmaz

*Istanbul University, Department of Geological Engineering, 34320 Avclar, Istanbul, Turkey
aysal@istanbul.edu.tr*

The northern part of the Menderes metamorphic core structurally divided NS trending anticlinorium and the synclinorium. This syn-detached folding is result of the NS directed stretching of the metamorphic core rocks. The well-developed NS directed stretching lineation and shear zone in the metamorphic gneissic core rocks exposing along the anticlinorium indicate top to the N directed moment. The synclinorium structure between the uplifting anticlinorium form NS directed elongated basins which covered by the Neogene aged volcano-sedimentary successions. These basins are bounded by the NS trending faulting which are synchronically faulting with the NS directed folding. This NS folding are located the limbs of the uplifting anticlinorium. Syn-detachment faulting and folding are parallel to the NS directed stretching direction. The stretching parallel structure, lineation, faulting and folding were cuts by the EW directed youngest extensional faulting along the Simav graben in the north and Gediz graben in the south. The both of the NS directed stretching parallel lineation, folding and faulting and the EW directed stretching normal extensional younger faulting are product of the continuous stretching deformation of the Northern Menderes core during the uplifting by the major detachment zone. This detachment zone was representing by the NS directed stretching lineation with in the thick flat lying carapace zone. The EW directed extensional faults along the northern flank of the Simav Mountain are very typical seismogenic fault zone in the northern part of the Menderes core. This EW directed extensional fault aren't the detached zone on the contrary detached zone observed along the anticlinorium zone covered by the mylonitic carapace.

Buttressing in the hanginwall of a Mesozoic normal fault (Asturian Basin, NW Spain); section constructed via photogrammetric methods

Hodei Uzkeda¹, J. Poblet¹, M. Bulnes¹, S. Martín², J.C. García-Ramos^{1,3}

¹ Departamento de Geología, Universidad de Oviedo, Spain

² Departamento de Construcción e Ingeniería de Fabricación, Universidad de Oviedo, Spain

³ Museo del Jurásico de Asturias (MUJA), Spain

hodei@geol.uniovi.es

A detailed section across a major normal fault subsequently affected by contraction is constructed by means of photogrammetric methodology. The studied structure crops out at the cliffs east of the Rodiles beach (Asturias, northwestern Spain). Geologically it is situated within the extensional Permo-Mesozoic Asturian Basin partially inverted during the Cenozoic contraction responsible for the Pyrenean range and its western prolongation along the north Iberian Peninsula. The fault involves materials from the Jurassic, corresponding to the Rodiles Formation. This formation consists basically of an alternation of marls and limestones, being the latter more abundant in the lower member (Buerres), present in the footwall, than in the upper one (Santa Mera), which appears in the hangingwall.

The cliffs where the main fault and the related structures crop out offer an apparent section what makes a 3-D approach highly recommended, if not compulsory. In order to achieve such view a set of photogrammetry programs developed at our University was employed. This computer program works with stereoscopic pairs of photographs and allows drawing the geological features depicted in them. The photogeological interpretation obtained this way can be, via control points with known coordinates, placed in their actual position. This procedure permits to combine successive pairs of photographs and achieve a complete image of the structure. Once the interpretation is finished, the beds and structures drawn on the photographs can be projected in an adequate direction (i.e. parallel to the fold axes) onto a selected plane to reach a correct cross section.

The shortening of the main normal fault, whose strike is approximately NE-SW and dips moderately towards the SE, caused an effect of buttressing in its hangingwall. As a result of this, the rocks there underwent an intense deformation that provoked the reactivation of some previous smaller-scale normal faults and development of new decimetre to metre-scale thrusts and folds. Some of the old normal faults are cut and offset by the new reverse ones and by flexural-slip which seems to be the most relevant folding mechanism. Contractional deformation decreases as moving away from the main fault surface, for example, the number of thrusts reduces and the folds have greater interlimb angles.

3D geological reconstruction of Puerta-Pareja fault-propagation fold (Loranca Basin, Central Spain)

Manoel Valcarcel^{1,2}, Josep Anton Muñoz¹, Ruth Soto²

¹ Institut de Recerca Geomodels, Departament de Gedinàmica i Geofísica, Universitat de Barcelona, Spain

² Instituto Geológico y Minero de España, Spain

m.valcarcel@igme.es

The Puerta-Pareja fault-related fold is a NNE-SSW trending Alpine structure located in the Loranca Basin (Central Spain). The Loranca basin represents an intraplate basin filled up mainly with Oligocene-Lower Miocene continental sediments, bounded to the West and East by the Altomira and the Iberian Ranges, respectively. Subsurface data indicate the presence of a fold and thrust system in the area which detaches above the Upper Triassic evaporites (Keuper facies). The Puerta-Pareja fold belongs to this fold and thrust system. The pre-tectonic series affected by the Puerta-Pareja structure is Mesozoic and pre-Late Oligocene in age only outcropping the Paleocene to Early Oligocene materials. Syntectonic materials are Late Oligocene to Early Miocene in age and the structure is fossilized by Late Miocene to Present rocks. The main aim of this work is to describe and reconstruct in 3D the geometry of the fold and the main thrust surfaces from surface and subsurface data. The resulting 3D model will constitute the basis to understand its geometry, folding mechanism, kinematic evolution and origin in its regional context.

The workflow for 3D modelling in the present work is conditioned by the scarcity of pre-tectonic field data. This makes that the information from seismic profiles and well logs constitutes the main hard data to characterize the structure. Seismic and well interpretation, followed by a structural analysis validating it, has made possible to manually construct an isochrone map. Converting time-domain to depth-domain data is one of the critical steps of the process, even more considering the probable presence of a pull-up distortion under the main Puerta-Pareja thrusts. A velocity model (considering sonic information from well logs) has been generated to better constrain the depth conversion. The last step of the workflow has consisted of generating surfaces from the obtained isoline map using the Discrete Smooth Interpolation method.

The resulting 3D model of the Puerta-Pareja structure shows that it can be classified in a general sense as a fault-propagation fold (with a thrust displacement of about 1000 m) and contains some features that make it spatially complex when studied in detail. The geometry of the structure varies along strike, from a relatively simple fault-propagation fold with a secondary thrust with slight displacement to the South to a more complex geometry with two main thrusts following approximately a breakthrough style and a steeper secondary thrust to the North. This implies an important along strike variation in the total fault displacement from around 500 m in the South to around 1200 m in the North. Future 2D and 3D restoration will help to validate this 3D geometry.

Fracture formation and development in a crystalline basement reservoir, central Yemen

Resi Veeningen¹, Bernhard Grasemann¹, Kurt Decker¹, A. Hugh N. Rice¹, Ralf Bischoff²

¹ Dep. for Geodynamics and Sedimentology, University of Vienna, Austria

² OMV Exploration and Production, Vienna, Austria

resi.veeningen@univie.ac.at

The country of Yemen is located on the southwestern corner of the Arabian Plate. The geology of central Yemen is characterized by a horst-and-graben system which partly reactivated a complex, polymetamorphic, Proterozoic (Pan-African) basement along NW-SE trending faults. This basement is unconformably overlain by Jurassic marls and sandstones of the Kohlan Fm. Younger (Late Jurassic and Early Cretaceous) marine clastics and limestones are deposited during extensive rifting. These series are overlain by marine and continental Middle to Upper Cretaceous and Tertiary sediments. Since about 30 Ma, central Yemen has been marked by rifting related to the opening of the Red Sea and the Gulf of Aden, and associated magmatism of the Afar plume in the western part of Yemen.

The Habban Field reservoir is located approximately 320 km ESE of Sana'a. The reservoir is special due to the occurrence of hydrocarbons in the fractured crystalline basement. This study investigates micro- and macrostructural analysis on drill cores in order to understand the complex vein-fracture history at all scales. The drill cores taken from the crystalline basement consists of metamorphic rocks (quartzites, quartz porphyry's, gneisses and amphibolite) which has locally been intruded by large volumes of granites. Close to the metamorphic rocks, the granite is highly altered and relative porous.

In the polyphase cataclastic quartzites, fracture generations are hard to distinguish. The quartz probably originated from thick vein fillings that were fractured and healed at an early stage of deformation. Fluid inclusion analysis on quartz grains in both small veins and large areas gives the homogenization temperature (T_h), representing the lowest temperature range at which the quartz is crystallized. Fluid inclusions are also analysed in the reactivated healed and sealed calcite and dolomite vein cement in order to relate the growth of quartz (veins), the development of calcite/dolomite veins and the influx of hydrocarbons. C/O and S isotope analysis in respectively the calcite and the pyrite vein cement (as found in gneiss) provides, together with the fluid inclusion results and granite age dating, good insights in timing and temperature of all the processes involved during the development of the crystalline basement.

This all can be related to at least 3 different stages of extension, as found in both the metamorphic rock and the granite. From structural analysis of the drill cores, it is discovered that the earliest fault zone generation developed as veins filled with mainly chlorite, albite and sericite. The younger fracture generations are marked by 70°-90° dipping (intermediate in age) and <30° dipping (youngest generation) faults and veins.

Friction of marble under seismic deformation conditions in the presence of fluids

Marie Violay¹, S. Nielsen¹, E. Spagnuolo¹, G. Di Toro^{1,2}, S. Smith¹

1 Istituto Nazionale di Geofisica e Vulcanologia, Rome, Italy

2 Università di Padova, Dipartimento di Geoscienze, Padova, Italy

Marie.violay@ingv.it

Physical and chemical fluid/rock interactions control seismic rupture nucleation, propagation, arrest and recurrence. Several experimental studies explored the effects of pore fluid pressure (P_p) on the sliding behavior of faults. Most of them were performed with tri-axial apparatus at high temperature and high confining pressure. However, due to the experimental configuration, laboratory measurements were limited in terms of slip rate (< 1 mm/s) and displacement (< 1 cm) compared to natural earthquakes (e.g., average slip rate about 1 m/s).

Insight on the physical and chemical role of fluids during the seismic cycle can be gained using a novel rotary shear deformation apparatus, SHIVA (Slow to High Velocity Apparatus) which, by exploiting the large available power (300 kW), is capable to impose slip rates up to 6.5 m/s under normal stresses up to 50 MPa. Importantly, the rotary shear configuration allows large displacements (nominally infinite) and to investigate accelerating creep or other seismic precursory phenomena associated to fault slip in the presence of fluids. SHIVA owns a pore fluid vessel designed to reach 15 MPa of pore pressure. As a consequence, the apparatus extends the imposed deformation conditions towards more realistic conditions.

Here we present results from the first tests performed on Carrara (98% calcite) marble, which was selected because most seismic ruptures in Italy propagate in fluid-rich (usually H_2O and CO_2), calcite-bearing fault zones (e.g. Friuli Mw 6.4, 1976; Irpinia Mw 6.9, 1980; L'Aquila Mw 6.3 2009 earthquakes). Tests were conducted on hollow cylinders (50/30 mm ext/int diameter) at velocities of 1–6.5 m/s, normal stresses up to 40 MPa and fluid (H_2O in chemical equilibrium with the marble) pressure comprised between 0 (room-humidity conditions) and 15 MPa (fluid-saturated conditions). Fluid chemistry (Mg^{2+} , Ca^{2+} , HCO_3^- , pH, etc.) was determined before and after the experiments.

Under these deformation conditions, the friction coefficient decays exponentially from a peak (= static) $\mu_p \sim 0.8$ at the initiation of sliding towards a steady-state $\mu_{ss} \sim 0.1$. Once sliding stops, the friction coefficient recovers almost instantaneously a coefficient of friction $\mu_f = 0.2-0.6$ (fault healing). The experimental data suggest that:

1) μ_p and μ_{ss} are independent of the presence of fluids for a given imposed effective stress ($\sigma_{eff} = \sigma_n - p_p = 10$ MPa);

2) though μ_p and μ_{ss} are similar for experiments performed under the same effective normal stress under room-humidity ($\sigma_{eff} = \sigma_n = 10$ MPa) and fluid-saturated conditions ($\sigma_{eff} = \sigma_n - p_p = 10$ MPa), a comparison of the friction coefficient vs. slip curves shows that the decay is more abrupt in the case of room-humidity experiments: the presence of H_2O slightly buffers dynamic weakening during seismic slip;

3) sample shortens in the presence of fluids and under room-humidity conditions;

4) fault healing is smaller in the case of experiments performed in the presence of fluids;

5) the fluid (H_2O) after the experiment is enriched in Mg^{2+} and HCO_3^- : this chemical evolution suggest breakdown reactions (decarbonation of calcite) in the presence of H_2O as observed in springs after some large earthquakes in carbonate rocks (Sulem and Famin, 2008).

3D imaging and analysis of fracture networks, porosity and permeability in a reservoir dolomite, using micro-Computed Tomography

Maarten H. Voorn, A. Rath, U. Exner

*Department for Geodynamics and Sedimentology, University of Vienna, Austria
maarten.voorn@univie.ac.at*

A dense, multiscale fracture network crosscuts dolomites (early Triassic Hauptdolomit) in the basement of the Neogene Vienna Basin (Austria). The porosity induced by these fractures make the Hauptdolomit rocks a suitable gas reservoir, from which production is ongoing. For most reservoir rocks, petrophysical properties, such as porosity and permeability, are determined by standard laboratory methods. These methods however prove to not always be suitable for fractured reservoir rocks, and provide limited information on the internal distribution of the properties. Therefore, to be able to better assess such reservoir rocks and their potential, a different approach is required.

Micro-Computed Tomography (μ CT) is a non-destructive 3D imaging technique, using X-rays, which do not alter the physical properties of the samples. Various studies are available in literature, using this technique on different sample types, to inspect for example grain size distribution, porosity, and fracture surfaces. We use μ CT to three-dimensionally image the internal structural features of Hauptdolomit drill-core samples, from different drill sites and depths, provided by the OMV. From this 3D grey-scale data set, the fracture network has to be extracted, to be able to calculate porosity and permeability. The main problem is how to do this extraction in the least biased manner. Very different approaches exist in literature, ranging from simple thresholding to more sophisticated segmentation techniques. Also a more direct calculation of petrophysical properties is sometimes performed. Advantages and drawbacks of the different methods need to be investigated to find the most suitable technique for our rock sample data. Various (image) analysis software packages (ImageJ, Amira, MATLAB, and others) are used in this analysis of the data.

The resolution of the μ CT data is limited to approximately 20-50 μ m, depending on the used sample sizes. Higher resolution data, as well as information on e.g. vein filling cements, mineral growth, and cross-cutting relations of fractures, is provided by thin section analysis using the optical light microscope, Cathodoluminescence (CL) and Scanning Electron Microscopy (SEM). Thin sections are also created from the same samples, which have been scanned by μ CT as well. Furthermore, the mentioned standard laboratory methods (using e.g. helium porosimetry and gas permeability experiments) are performed on sample plugs.

First results indicate a multi-stage evolution of porosity, from several vein and fracture generations. The youngest structures are partly open by dissolving the calcitic cement or by evolving mode I cracks. The older veins are partially reactivated in various cataclastic fault zones, which can have high porosities.

The different data sets are used for comparison, as well as for calibration between the techniques. The final goal is to get a 3D view of the fracture network, the porosity and the permeability of various Hauptdolomit samples, on various scales (μ m to dm), which can serve as an input for upscaling permeability to the reservoir scale. This is a clear improvement over standard laboratory methods alone.

Compaction related microstructure in chromitites from the Merensky Reef (Bushveld Complex, South Africa)

Zoja Vukmanovic^{1,2}, S.J. Barnes¹, S.M. Reddy³, B. Godel¹, M.L. Fiorentini²

¹ Australian Commonwealth Scientific and Research Organization (CSIRO), Kensington WA 6151, Australia

² University of Western Australia, Centre of Exploration and Targeting, Crawley WA 6009, Australia

³ Curtin University of Technology, Bentley, WA 6102, Australia

zoja.vukmanovic@csiro.au

The Merensky Reef is a thin (< 1 m), highly continuous platinum-rich layer in the Bushveld Complex (South Africa). The samples studied here are characteristic of typical Merensky Reef, from bottom to top: lower chromitite layer (0.7-1 cm), coarse grained melanonorite (~10 cm), upper chromitite layer (~1 cm) and overlying melanonorite. Chromites from the lower and upper chromitite layers show morphological differences. Chromites from the lower chromitite layer have complex embayed and branching “amoeboidal” morphologies and often contain small sulphide and silicate inclusions. In contrast, the chromite grains in the upper chromitite are idiomorphic octahedral and are free of silicate inclusions. Both lower and upper chromitites contain interstitial pyroxenes, plagioclase, sulphides (pentlandite, pyrrhotite and chalcopyrite) and platinum group minerals.

Electron backscatter diffraction analysis (EBSD) was used to reveal internal microstructures within chromite and sulphide in samples from both chromitite layers. EBSD shows plastic deformation in amoeboidal chromites in the lower chromitite (up to 10° of misorientation), whereas idiomorphic chromites from the upper chromitite show little or no sign of plasticity ($\leq 3^\circ$ of misorientation) and no crystallographic preferred orientation. In both chromitites, all sulphides record crystal-plastic deformation.

The deformation observed in chromites and sulphides is consistent with deformation recorded by the silicates and with the vertical 3D-distribution of the sulphides. All of which are attributed to compaction during cooling of the overlying magma column. According to Godel et al (2007), crystallisation of the lower chromitite layer and the melanorite took place from an injection of new magma on the top of the almost completely solidified anorthosite. The upper chromitite layer formed by a second injection of magma while the melanonorite was still a partially crystalline mush (Cawthorn and Boerst 2006). The more rigid interface between solid anorthosite and overlying magma focused the deformation in the early crystallized phases, chromites and in the late magmatic sulphides. The chromites from the upper chromitite layer crystallised above the “mushy” melanonorite and do not record any signs of deformation, as deformation was accommodated by compaction of the weaker semi-solid melanonorite.

The origin of the amoeboidal chromites remains unclear. The larger amoeboidal chromites in the lower layer were more prone to record plastic deformation than adjacent finer idiomorphic chromites, which were more capable of accommodating compaction by sliding past one another rather than deforming internally. Internal microstructures indicate that the amoeboidal grains were not developed by late stage sintering of multiple idiomorphic equant grains as has been suggested previously (Hulbert and Von Gruenewaldt 1985). The amoeboidal grains evidently developed as single crystals, possibly with originally dendritic morphologies, prior to most of the compaction. However, the presence of deformation microstructures in adjacent chalcopyrite grains indicates that compaction-related deformation continued until very close to the solidus temperature of the rock.

REFERENCES

- Cawthorn, R. G. ; Boerst, K.(2006) *Journal of Petrology*, 47(8):1509-1530
Godel, B.; Barnes, S.-J.; Maier, W. D. (2007) *Journal of Petrology*, 48(8):1569-1604.
Hulbert L.J, Von Gruenewaldt G (1985). *Economic Geology* 80(4):872-895.

Seismic properties and microstructures of serpentinite mylonites

Tohru Watanabe¹, Yuhto Shirasugi¹, Katsuyoshi Michibayashi²

¹ Department of Earth Sciences, University of Toyama, Japan

² Institute of Geosciences, Shizuoka University, Japan

twatnabe@sci.u-toyama.ac.jp

Serpentinites play key roles in subduction zone processes including transportation of water, seismogenesis, slab-mantle coupling, and exhumation of high-pressure rocks. Geophysical mapping of serpentinitized regions in the mantle wedge leads to further understanding of these processes. Direct study of serpentinites is critical to the interpretation of indirect geophysical observations. Antigorite is the dominant serpentine at high-pressures in subduction zones. Reflecting its crystallographic structure, deformed antigorite-bearing rocks expected in the mantle wedge should show strong seismic anisotropy. Some studies have suggested a serpentinitized layer as a cause of shear wave splitting observed in subduction zones. However, seismic properties predicted from microstructures with conventional averaging schemes have large uncertainty. When a rock is composed of minerals with strong elastic anisotropy, Voigt and Reuss averages are far apart. The geometrical information of mineral grains should be taken into account for a better prediction. It is therefore essential to measure seismic velocities of deformed antigorite-bearing rocks to understand what geometrical information is needed. We have, thus, performed velocity measurement and microstructural analysis on antigorite-bearing deformed rocks, and made comparison between measured and calculated velocities.

Rock samples were collected from the Happo ultramafic complex, Central Japan. Compressional and shear wave velocities were measured by the pulse transmission technique at room temperature and confining pressures of up to 180 MPa. Microstructure was examined by optical microscopy and SEM-EBSD. Serpentinite mylonites show strong anisotropy of velocity. The compressional wave velocity is fastest in the direction parallel to the lineation, and slowest in the direction perpendicular to the foliation. The shear wave oscillating parallel to the foliation has higher velocity than that oscillating perpendicular to the foliation. As the antigorite content increases, the mean velocity decreases but both azimuthal and polarization anisotropies are enhanced. Voigt, Reuss and Hill averages of elastic constants were calculated from CPO data and modal composition by using Petrophysics Software (developed by Dr. D. Mainprice). All averaging schemes produce velocity anisotropy qualitatively similar to measurements. Measured velocities are found between Reuss and Hill averages. We suggest that the relatively low velocity is due to the platy shape of antigorite grains, the well developed shape fabric and their strong elastic anisotropy. The configuration of grains should be an important factor for calculating seismic velocities in an aggregate composed of strongly anisotropic materials, such as sheet silicates.

Partitioning of lithosphere stretching and thinning at continental rifted margins between pre- and syn-breakup deformation: Norwegian margin study

John G. Watson¹, N. J. Kusznir², A. Roberts³

1 Fugro Robertson Limited, Llandudno, North Wales LL30 1SA

2 Earth Interior Dynamics, University of Liverpool, Liverpool L69 3BX, UK

3 Badley Geoscience Limited, North Beck House, North Beck Lane, Hundleby, Spilsby, Lincolnshire, PE23 5NB, UK

The Norwegian rifted continental margin was formed by the breakup at 55Ma and earlier Mesozoic rifting of the North Atlantic. The continental margin reveals pre-breakup lithosphere deformation during the Triassic, Jurassic and Cretaceous Periods. This study examines the Lofoten, Vøring and Møre margin segments in order to understand better the evolution of the Norwegian margin. Interpreted seismic crustal profiles have been analysed to determine continental lithosphere thinning and upper crustal extension from the Triassic period to present day. Continental crustal structure and thinning coupled with the location of both the ocean continent transition (OCT) and the continent ocean boundary (COB) have also been addressed. This study shows that the Norwegian rifted margin experienced breakup depth-dependent lithosphere stretching and thinning where whole lithosphere stretching and thinning exceeds that of the upper crust. Earlier pre-breakup lithospheric deformation during the Triassic, Jurassic and Early Cretaceous rifting is shown to be depth-uniform leading to intra-continental rift basin formation. The non-coaxial superposition of lithosphere thinning from the earlier intra-continental rift events with Early Tertiary breakup thinning has led to a complex and laterally varying distribution of thinned continental lithosphere. It is important to understand the structure and rifting history in order to partition the stretching and thinning of the Norwegian continental margin lithosphere. By these methods better predictions of the subsidence and heat flow histories of the Norwegian margin can be deduced.

Kinematic constraints on lithospheric-scale oroclinal bending of the Ibero-Armorican Arc along the northern margin of Gondwana: a paleomagnetic and structural synthesis

Arlo Brandon Weil¹, Gabriel Gutiérrez-Alonso²

¹ Department of Geology, Bryn Mawr College, Bryn Mawr, PA 19010, U.S.A.

*² Universidad de Salamanca, Departamento de Geología, Salamanca, 37008, Spain
aweil@brynmawr.edu*

The Paleozoic Variscan orogeny was a large-scale collisional event that involved amalgamation of multiple continents and micro-continents. Existing paleomagnetic and structural analyses of the western Variscan orogen, notably the Ibero-Armorican Arc (IAA), suggests that this region underwent oroclinal bending of an originally near-linear orogen during the latest stages of Variscan deformation in the late Paleozoic. Closure of the Rheic Ocean resulted in E-W shortening (in present-day coordinates) in the Carboniferous, which produced a near linear N-S trending, east verging, fold-thrust belt. Subsequent N-S shortening near the Carboniferous-Permian boundary resulted in oroclinal bending. This late-stage orogenic event remains an enigmatic part of the final amalgamation of Pangaea.

The present-day 180° of arc curvature of the IAA has inspired many tectonic models explaining how this orogen was created, with little agreement between different models. While there is general consensus that two separate phases of deformation occurred, various models have considered that curvature was caused by: dextral transpression around a Gondwanan indenter; strike-slip wrench tectonics; or a change in tectonic transport direction over time as a result of a continuously changing stress field; whereas more recent models explain the curvature by the formation of an orocline. Deciphering the kinematic history of a curved orogen like the IAA is difficult. To classify an orogen as an orocline, two deformation phases need to be differentiated: an initial compressive phase that forms a relatively linear belt with little to no rotation of developing structures, and a second phase that causes vertical-axis rotation of existing orogenic limbs. Historically the most robust technique to accurately quantify vertical axis-rotation in curved orogens is paleomagnetic analysis. A review of existing and new Variscan paleomagnetic data from Iberia will be presented that argues in support of secondary bending of an originally linear orogenic system.

New data from the Esla tectonic unit, which lies along the southern boundary of the IAA core in the Cantabria Asturias Arc (CAA), helps elucidate rotation kinematics of individual thrust sheets during oroclinal bending. The Esla Unit is a particularly complex region due to the interaction of thin-skinned tectonic structures and deeper duplex systems that underlie thrust sheets. Similar to other regions of the CAA, the Esla Unit carries a secondary magnetization that was acquired in the Late Carboniferous. Protracted deformation during oroclinal bending caused local reactivation and rotation of individual thrust sheets that define the Esla thrust system. This reactivation and subsequent structural modification revises existing kinematic and tectonic models of oroclinal bending in the CAA, especially in the interactions of distinct foreland thrust systems in the CAA (e.g., the Ponga and Picos de Europa units) that were modified and/or emplaced during late-stage north-south shortening.

Together with over five hundred additional paleomagnetic sites from throughout Iberia, these data constrain oroclinal bending of the IAA to have occurred late in the latest Carboniferous over about a 10 million year time window. This agrees well with recent geodynamical models and structural data that relate oroclinal bending with lithospheric delamination within the Western Variscan belt.

Ductile and brittle deformation structures of the Mäntsälä granodiorite batholith in southern Finland; observation at three scales

Marit Wennerström¹, Mira Markovaara-Koivisto²

¹ Geological Survey of Finland, Finland

² Department of Civil and Environmental Engineering, Aalto University, Finland

Marit.Wennerstrom@gtk.fi

The polydeformed granodiorite batholith in southern Finland was earlier modelled in 3D to define the rock quality in a quarry in it. In the present study the influence of ductile deformation structures to brittle deformation properties was examined. During the study field observations were made at three different scales. Two ca. 10 km long survey lines with 9 outcrop observations each were drawn across the batholith in N-S and E-W directions. Structural geological mapping was done at the macro scale in the quarry and the structures in oriented samples from the quarry were examined. The validity of observations was tested using a detailed scanline measurement form modeled in the project.

The Mäntsälä granodiorite batholith belongs to systematic dome-and-basin structures in southern Finland. The structural pattern of the foliations suggests that the lower tectonic slices of crust are exposed in the dome windows. Migmatitic mica gneisses in the batholith centre provide evidence of several folding generations prior to the formation of the open rounded dome structure. Vertical foliations dominate in the centre of the batholith and foliation dips steeply or moderately to the NE on the northern and southern border zones tracing the orientations of the outer contacts. The batholith abuts on the NE-trending major fault system in the west. In the batholith vertical fractures trend mostly to the NE and moderately dipping fractures dip to ENE or WSW. At a few outcrops fractures follow slickenside planes or foliation, when gneiss enclaves occur at that orientation.

In the quarry two open fold phases intersect each other forming a macro scale dome and basing structure. Fractures seldom parallel the schistosity, only when mafic interlayers intensify the structural anisotropy. NE-trending cutting vertical fractures have as infilling mica, chlorite and/or calcite and sometimes palygorskite indicating at least two brittle deformation phases. Subvertical faults with above mentioned infillings trend NW. The rock mostly shows sparse jointing in the quarry. Some vertical or subvertical fracture zones and tightly spaced joint sets trend NE and NW.

First studies of the oriented samples from the quarry show cutting behavior of fractures relative to schistositities. In some samples fractures with infillings shortly parallel one foliation orientation. The ductile deformation of the batholith has mostly inhibited the generation of foliation parallel weakness planes. The steep brittle structures mainly trend to two directions, NE and NW. This information is useful in planning the use of the rock for different purposes.

New conceptual model for how metamorphism and deformation interact in porous materials

John Wheeler¹, S. Llana-Fúnez^{1,2}, D. R. Faulkner¹

¹ Dept. Earth and Ocean Sciences, Liverpool University, L69 3GP, Liverpool, UK

² Dept. Geología, Universidad de Oviedo, 33005 Oviedo, Spain

johnwh@liv.ac.uk

There is no doubt that fluid pressure is a prime influence on brittle failure and consequently we need to understand how fluid pressure evolves in the Earth. There are many places and events in the Earth that lead to fluid pressure deviating from lithostatic pressure: for example, during earthquakes, in basins and in geothermal fields. Since pressure has an effect on metamorphic equilibria and reaction rates, we need to know how fluid and lithostatic pressures together influence metamorphic reaction. Dehydration and rehydration reactions will in turn influence fluid pressure so we need to understand the feedbacks.

For the past 50 years assertions have been made in the geoscience literature about how metamorphism should be dealt with in systems under stress. Many of these assertions are flawed. We present a conceptual generic model based on the thermodynamic theory of systems under stress. In our model, there is no equilibrium, reactions will occur by chemical transport along various pathways (e.g. pores, grain boundaries) and different pathways have different energy drops but also different kinetics.

We have run an extensive set of experiments on gypsum dehydration (to bassanite) to address key questions relating to fluid pressure evolution and, in parallel, have developed a numerical model for dehydration. Experiments show that the rate of gypsum dehydration is strongly influenced by pore fluid pressure and not by confining pressure. We show how these results fit into our conceptual model, but also how they may be just one aspect of behaviour to be expected on longer timescales. Our conceptual model will be key to understanding fluid pressure evolution during metamorphism over the range of timescales expected for geological events.

LIST OF CONFERENCE PARTICIPANTS

Gema	Alías López	Universitat de Barcelona	Spain	galias@ub.edu
Jesús	Aller	Universidad de Oviedo	Spain	aller@geol.uniovi.es
Juan Luis	Alonso	Universidad de Oviedo	Spain	jalonso@geol.uniovi.es
Loreto	Antón	Universidad Nacional de Educación a Distancia, UNED	Spain	lanton@ccia.uned.es
Nicholas	Austin	Imperial Oil	USA	nick.j.austin@gmail.com
Juan Carlos	Balaný	Universidad Pablo Olavide	Spain	jcbalrou@upo.es
Daniel	Ballesteros	Universidad de Oviedo	Spain	ballesteros@geol.uniovi.es
Leticia	Barcos Murcia	Universidad Pablo Olavide	Spain	lbarmur@upo.es
Fernando	Bastida	Universidad de Oviedo	Spain	bastida@geol.uniovi.es
Michel	Bestmann	University Erlangen-Nuremberg	Germany	michel@geol.uni-erlangen.de
Marco	Billia	University of Otago	New Zealand	marco@geology.co.nz
Silvia	Blanco-Ferrera	Universidad de Oviedo	Spain	silvia@geol.uniovi.es
Paul	Bons	University of Tuebingen	Germany	paul.bons@uni-tuebingen.de
Simon	Brocklehurst	University of Manchester	UK	simon.brocklehurst@manchester.ac.uk
Siebe	Breed	Universidad de Oviedo	Spain	siebe@siebebreed.nl
Katharine	Brodie	University of Manchester	UK	Kate.Brodie@manchester.ac.uk
Zita	Bukovska	Charles University	Czech Rep.	zita.bukovska@natur.cuni.cz
Mayte	Bulnes	Universidad de Oviedo	Spain	maite@geol.uniovi.es
Benedito	Calejo Rodríguez	Centro Geologia Univ Porto	Portugal	bjc.rodrigues@gmail.com
Pablo	Calvín	University of Zaragoza	Spain	Pablo_calvin@hotmail.com
Irene	Cantarero	Universitat de Barcelona	Spain	i_cantarero@ub.edu
James	Connolly	ETH Zürich	Switzerland	connolly@erdw.ethz.ch
Dyanna	Czeck	University of Wisconsin-Milwaukee	USA	dyanna@uwm.edu
Irene	de Felipe	Universidad de Oviedo	Spain	defelipe@geol.uniovi.es
Manuel	Díaz-Azpiroz	Universidad Pablo Olavide	Spain	mdiaazp@upo.es
Amy Clare	Ellis	University of Manchester	UK	Amy.Ellis@postgrad.manchester.ac.uk
José Julián	Esteban	Universidad del País Vasco	Spain	jj.esteban@ehu.es
Ulrike	Exner	University of Vienna	Austria	ulrike.exner@univie.ac.at
Francisco J.	Fernández	Universidad de Oviedo	Spain	brojos@geol.uniovi.es
Carlos	Fernández	Universidad de Huelva	Spain	fcarlos@uhu.es
David	Fernández-Blanco	Vrije Universiteit Amsterdam	The Netherlands	david.fernandez@falw.vu.nl
Natalia	Fortunatti	Universidad Nacional del Sur	Argentina	nfortuna@uns.edu.ar
Marcel	Frehner	ETH Zürich	Switzerland	marcel.frehner@erdw.ethz.ch
Jun-ichi	Fukuda	Tohoku University	Japan	jfukuda@dges.es.tohoku.ac.jp
Jorge	Ginés	Fugro NPA Limited	UK	j.gines@fugro-npa.com
Enrique	Gómez-Rivas	University of Tuebingen	Germany	enrique.gomez-rivas@uni-tuebingen.de
Raphaël	Gottardi	University of Minnesota	USA	gotta004@umn.edu
Albert	Griera	Universitat Autònoma de Barcelona	Spain	albert.griera@uab.cat
Djordje	Drujic	Dalhousie University	Canada	gdrujic@dal.ca
Gabriel	Gutiérrez-Alonso	Universidad de Salamanca	Spain	gabi@usal.es
Miguel	Gutiérrez-Medina	Universidad de Cantabria	Spain	miguel.gutierrez@unican.es
Abigail	Hackston	University of Manchester	UK	abigail.hackston@postgrad.manchester.ac.uk
Tom	Haerincx	Katholieke Universiteit Leuven	Belgium	tom.haerincx@ees.kuleuven.be
Mike	Haertel	University of Bern	Switzerland	mike.haertel@geo.unibe.ch
Angela	Halfpenny	CSIRO	Australia	Angela.halfpenny@csiro.au
Suzanne	Hangx	Shell	The Netherlands	Suzanne.Hangx@shell.com
Pedro Pablo	Hernaiz Huerta	INYPESA Informes y Proyectos S.A.	Spain	phh@inypsa.es
Ken-ichi	Hirauchi	Hiroshima University	Japan	k-hirauchi@hiroshima-u.ac.jp
Benjamin	Holtzman	Columbia University	USA	benh@ldeo.columbia.edu
Esther	Izquierdo-Llavall	University of Zaragoza	Spain	estheriz@unizar.es
Silvia	Japas	Universidad de Buenos Aires	Argentina	msjapas@gl.fcien.uba.ar
Alberto	Jiménez-Díaz	Universidad Complutense de Madrid	Spain	ajimenezdiaz@geo.ucm.es
Montserrat	Jiménez-Sánchez	Universidad de Oviedo	Spain	mjimenez@geol.uniovi.es

Rüdiger	Killian	Basel University	Switzerland	ruediger.killian@unibas.ch
Richard	Lisle	Cardiff University	UK	Lisle@cardiff.ac.uk
Sergio	Llana-Fúnez	Universidad de Oviedo	Spain	slf@geol.uniovi.es
Maria Gema	Llorens	University of Tuebingen	Germany	gemalloreng@gmail.com
Tina	Lohr	ERC Equipoise Limited	UK	tinal@ercequipoise.com
Carlos	Lopez	Universidad de Oviedo	Spain	clopez@geol.uniovi.es
Irene	López Rodríguez	Universidad de Oviedo	Spain	irene@geol.uniovi.es
Marco	López-Sánchez	Universidad de Oviedo	Spain	malopez@geol.uniovi.es
Alberto	Marcos	Universidad de Oviedo	Spain	marcos@geol.uniovi.es
Elisabetta	Mariani	University of Liverpool	UK	mariani@liverpool.ac.uk
Mira	Markovaara-Koivisto	Aalto University	Finland	mira.markovaara-koivisto@aalto.fi
Katarlina				
Luca	Menegon	Tromsø University	Norway	luca.menegon@uit.no
Daniel	Metodiev	National Laboratory of Energy and Geology	Portugal	daniel.metodiev@lneg.pt
Mar	Moragas	CSIC	Spain	mmoragas@ictja.csic.es
Luiz FG	Morales	GFZ German Research Centre for Geosciences	Germany	Morales@gfz-potsdam.de
Noel	Moreira	Centro de Ciência Viva de Estremoz e LIRIO	Portugal	nmoreira@estremoz.cienciaviva.pt
Isabel	Moriano	Universidad de Oviedo	Spain	imoriano@geol.uniovi.es
Mustapha	Namouh	Université Cadi Ayyad	Morocco	mustaphanamouh@yahoo.fr
Marianne	Negrini	Universitetet i Tromsø	Norway	marianne.negrini@uit.no
André	Niemeijer	Utrecht University	The Netherlands	niemeijer@geo.uu.nl
Matej	Pec	University of Basel	Switzerland	matej.pec@unibas.ch
Andrés	Pérez-Estáun	CSIC	Spain	andres@itja.csic.es
Fernando	Pérez-Valera	Universidad de Jaén	Spain	fperez@ujaen.es
Josep	Poblet	Universidad de Oviedo	Spain	jpoblet@geol.uniovi.es
Carlos	Ponce	Universitat Autònoma de Barcelona	Spain	carlos.ponce@uab.cat
Alejandra	Quintanilla-Terminel	Massachusetts Institute of Technology	USA	alequte@mit.edu
Giorgio	Ranalli	Carleton University	Canada	granalli@earthsci.carleton.ca
Lidia	Rodríguez Mendez	Universidad del País Vasco	Spain	lidia.rodriguez@ehu.es
Ernest	Rutter	University of Manchester	UK	e.rutter@manchester.ac.uk
Pablo	Santolaria	Universidad de Zaragoza	Spain	psotin@unizar.es
Hugh	Sinclair	University of Edinburgh	UK	Hugh.Sinclair@ed.ac.uk
Manuel	Sintubin	Katholieke Universiteit Leuven	Belgium	manuel.sintubin@ees.kuleuven.be
Alexis	Soares	Centro Ciência Viva de Estremoz e LIRIO	Portugal	asoares@estremoz.cienciaviva.pt
João	Sousa	Universidade do Minho	Portugal	jpns@portugalmail.pt
Angela	Suárez	IGME	Spain	a.suarez@igme.es
Joe	Tant	University of Manchester	UK	Joseph.tant@postgrad.manchester.ac.uk
Dan	Tatham	University of Liverpool	UK	tatham@liverpool.ac.uk
Stefano	Tavani	Universitat de Barcelona	Spain	stefano.tavani@ub.edu
Taija	Torvela	University of Helsinki	Finland	taija.torvela@helsinki.fi
Claudia	Trepmann	Ludwig-Maximilians-Universität München	Germany	claudia.trepmann@lmu.de
Şener	Üşümezsoy	Istanbul University	Turkey	aysal@istanbul.edu.tr
Hodei	Uzkeda	Universidad de Oviedo	Spain	hodei@geol.uniovi.es
Manoel	Valcarcel	Universitat de Barcelona	Spain	m.valcarcel@igme.es
Resi	Veeningen	University of Vienna	Austria	resi.veeningen@univie.ac.at
Marie	Violay	Istituto Nazionale di Geofisica e Vulcanologia (INGV)	Italy	Marie.violay@ingv.it
Maarten	Voorn	University of Vienna	Austria	maarten.voorn@univie.ac.at
Zoja	Vukmanovic	Australian Commonwealth Scientific and Research Organization (CSIRO)	Australia	zoja.vukmanovic@csiro.au
Tohru	Watanabe	University of Toyama	Japan	twatanabe@sci.u-toyama.ac.jp
John	Watson	Fugro Robertson Limited	UK	john.watson@fugro-robertson.com
Arlo	Weil	Bryn Mawr College	USA	aweil@brynmawr.edu
Marit	Wennerström	Geological Survey of Finland	Finland	Marit.Wennerstrom@gtk.fi
John	Wheeler	University of Liverpool	UK	johnwh@liverpool.ac.uk

ACKNOWLEDGEMENTS

We would like to thank postgraduates that helped during the conference: Siebe Breed, Irene López Rodríguez and Erica de la Riva Rodríguez.

Financial support in addition to the conference fee paid by DRT participants was necessary in order to run the meeting. We acknowledge the following institutions and companies for the support given without which we could not have organised this event.

Ministerio de Ciencia y Tecnología: grants RYC-2008-02067, Consolider Topolberia CSD2006-00041, FRADUCSIS project CGL2010-14890, CGL2011-13171-E (*proposal in evaluation*)

Gobierno del Principado de Asturias, Conserjería de Educación y Universidades, (*proposal in evaluation*)

Universidad de Oviedo

Facultad and Departamento de Geología

Xstrata Zinc

Cajastur

Ciudad de la Energía, Gobierno de España

Tectask

Fugro

Instituto Universitario de Xeoloxía Isidro Parga Pondal

